





GRB221009A



Are axion-like particles required to explain the observations of very high energy photons from

GRB221009A

Manuel Meyer, Katrine Kennedy, Eike Ravensburg
CP3 Origins, University of Southern Denmark

mey@sdu.dk

20th Patras Workshop on Axions, WIMPs and WISPs
September 23, 2025

Are axion-like particles required to explain the observations of very high energy photons from

GRB221009A

Manuel Meyer, Katrine Kennedy, Eike Ravensburg
CP3 Origins, University of Southern Denmark

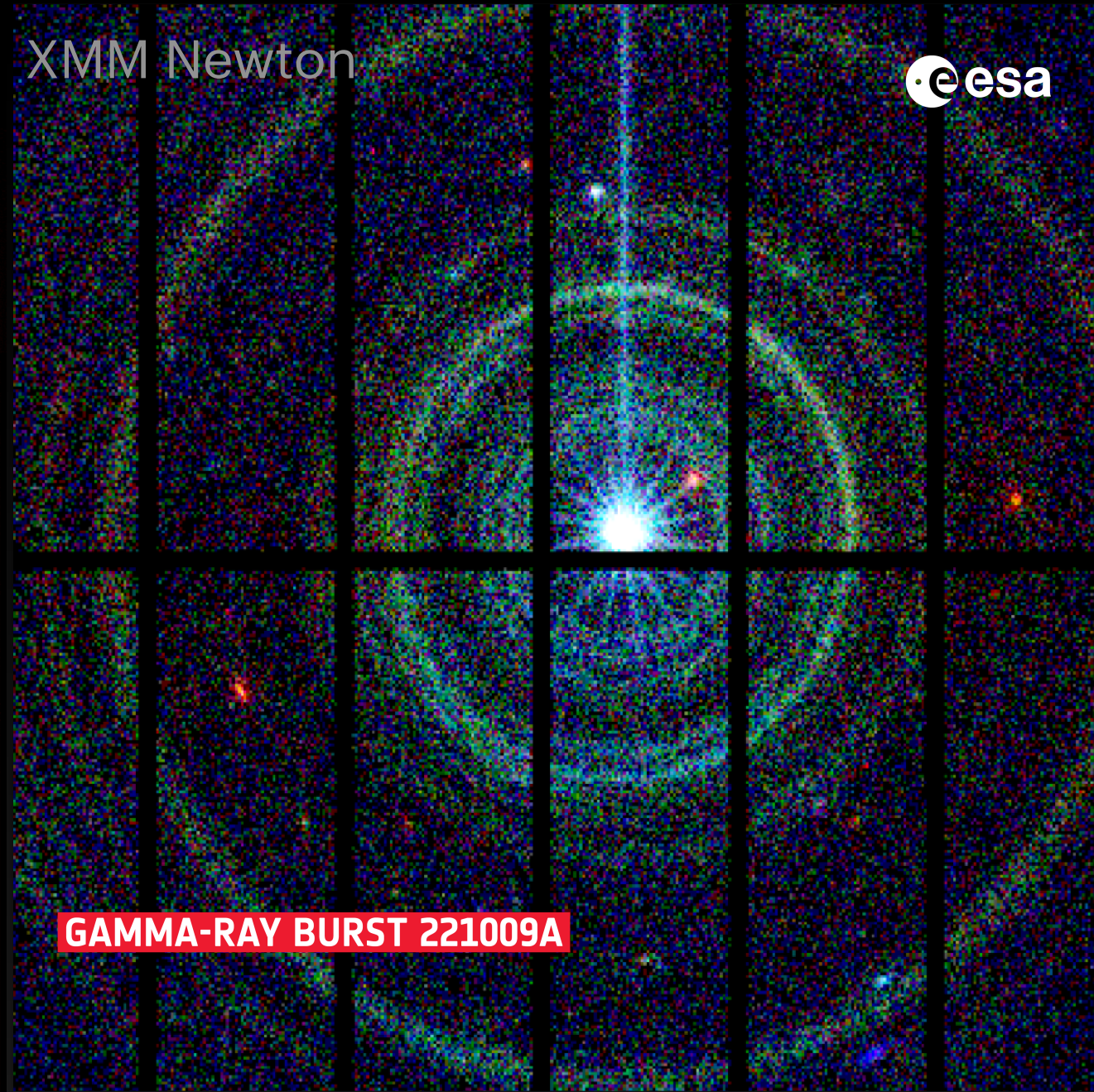
mey@sdu.dk

20th Patras Workshop on Axions, WIMPs and WISPs
September 23, 2025

erc SDU

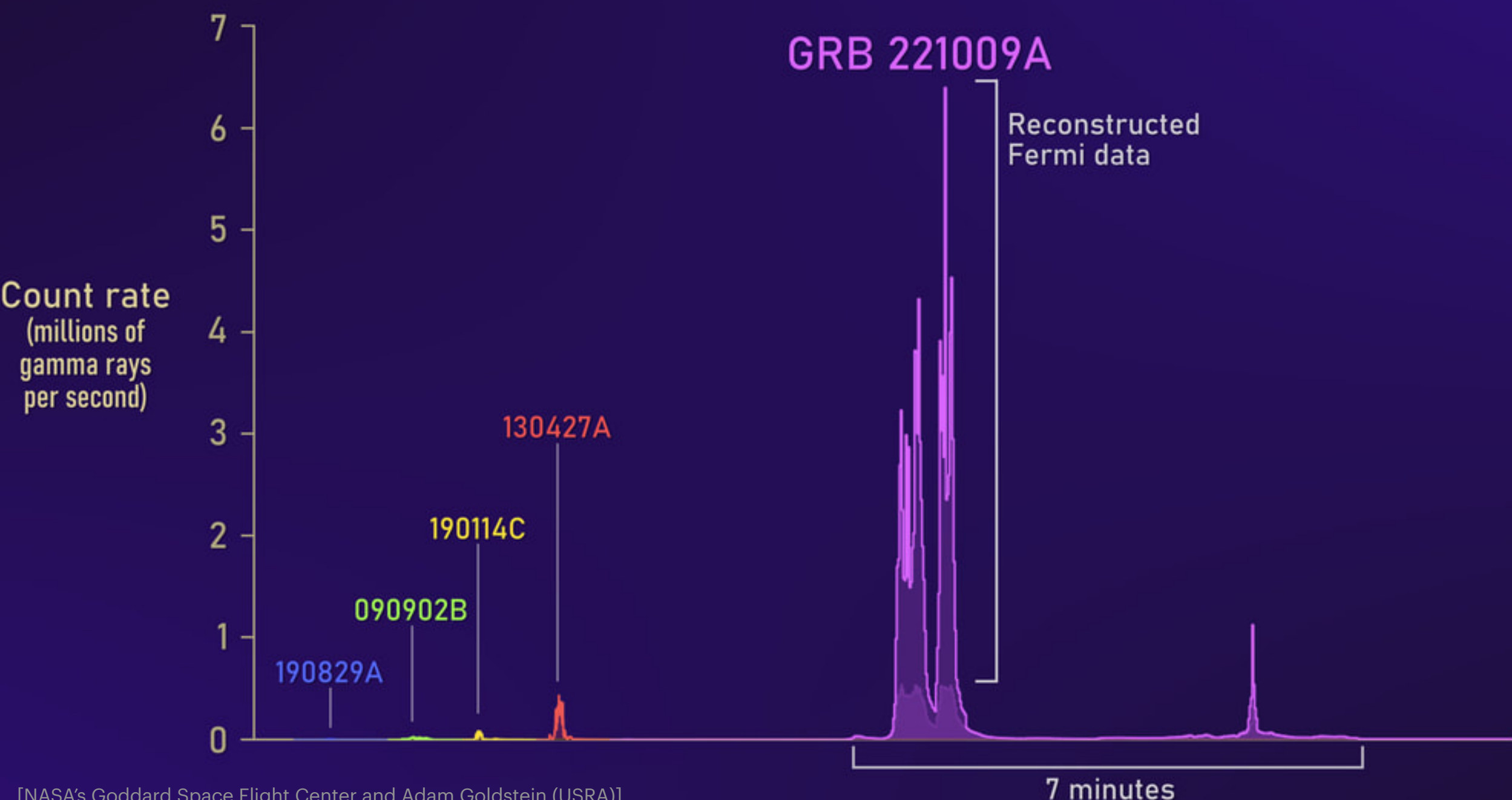


E > 100 MeV
10 hours of observation
 $20^\circ \times 20^\circ$
Credit: NASA/DOE/Fermi LAT Collaboration

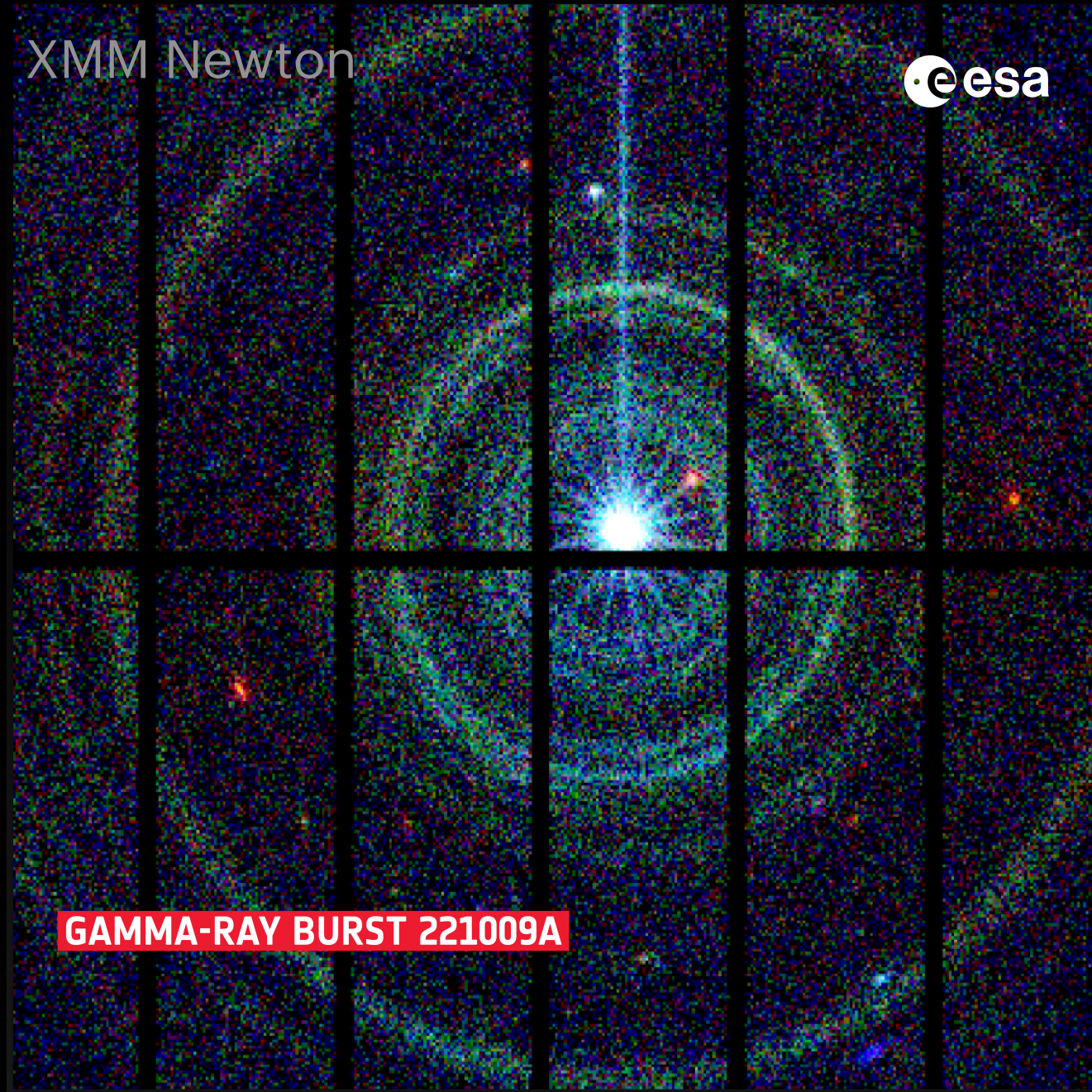


GRB221009A — BOAT

The BOAT GRB in Context



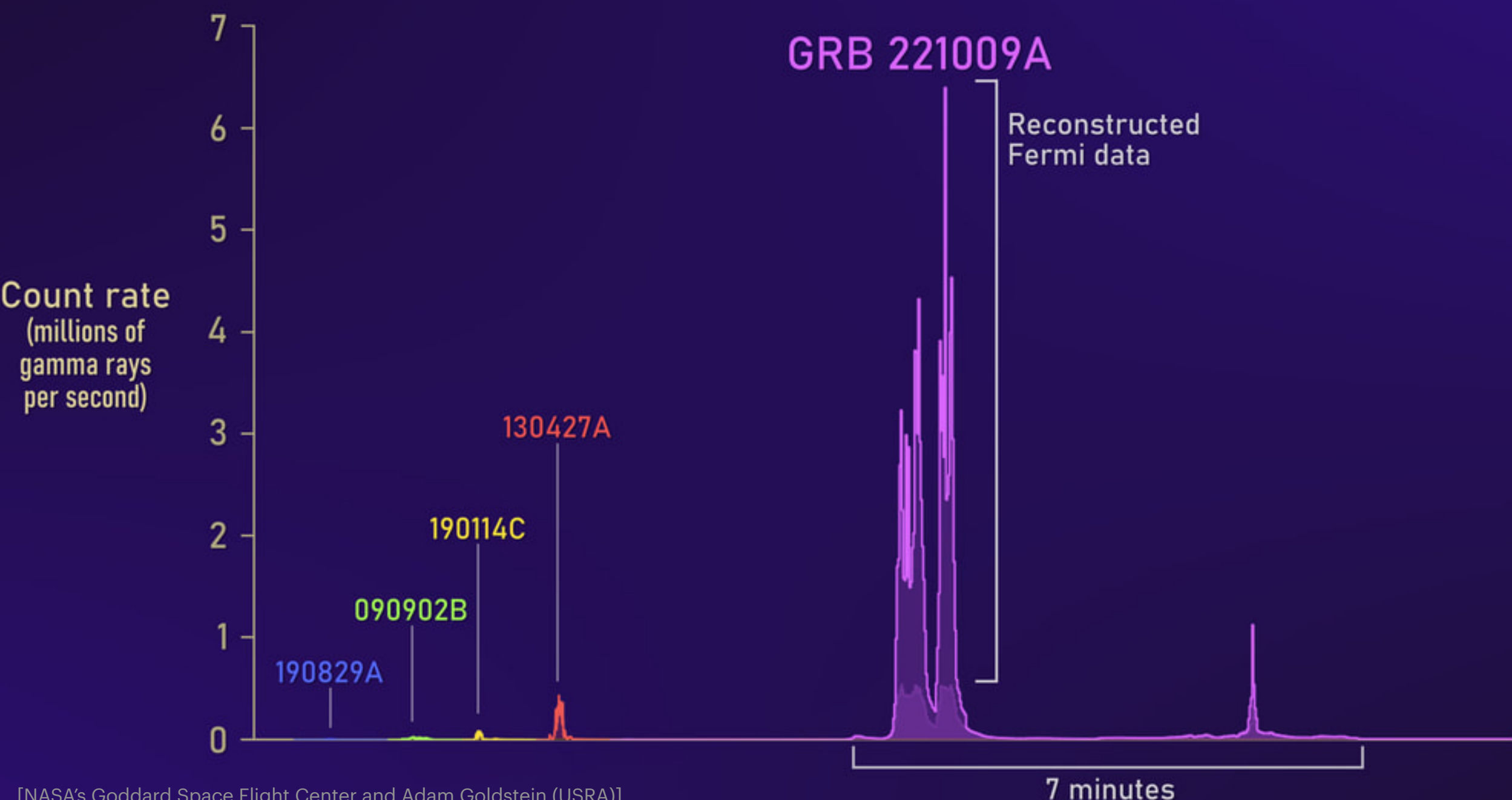
E > 100 MeV
10 hours of observation
 $20^\circ \times 20^\circ$
Credit: NASA/DOE/Fermi LAT Collaboration



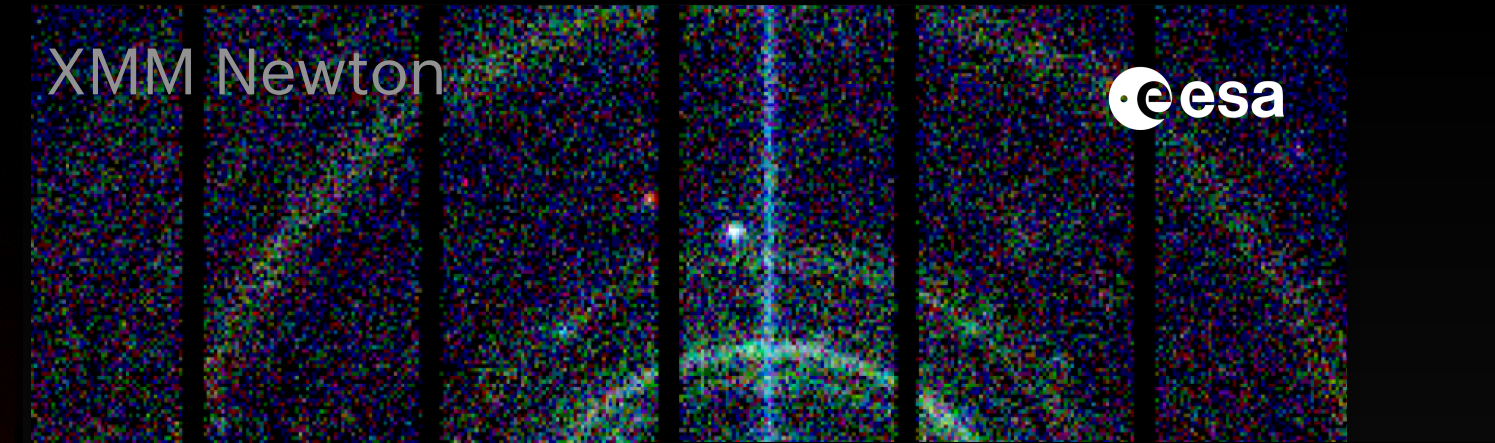
GRB221009A — BOAT

- Brightest GRB ever observed

The BOAT GRB in Context



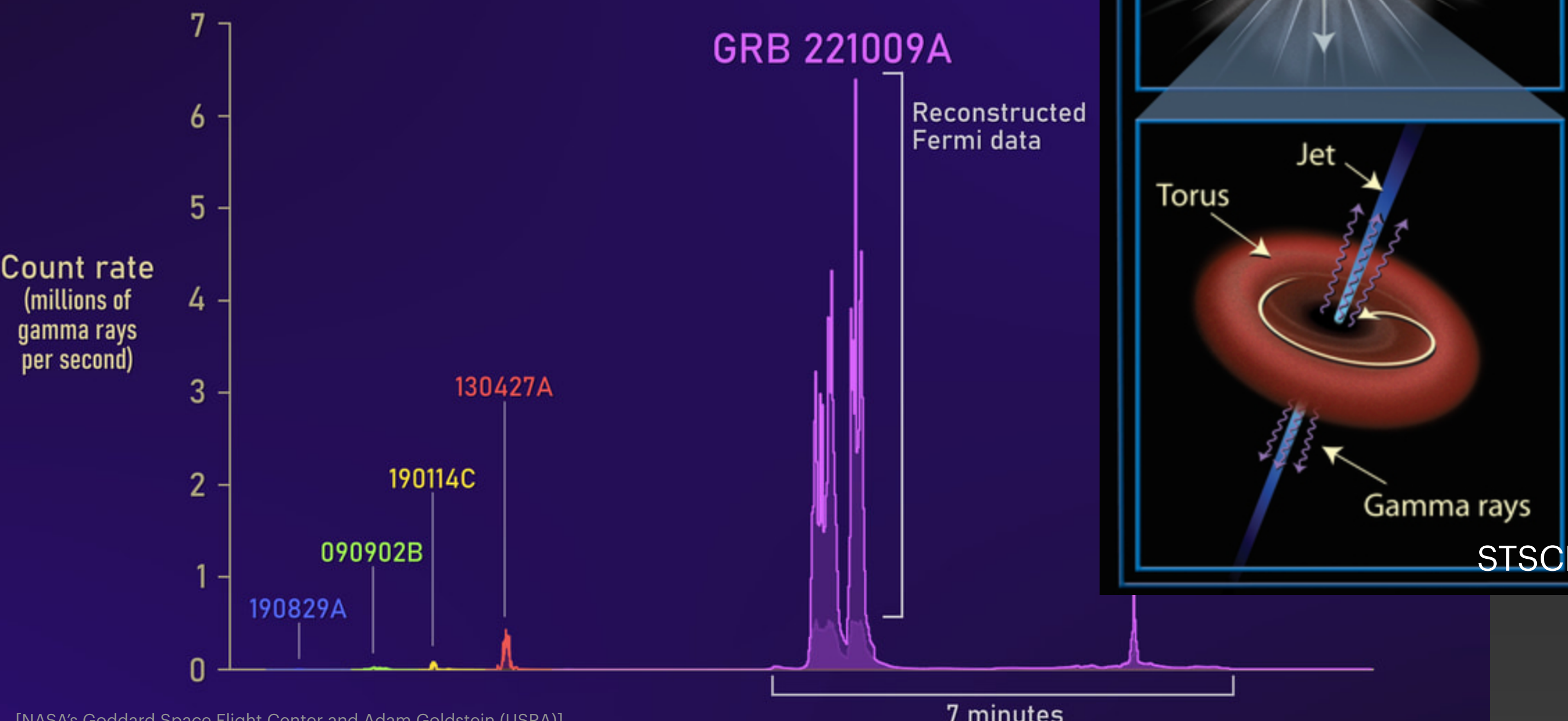
E > 100 MeV
10 hours of observation
 $20^\circ \times 20^\circ$
Credit: NASA/DOE/Fermi LAT Collaboration



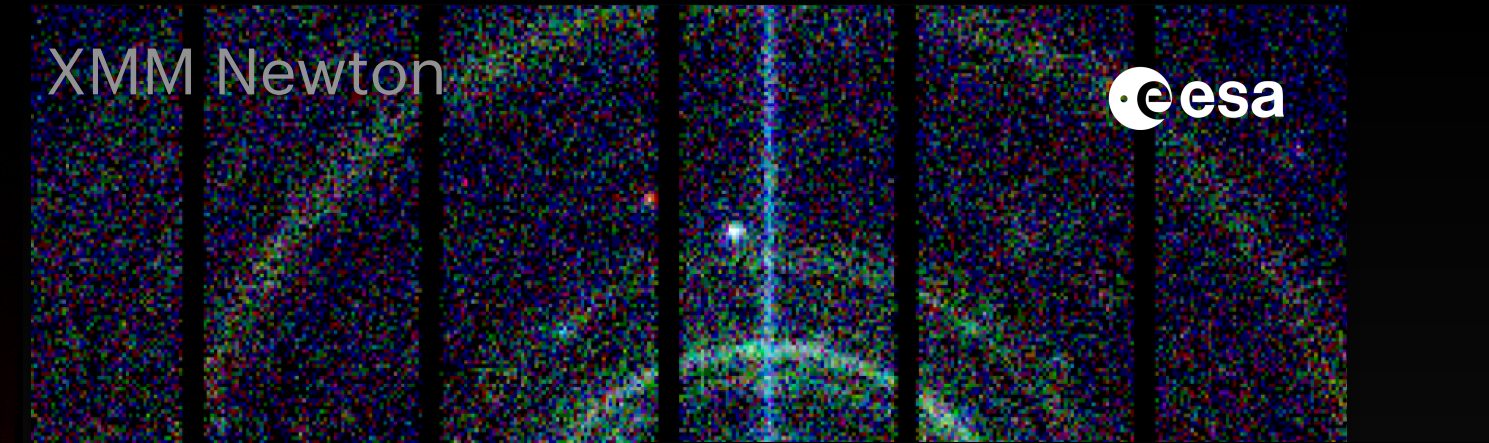
GRB221009A — BOAT

- Brightest GRB ever observed
- Probable precursor: collapsar

The BOAT GRB in Context



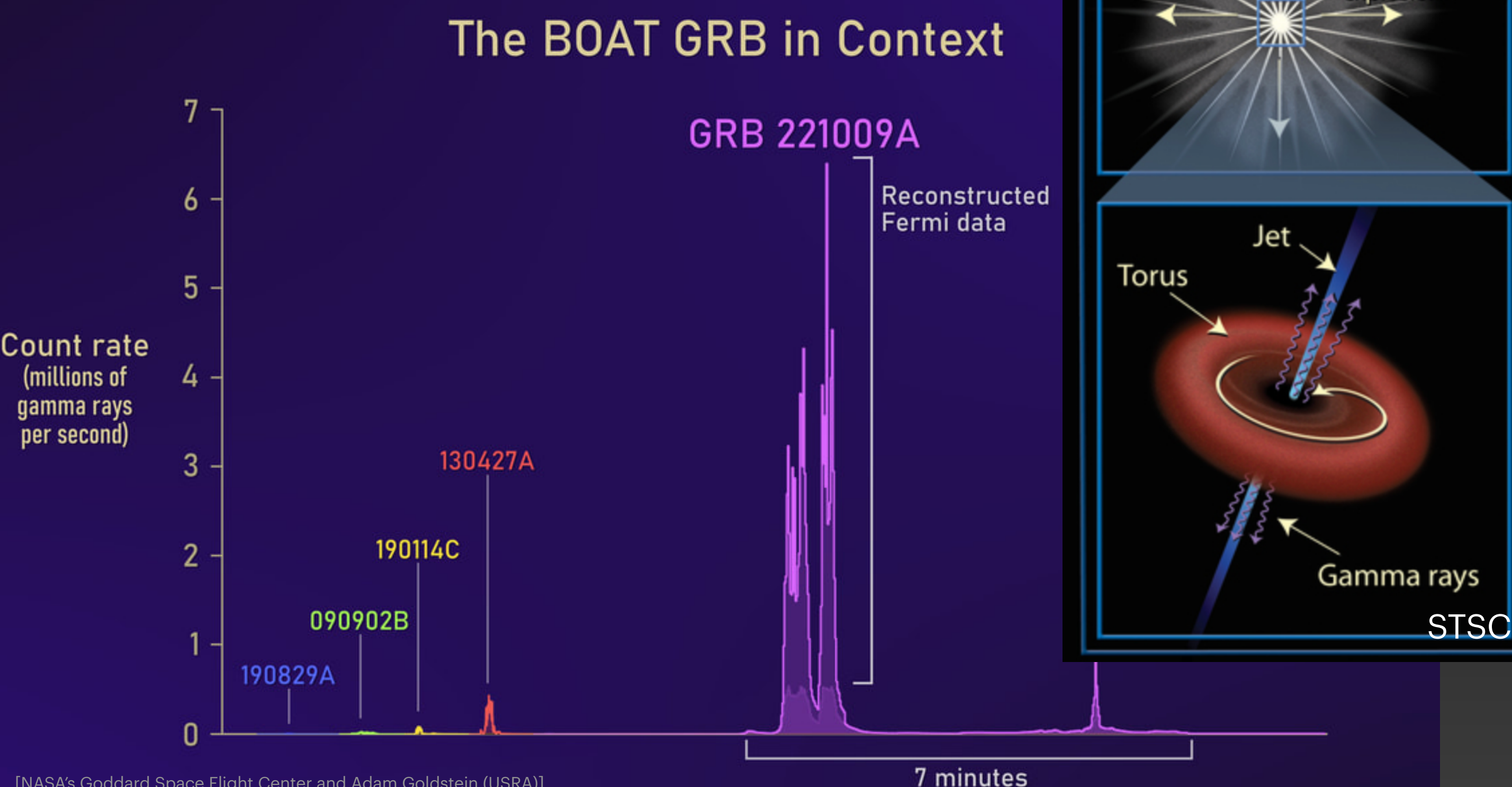
E > 100 MeV
10 hours of observation
 $20^\circ \times 20^\circ$
Credit: NASA/DOE/Fermi LAT Collaboration



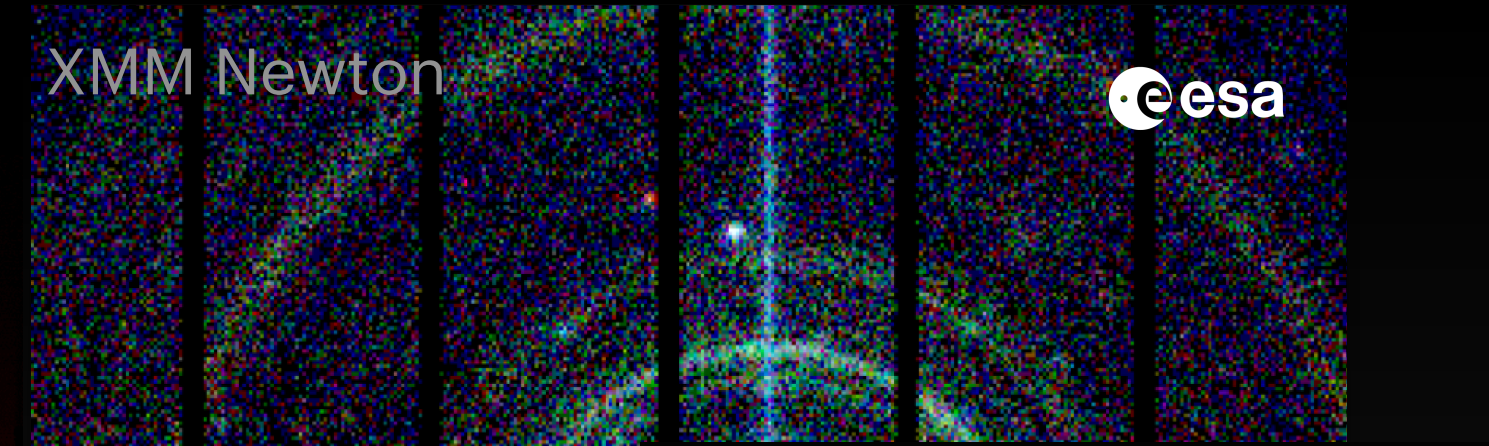
GRB221009A — BOAT

- Brightest GRB ever observed
- Probable precursor: collapsar
- Redshift $z = 0.1505$
($D_L \approx 2.4 \times 10^9$ ly) from Cal, II absorption lines measured with VLT X-Shooter

[Malesani et al., 2023, arXiv:2302.07891]

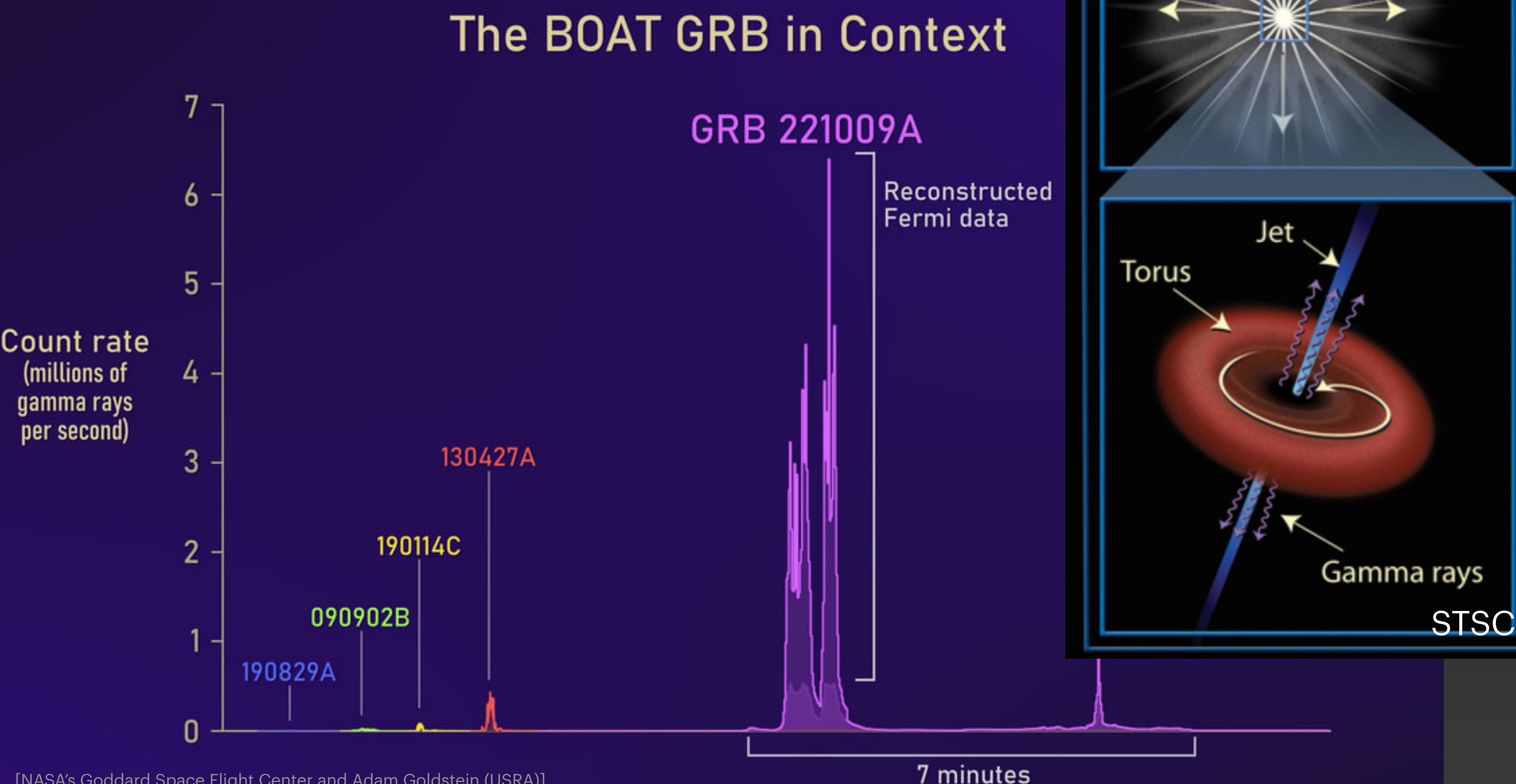


E > 100 MeV
10 hours of observation
 $20^\circ \times 20^\circ$
Credit: NASA/DOE/Fermi LAT Collaboration



GRB221009A — BOAT

- Brightest GRB ever observed
- Probable precursor: collapsar
- Redshift $z = 0.1505$
($D_L \approx 2.4 \times 10^9$ ly) from Cal, II absorption lines measured with VLT X-Shooter
[Malesani et al., 2023, arXiv:2302.07891]
- *Fermi* LAT detected 99.4 GeV photon
(record from GRB) at $T_0 + 240$ s
[Axelsson et al., 2025, arXiv:2409.04580]



Why exciting for axion enthusiasts?

GCN Circular 32677

Subject LHAASO observed GRB 221009A with more than 5000 VHE photons up to around 18 TeV
Event [GRB 221009A](#)
Date 2022-10-11T09:21:54Z (3 years ago)
From Judith Racusin at GSFC <judith.racusin@nasa.gov>

Yong Huang, Shicong Hu, Songzhan Chen, Min Zha, Cheng Liu, Zhiguo Yao and Zhen Cao report on behalf of the LHAASO experiment

We report the observation of GRB 221009A, which was detected by Swift (Kennea et al. GCN #[32635](#)), Fermi-GBM (Veres et al. GCN #[32636](#), Lesage et al. GCN #[32642](#)), Fermi-LAT (Bissaldi et al. GCN #[32637](#)), IPN (Svinkin et al. GCN #[32641](#)) and so on.

GRB 221009A is detected by LHAASO-WCDA at energy above 500 GeV, centered at RA = 288.3, Dec = 19.7 within 2000 seconds after T0, with the significance above 100 s.d., and is observed as well by LHAASO-KM2A with the significance about 10 s.d., where the energy of the highest photon reaches 18 TeV.

This represents the first detection of photons above 10 TeV from GRBs.

The LHAASO is a multi-purpose experiment for gamma-ray astronomy (in the energy band between 10^{11} and 10^{15} eV) and cosmic ray measurements.

Why exciting for axion enthusiasts?

GCN Circular 32677

Subject LHAASO observed GRB 221009A with more than 5000 VHE photons up to around 18 TeV
Event [GRB 221009A](#)
Date 2022-10-11T09:21:54Z (3 years ago)
From Judith Racusin at GSFC <judith.racusin@nasa.gov>

Yong Huang, Shicong Hu, Songzhan Chen, Min Zha, Cheng Liu, Zhiguo Yao and Zhen Cao report on behalf of the LHAASO experiment

We report the observation of GRB 221009A, which was detected by Swift (Kennea et al. GCN #[32635](#)), Fermi-GBM (Veres et al. GCN #[32636](#), Lesage et al. GCN #[32642](#)), Fermi-LAT (Bissaldi et al. GCN #[32637](#)), IPN (Svinkin et al. GCN #[32641](#)) and so on.

GRB 221009A is detected by LHAASO-WCDA at energy above 500 GeV, centered at RA = 288.3, Dec = 19.7 within 2000 seconds after T0, with the significance above 100 s.d., and is observed as well by LHAASO-KM2A with the significance about 10 s.d., where the energy of the highest photon reaches 18 TeV.

This represents the first detection of photons above 10 TeV from GRBs.

The LHAASO is a multi-purpose experiment for gamma-ray astronomy (in the energy band between 10^{11} and 10^{15} eV) and cosmic ray measurements.

Why exciting for axion enthusiasts?

GCN Circular 32677

Subject LHAASO observed GRB 221009A with more than 5000 VHE photons up to around 18 TeV
Event [GRB 221009A](#)
Date 2022-10-11T09:21:54Z (3 years ago)
From Judith Racusin at GSFC <judith.racusin@nasa.gov>

Yong Huang, Shicong Hu, Songzhan Chen, Min Zha, Cheng Liu, Zhiguo Yao and Zhen Cao report on behalf of the LHAASO experiment

We report the observation of GRB 221009A, which was detected by Swift (Kennea et al. GCN #[32635](#)), Fermi-GBM (Veres et al. GCN #[32636](#), Lesage et al. GCN #[32642](#)), Fermi-LAT (Bissaldi et al. GCN #[32637](#)), IPN (Svinkin et al. GCN #[32641](#)) and so on.

GRB 221009A is detected by LHAASO-WCDA at energy above 500 GeV, centered at RA = 288.3, Dec = 19.7 within 2000 seconds after T0, with the significance above 100 s.d., and is observed as well by LHAASO-KM2A with the significance about 10 s.d., where the energy of the highest photon reaches 18 TeV.

This represents the first detection of photons above 10 TeV from GRBs.

The LHAASO is a multi-purpose experiment for gamma-ray astronomy (in the energy band between 10^{11} and 10^{15} eV) and cosmic ray measurements.

Very unlikely to observe $E = 18$ TeV photon from source at $z = 0.151$ – need new physics?

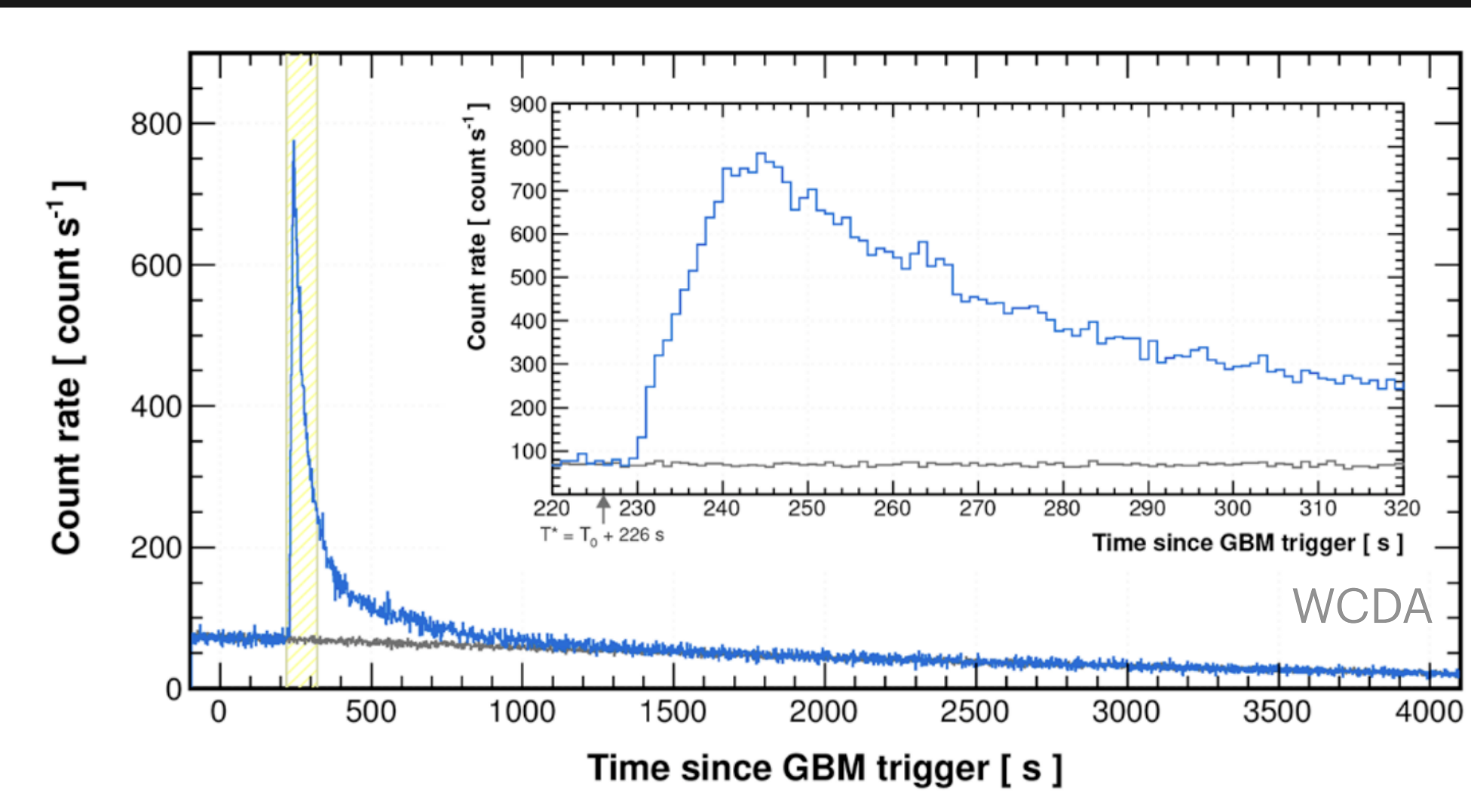
VHE photons seen with LHAASO



LHAASO Mt Haizi, Sichuan, China

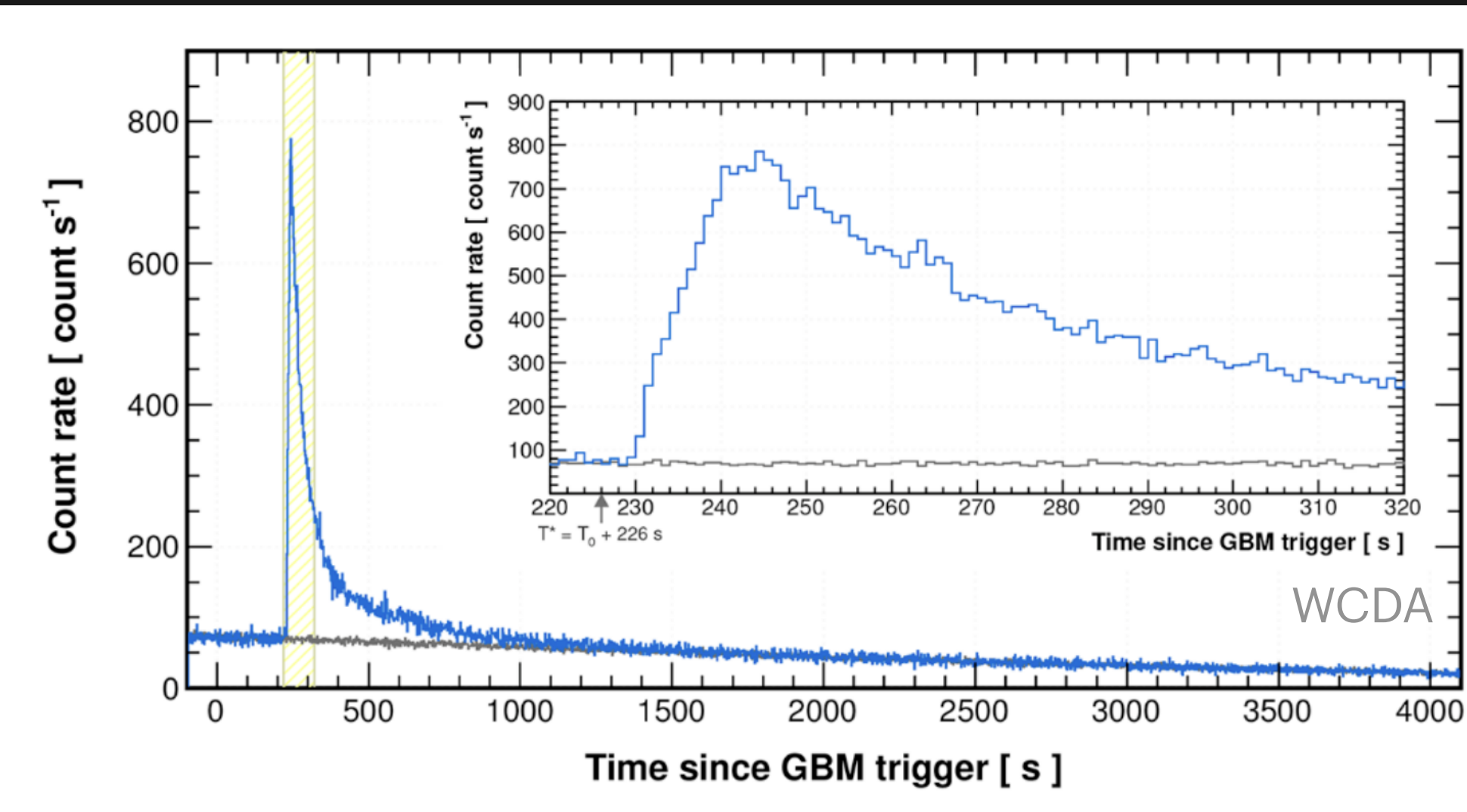
VHE photons seen with LHAASO

- WCDA: > 64,000 gamma rays between 0.2 TeV and 7 TeV in ~3000s



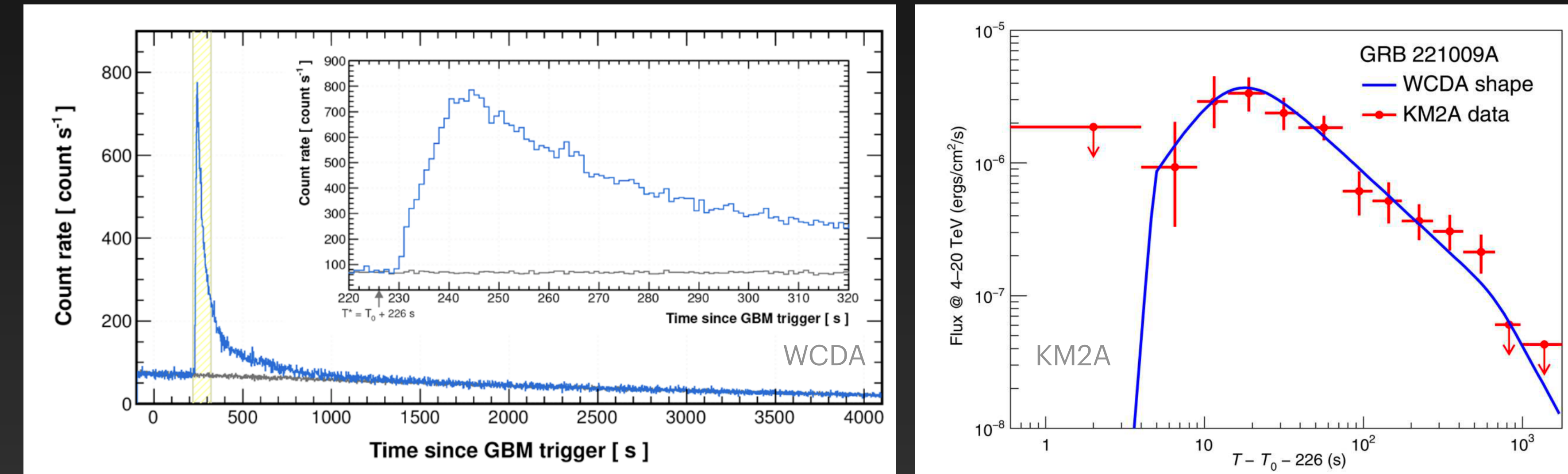
VHE photons seen with LHAASO

- WCDA: > 64,000 gamma rays between 0.2 TeV and 7 TeV in ~3000s
- Light curve suggests jet opening angle of 1.6°



VHE photons seen with LHAASO

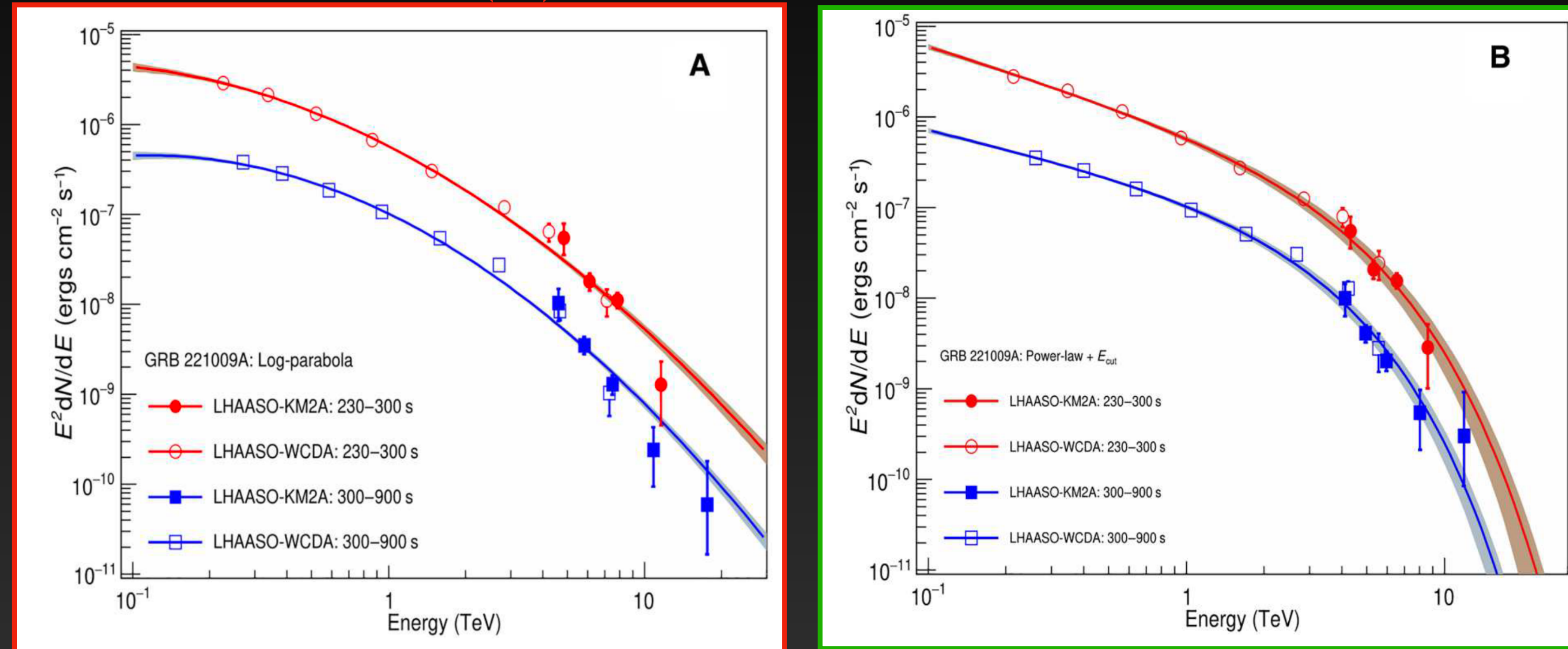
- WCDA: > 64,000 gamma rays between 0.2 TeV and 7 TeV in ~3000s
- Light curve suggests jet opening angle of 1.6°
- KM2A: 140 gamma rays between 3 and $\gtrsim 13$ TeV in ~900s



Combined WCDA+KM2A spectrum

Log parabola (LP): $\frac{dN}{dE} = N \left(\frac{E}{E_0} \right)^{-\alpha-\beta \ln(E/E_0)}$

Power law with exp. cutoff: $\frac{dN}{dE} = N \left(\frac{E}{E_0} \right) e^{-E/E_{\text{cut}}}$

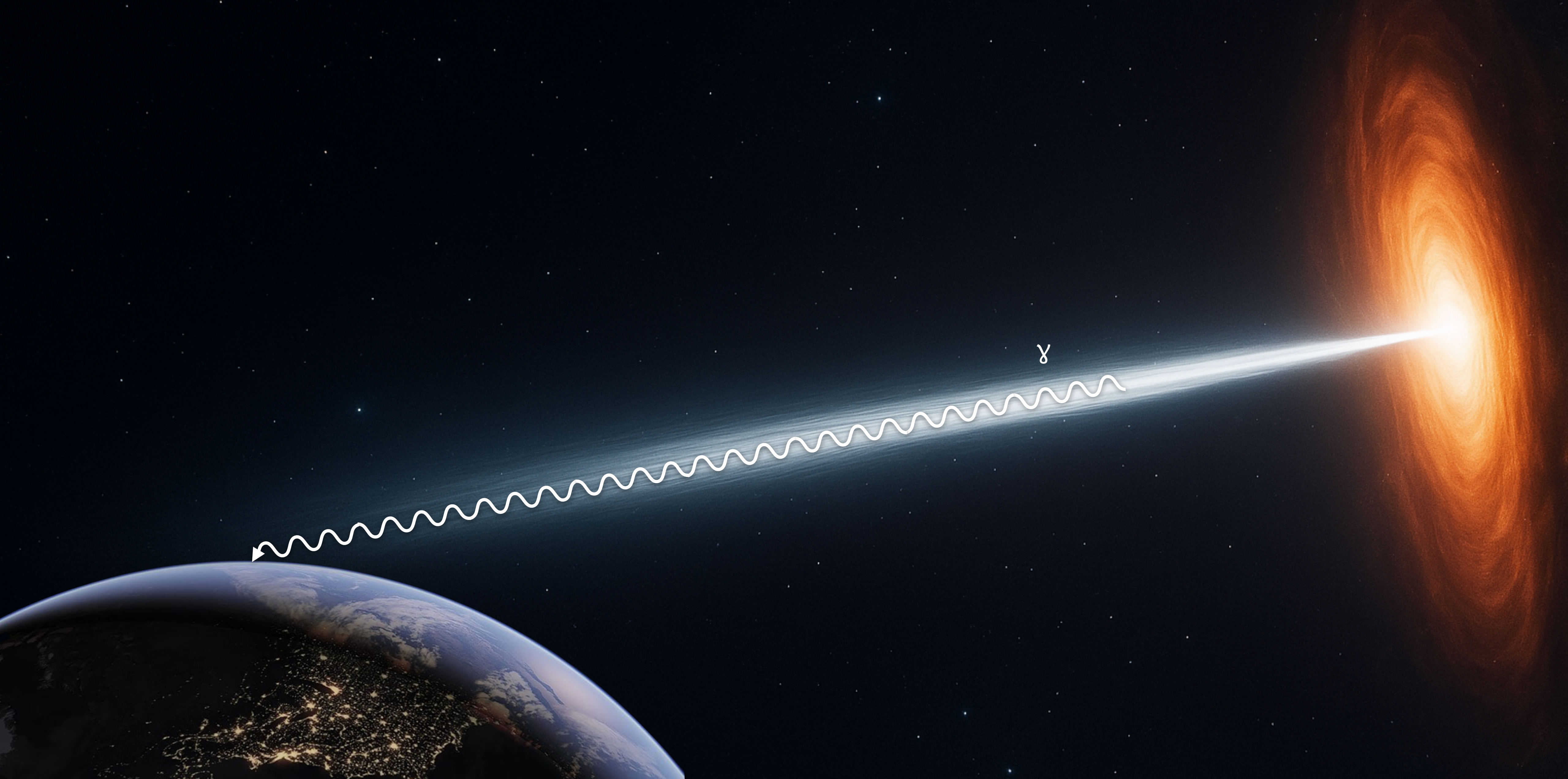


- Reconstruction depends on assumed source spectrum
- Maximum photon energies: $E_{\text{max}}^{\text{LP}} = 17.8^{+7.4}_{-5.1} \text{ TeV}$ whereas $E_{\text{max}}^{\text{EPL}} = 12.2^{+3.5}_{-2.4} \text{ TeV}$
- EPL spectrum provides better fit for combined data set

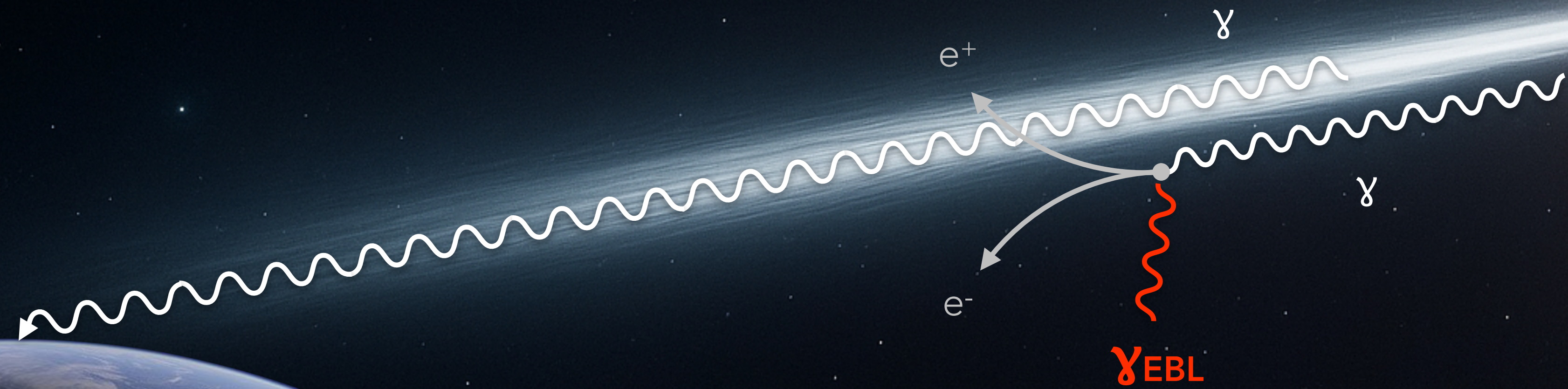
Absorption of VHE gamma rays



Absorption of VHE gamma rays

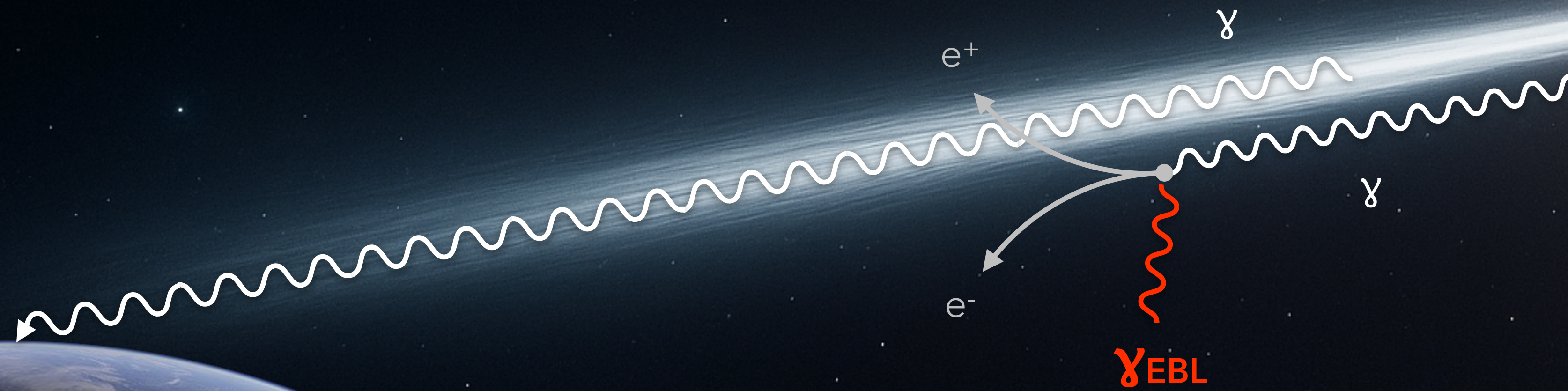


Absorption of VHE gamma rays



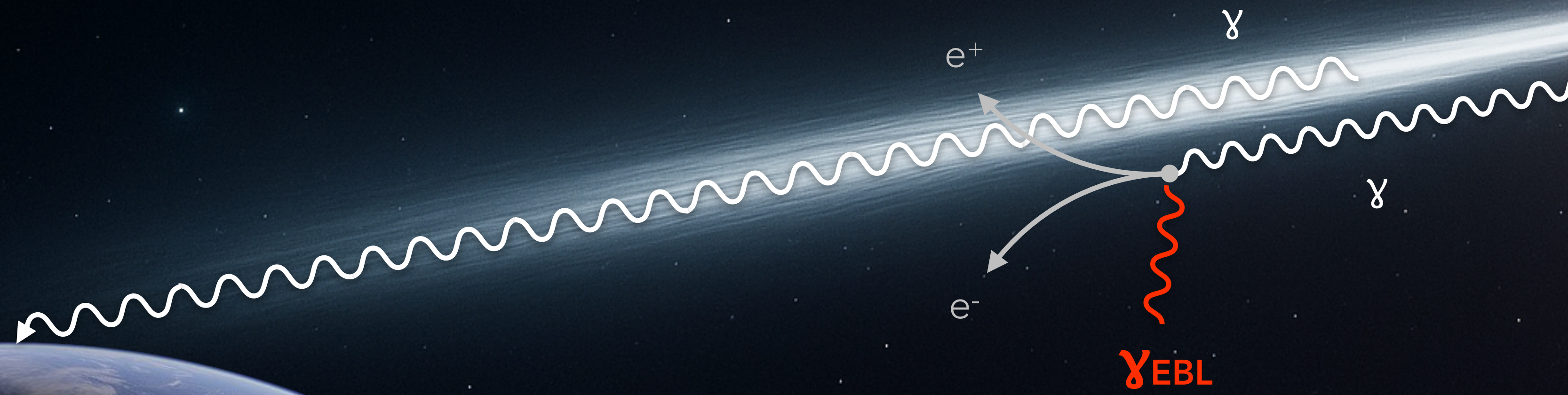
Absorption of VHE gamma rays

$$F_{\text{obs}} = F_{\text{int}} \exp(-\tau_{\gamma\gamma}(E, z))$$



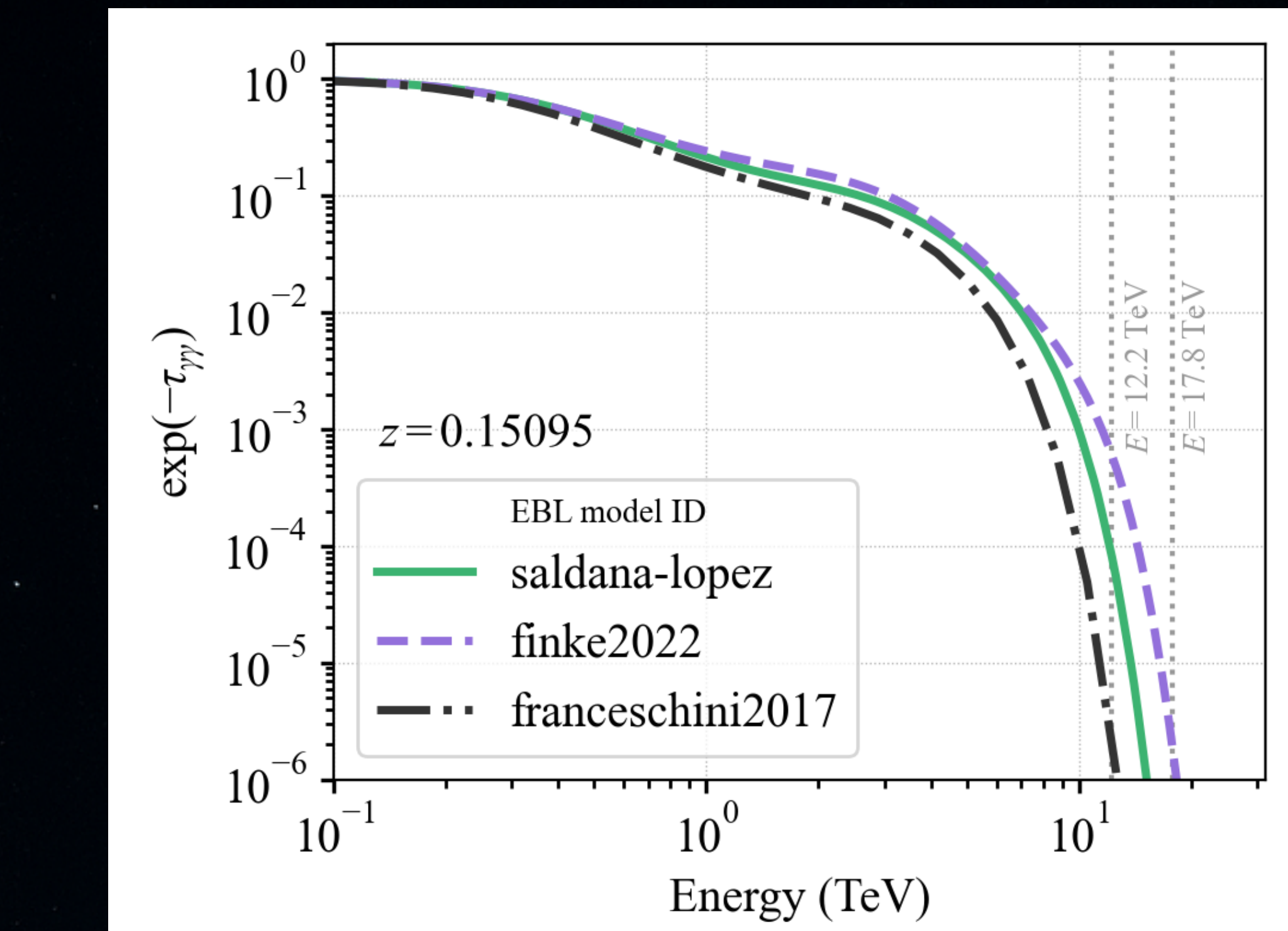
Absorption of VHE gamma rays

$$F_{\text{obs}} = F_{\text{int}} \exp(-\tau_{\gamma\gamma}(E, z))$$



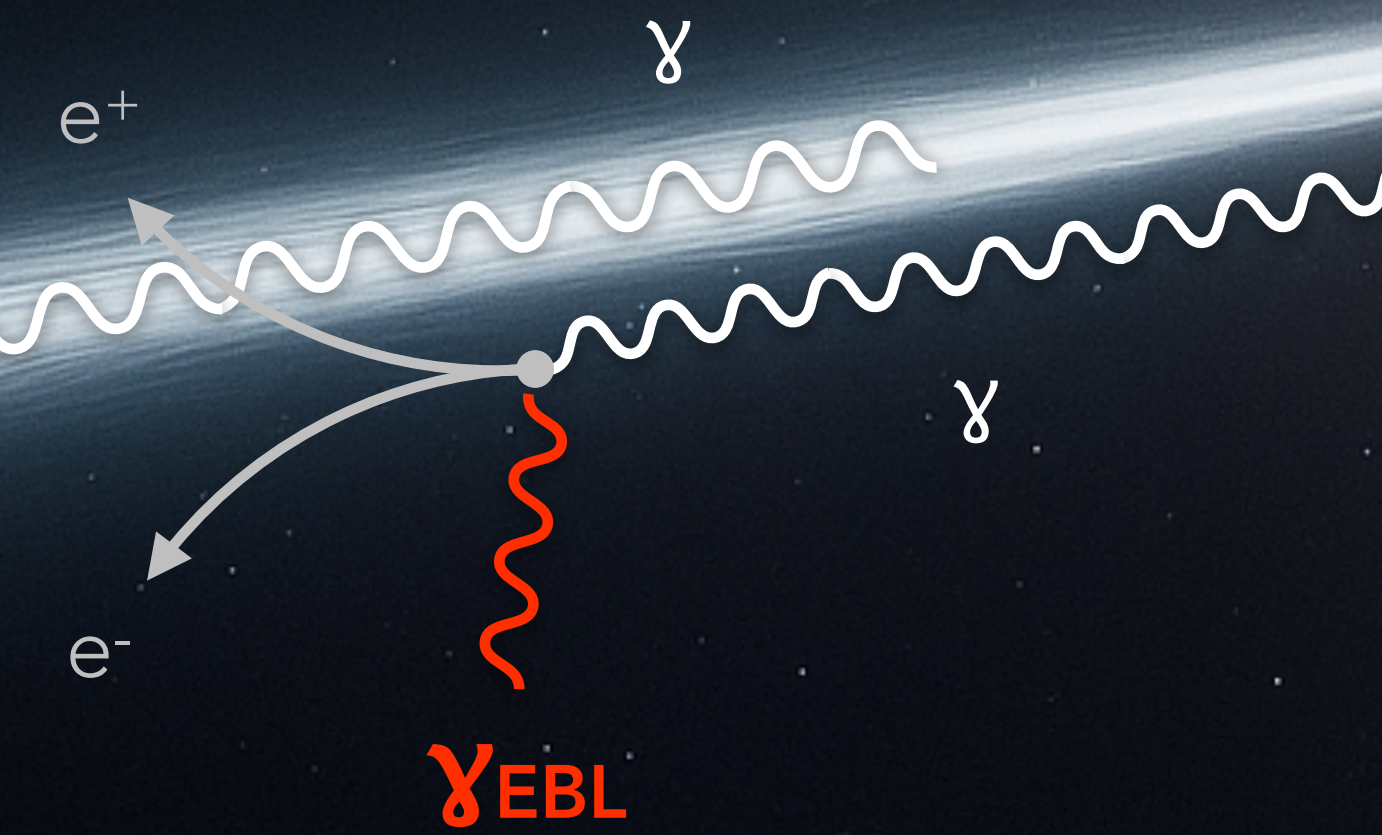
$\tau_{\gamma\gamma}(E, z)$ depends on (not precisely known)
intensity of extragalactic background light (EBL)
→ rely on EBL models

Transmission for selection of recent EBL models



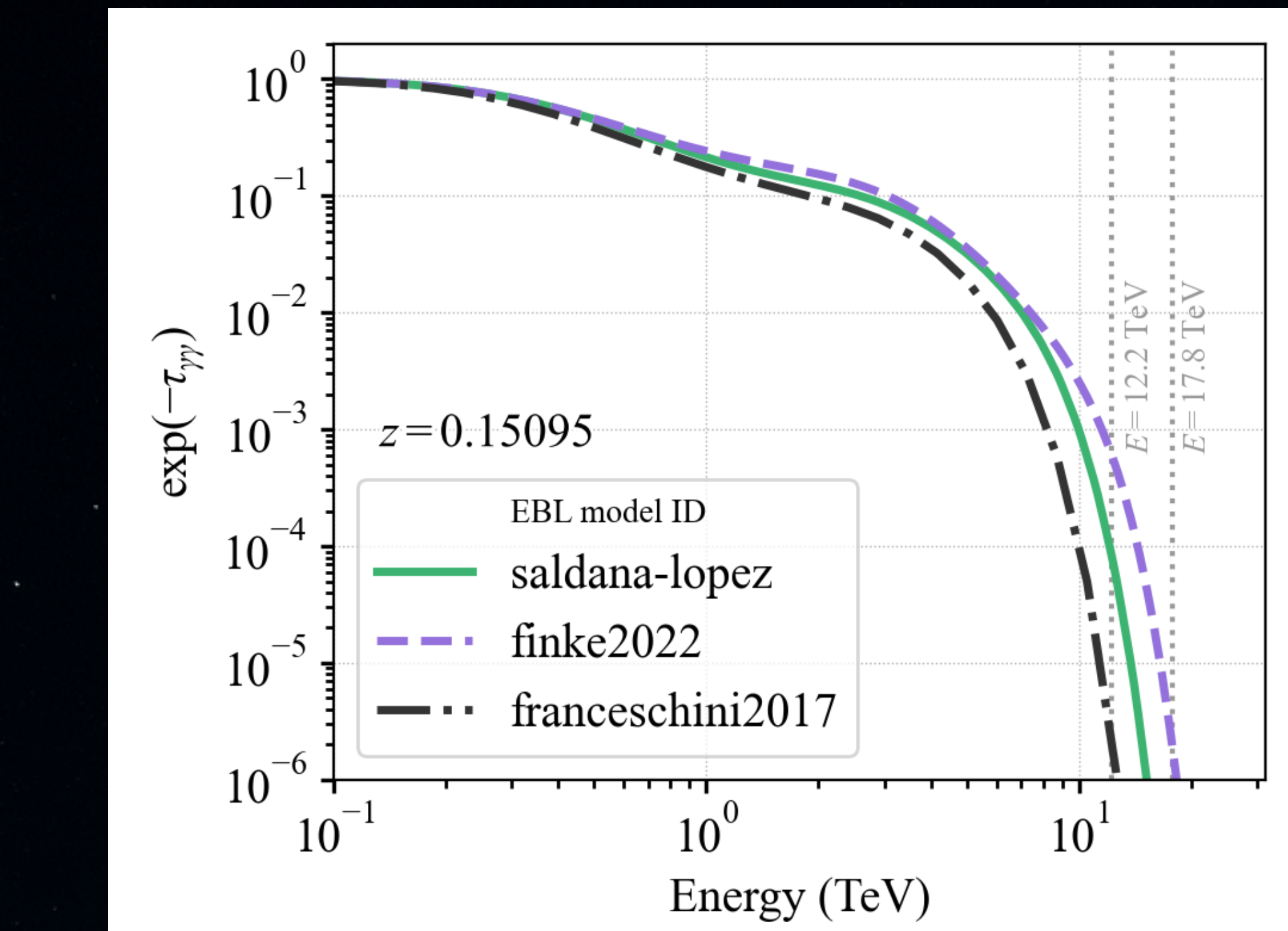
Absorption of VHE gamma rays

$$F_{\text{obs}} = F_{\text{int}} \exp(-\tau_{\gamma\gamma}(E, z))$$



$\tau_{\gamma\gamma}(E, z)$ depends on (not precisely known)
intensity of extragalactic background light (EBL)
→ rely on EBL models

Transmission for selection of recent EBL models

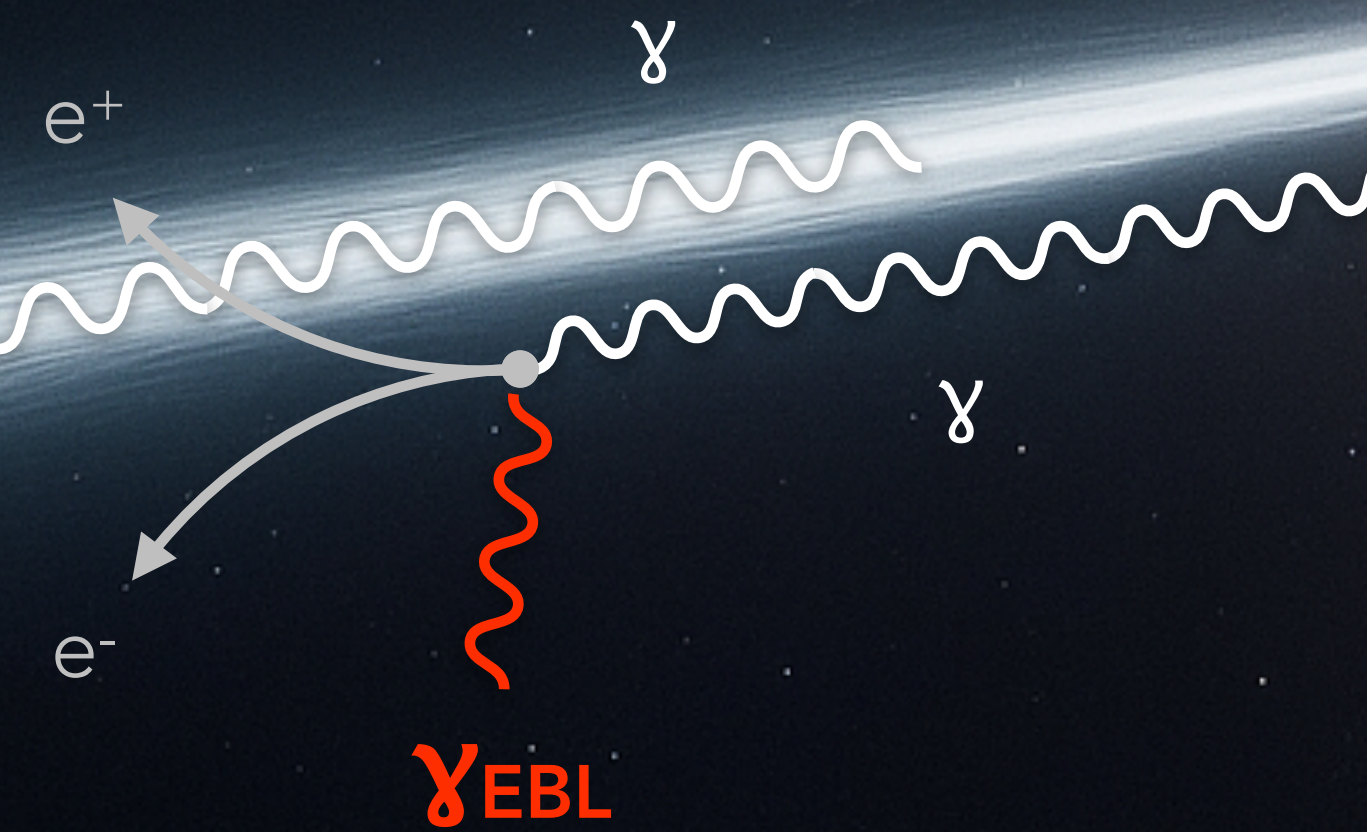


Absorption of VHE gamma rays

Depending on energy and EBL model:

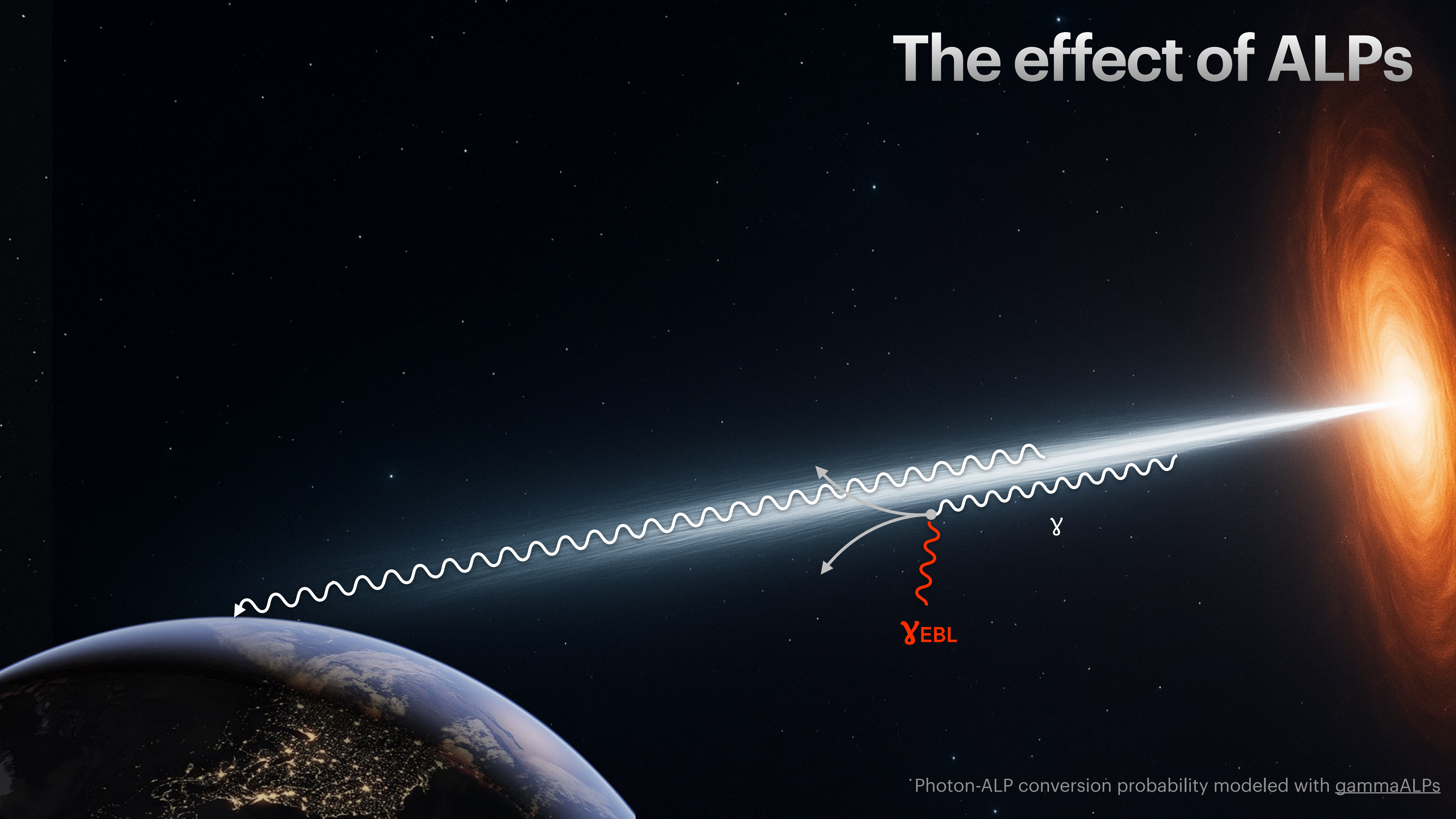
$$8 \times 10^{-13} \lesssim e^{-\tau_{\gamma\gamma}} \lesssim 6 \times 10^{-4}$$

$$F_{\text{obs}} = F_{\text{int}} \exp\left(-\tau_{\gamma\gamma}(E, z) \right)$$



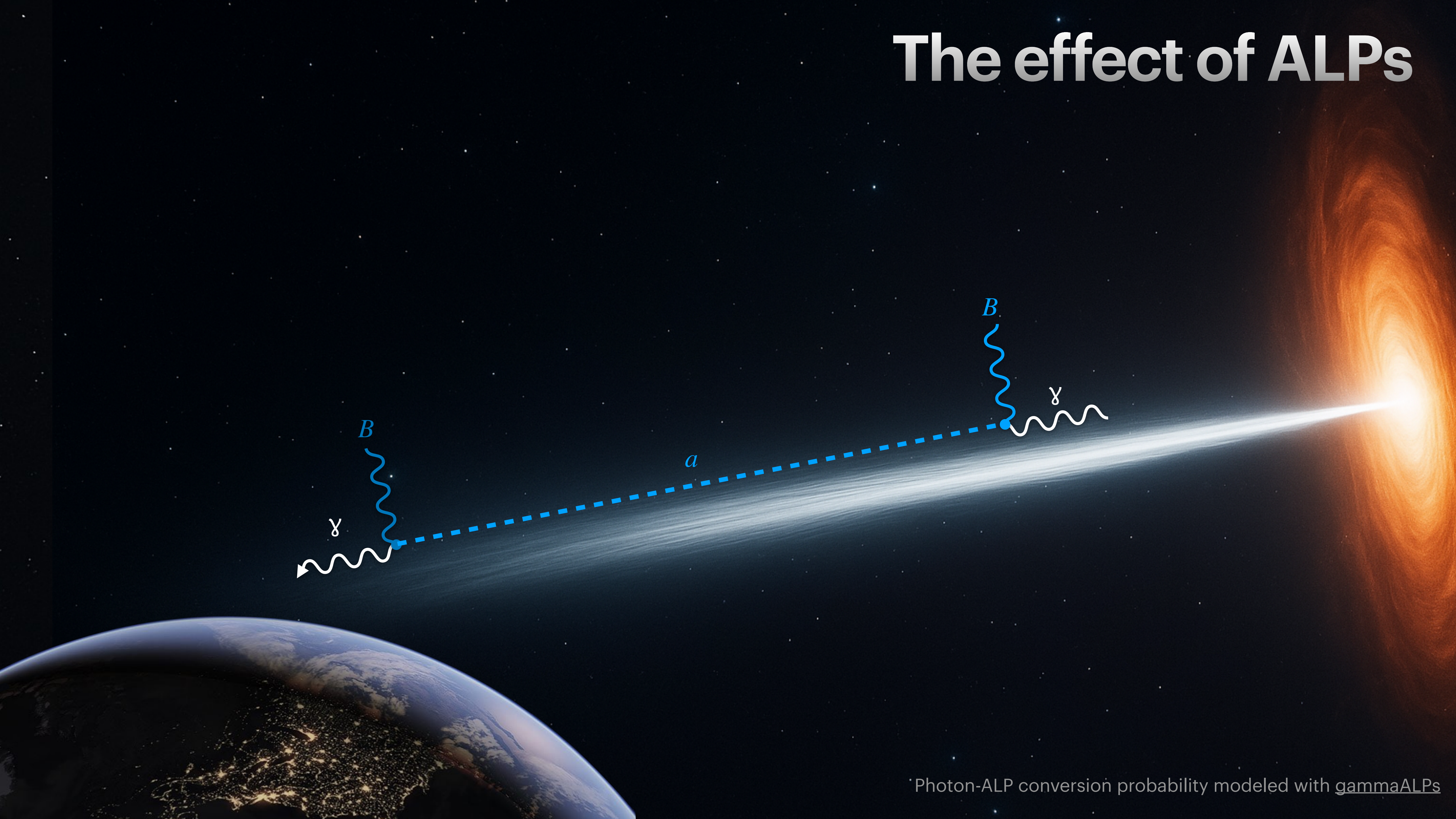
$\tau_{\gamma\gamma}(E, z)$ depends on (not precisely known)
intensity of extragalactic background light (EBL)
→ rely on EBL models

The effect of ALPs



Photon-ALP conversion probability modeled with [gammaALPs](#)

The effect of ALPs

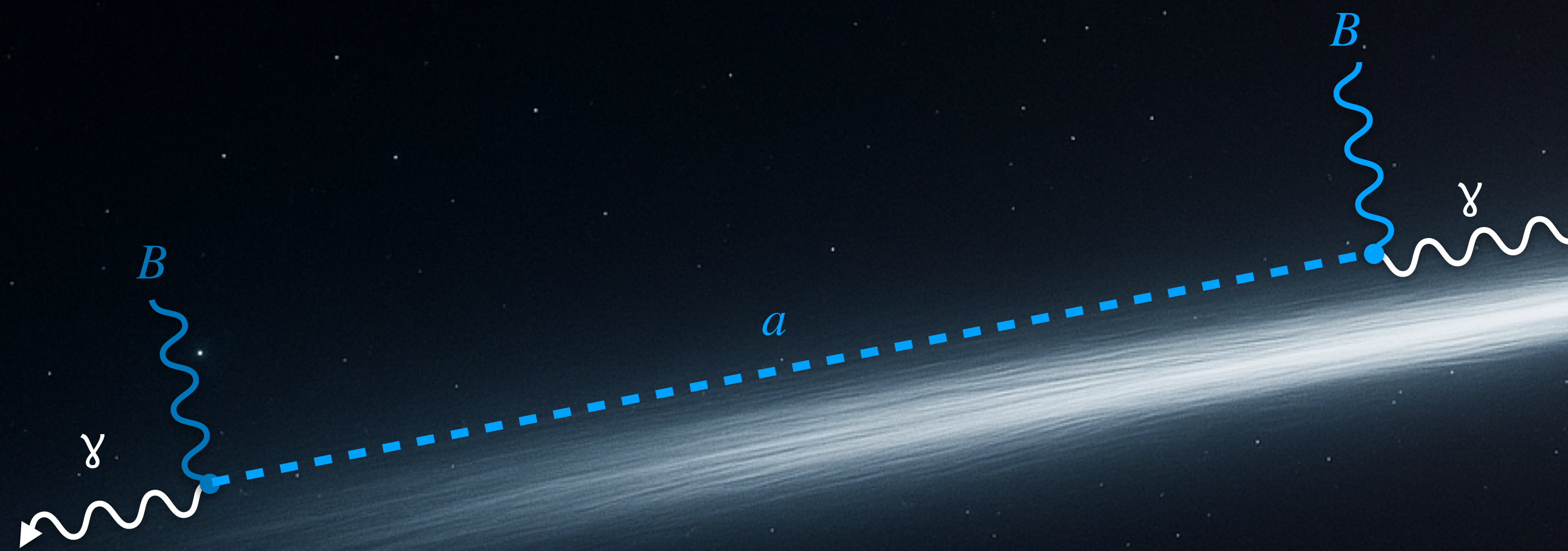


Photon-ALP conversion probability modeled with [gammaALPs](#)

The effect of ALPs

ALP production in B field of host galaxy

(Inside GRB, photon-ALP conversion negligible,
see, e.g., [Baktash, Horns, MM \(2022\)](#), [Galanti et al. \(2023\)](#))



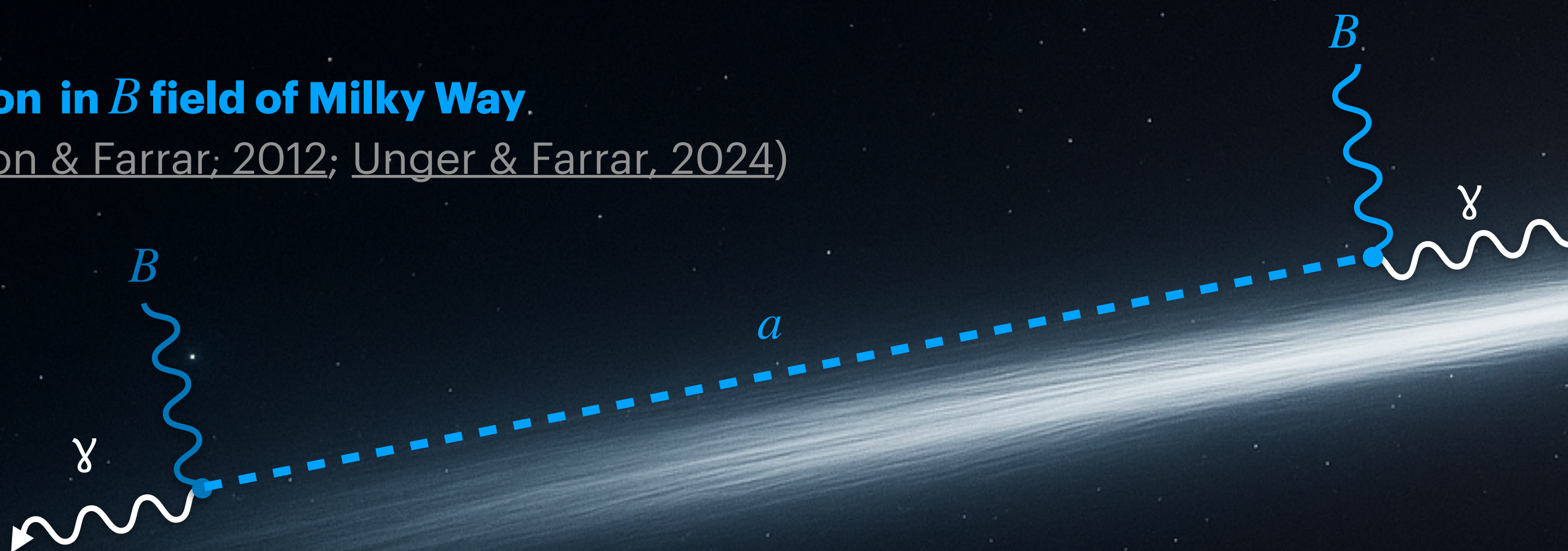
The effect of ALPs

ALP production in B field of host galaxy

(Inside GRB, photon-ALP conversion negligible,
see, e.g., [Baktash, Horns, MM \(2022\)](#), [Galanti et al. \(2023\)](#))

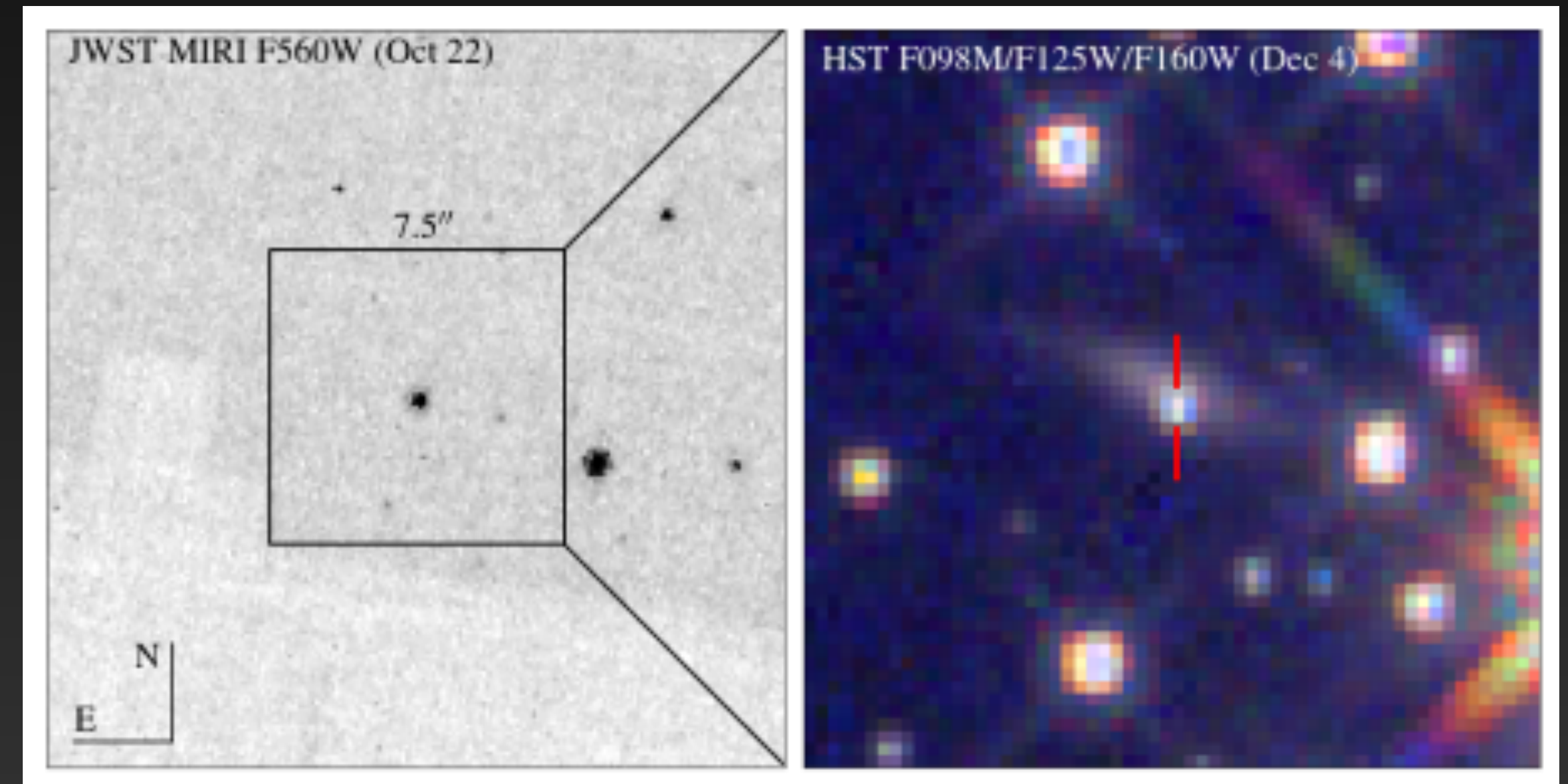
Reconversion in B field of Milky Way

(Assumed models: [Jansson & Farrar; 2012](#); [Unger & Farrar, 2024](#))



What do we know about the host galaxy of GRB221009A?

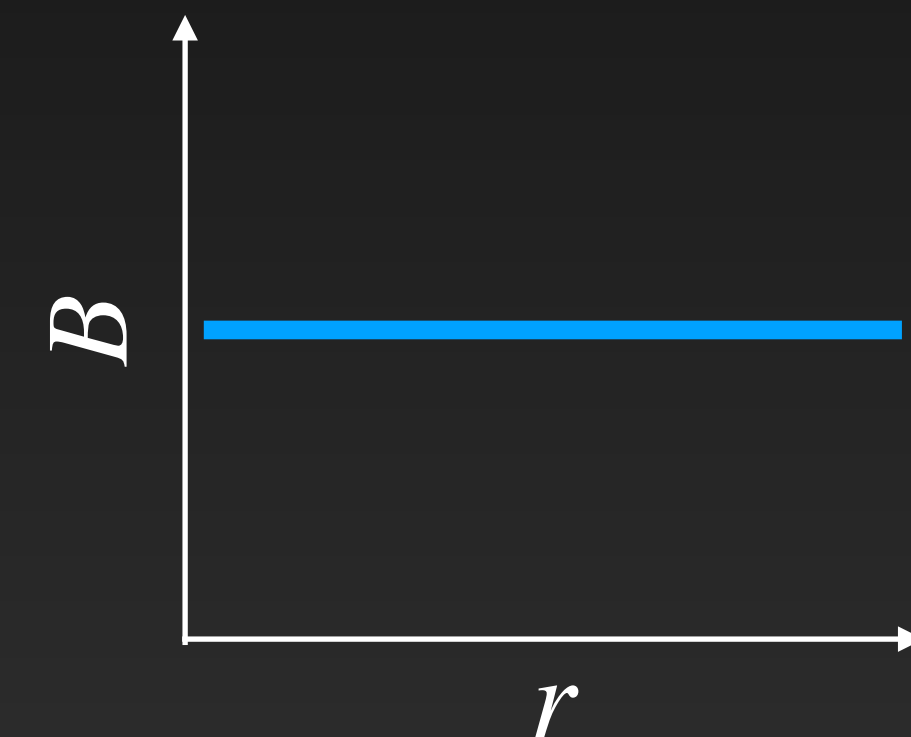
- Observed with JWST and HST
- Appears to be disc galaxy
- Observed edge-on
- Half-light radius $R_e = (2.45 \pm 0.20)\text{kpc}$
- GRB (projected) offset from center by 0.65 kpc
- Mass $\log(M/M_\odot) = 9.00^{+0.23}_{-0.47}$



Modeling the B field of the host galaxy

Constant \mathbf{B} field

[e.g. LHAASO Collaboration
2023, Sci. Adv., 9, 46]

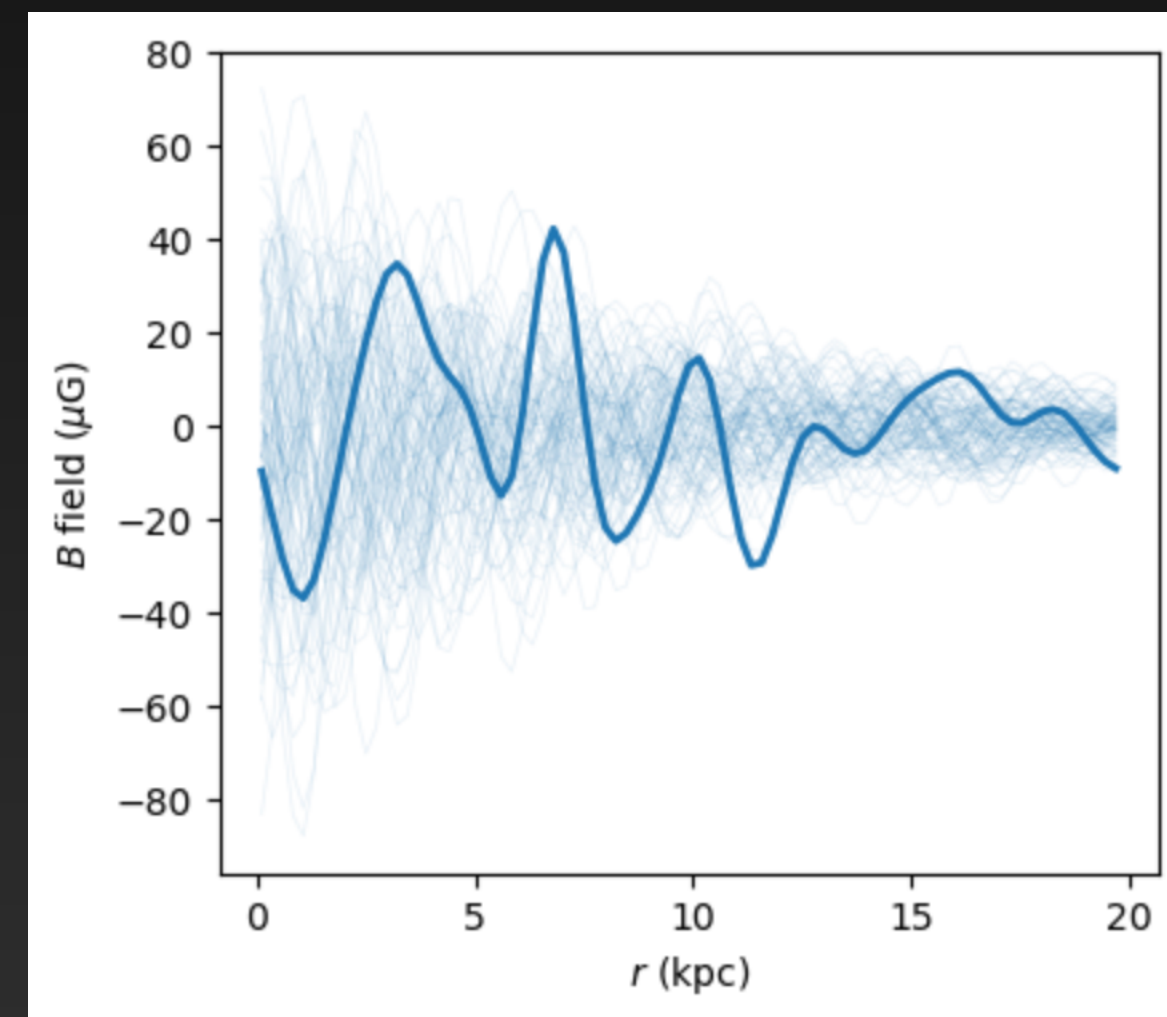


$$B_0 = 5\mu\text{G}$$

$$L_0 = 2R_e$$

Turbulent \mathbf{B} fields (spiral and starburst)

[Galanti et al. (2023)]

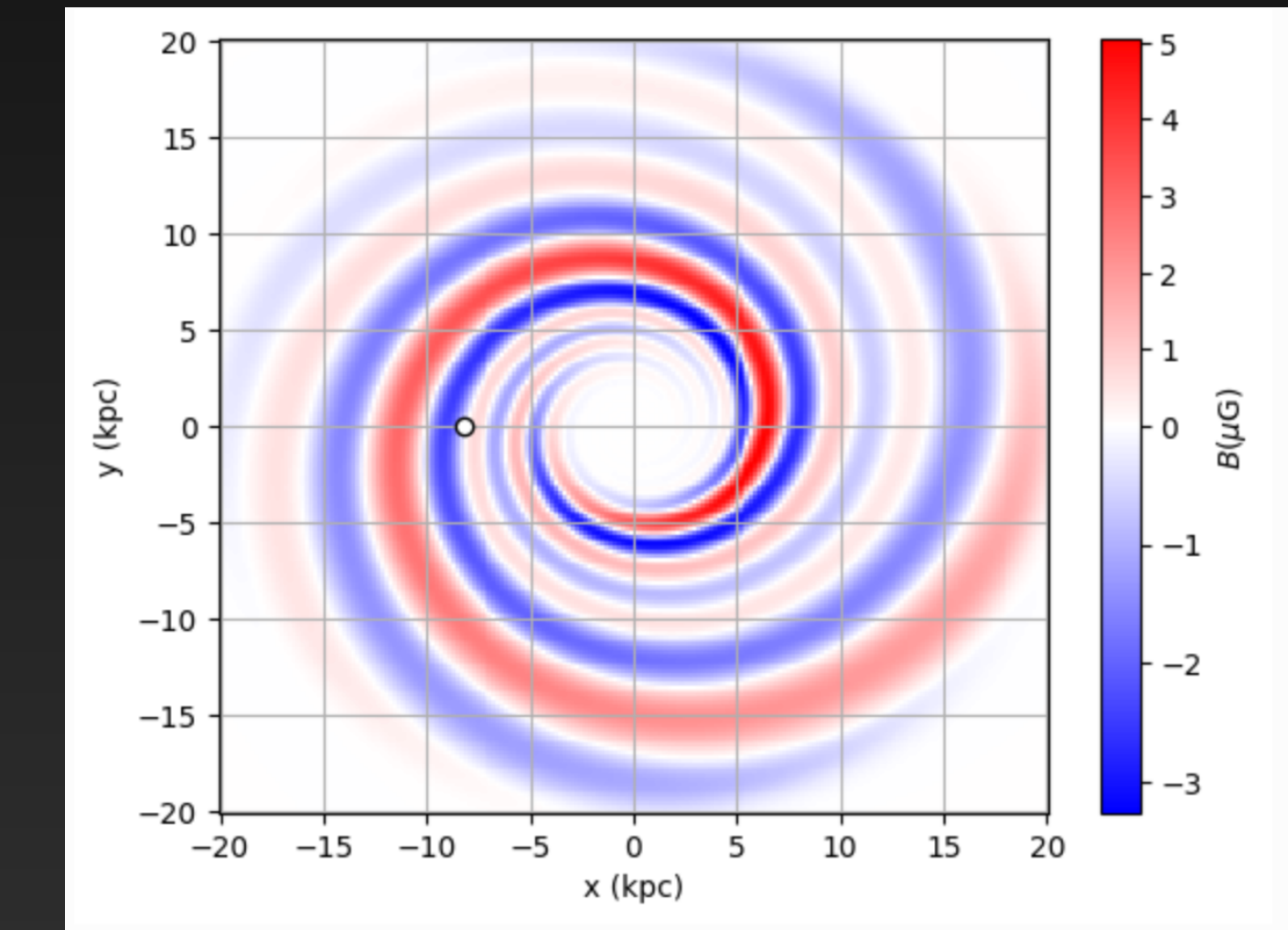


$$B_0 = (20,50)\mu\text{G} \times \exp(-r/r_0)$$

$$r_0 = (15,10) \text{ kpc}$$

Spiral-like galaxy

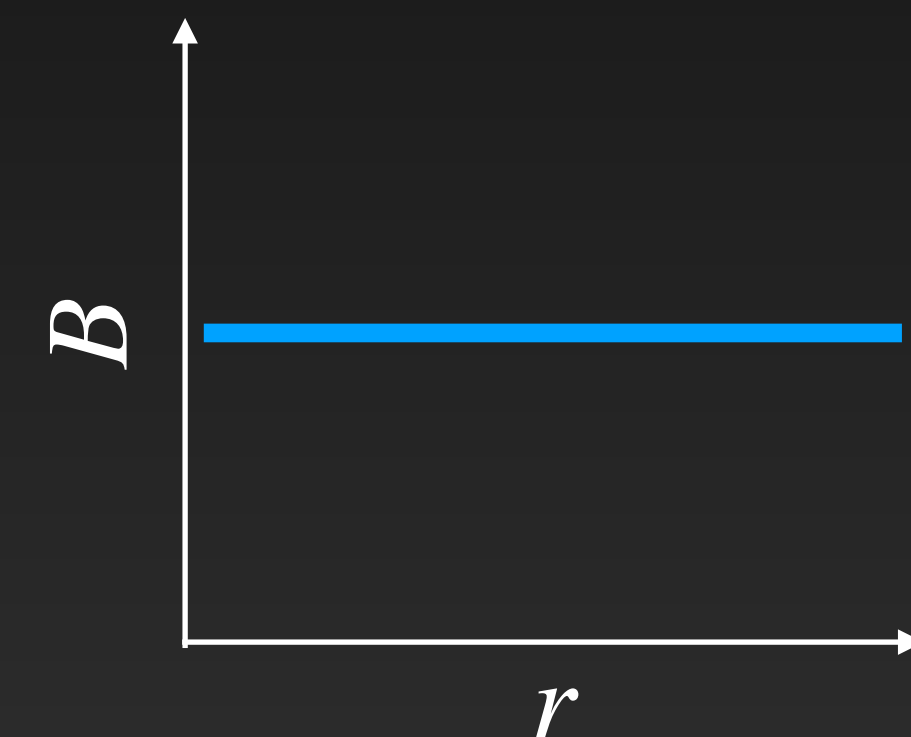
[e.g. Carenza & Marsh (2022),
Troitsky (2024)]



Modeling the B field of the host galaxy

Constant B field

[e.g. LHAASO Collaboration
2023, Sci. Adv., 9, 46]

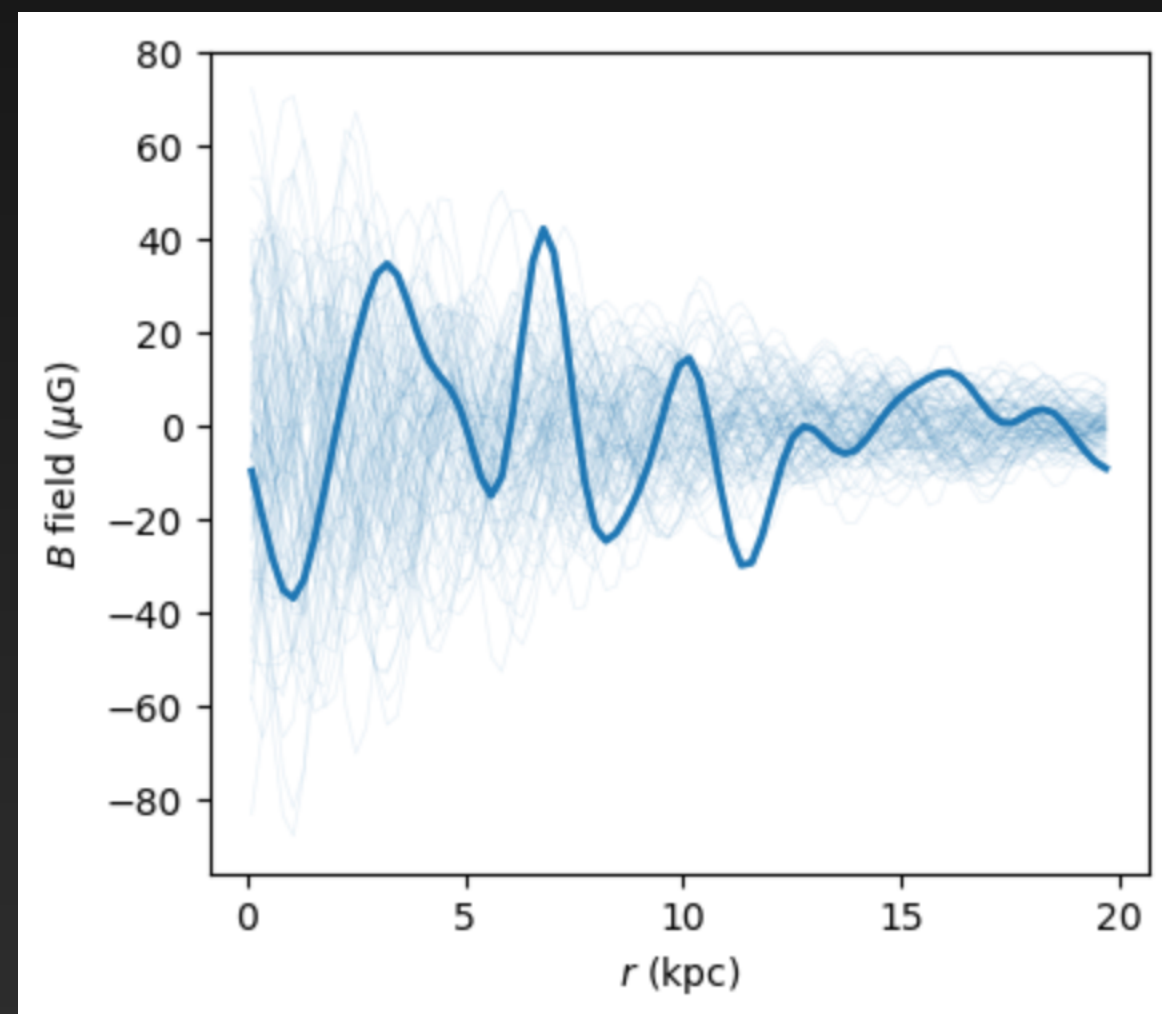


$$B_0 = 5\mu\text{G}$$

$$L_0 = 2R_e$$

Turbulent B fields (spiral and starburst)

[Galanti et al. (2023)]

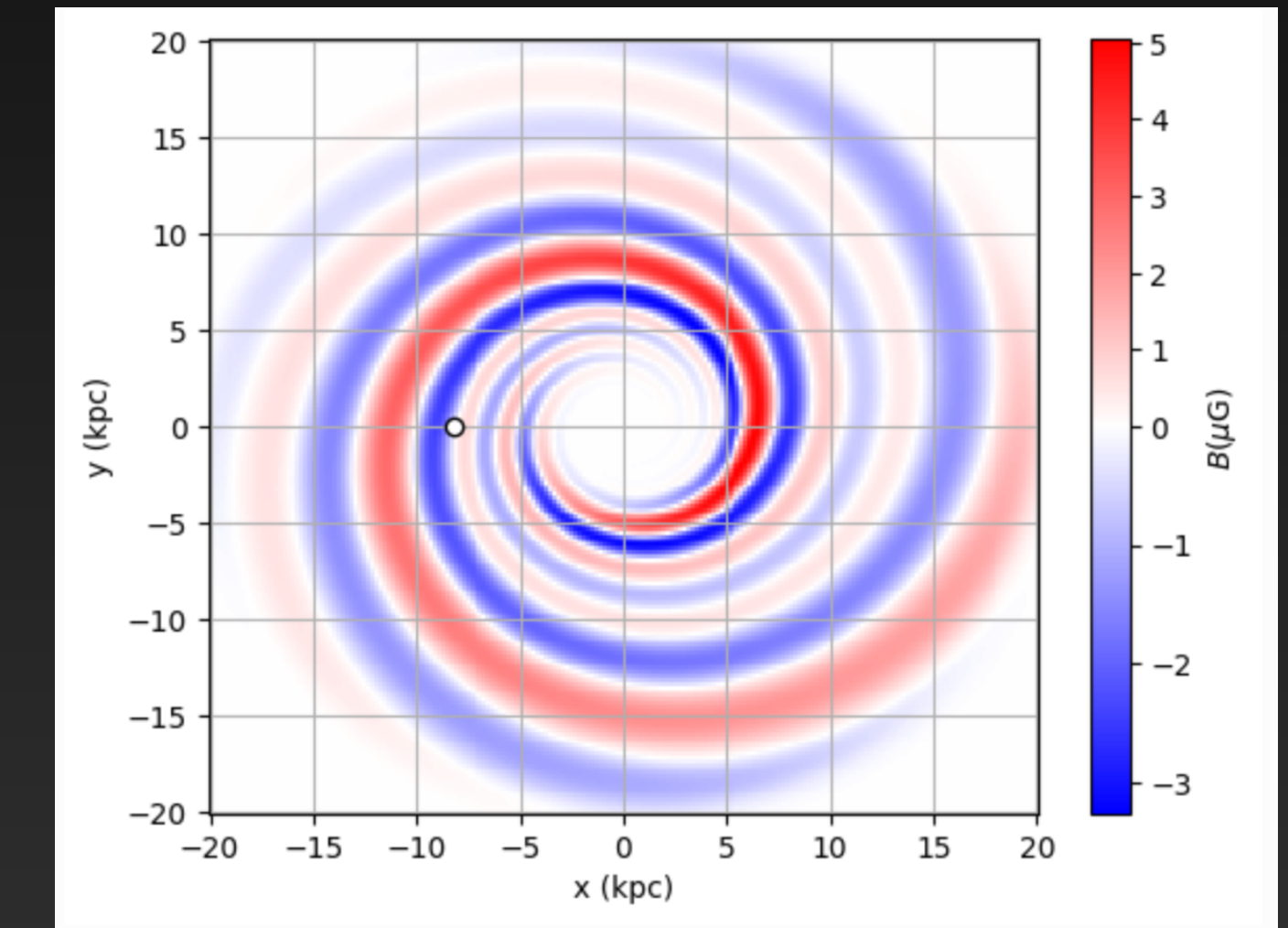


$$B_0 = (20,50)\mu\text{G} \times \exp(-r/r_0)$$

$$r_0 = (15,10)\text{kpc}$$

Spiral-like galaxy

[e.g. Carenza & Marsh (2022),
Troitsky (2024)]

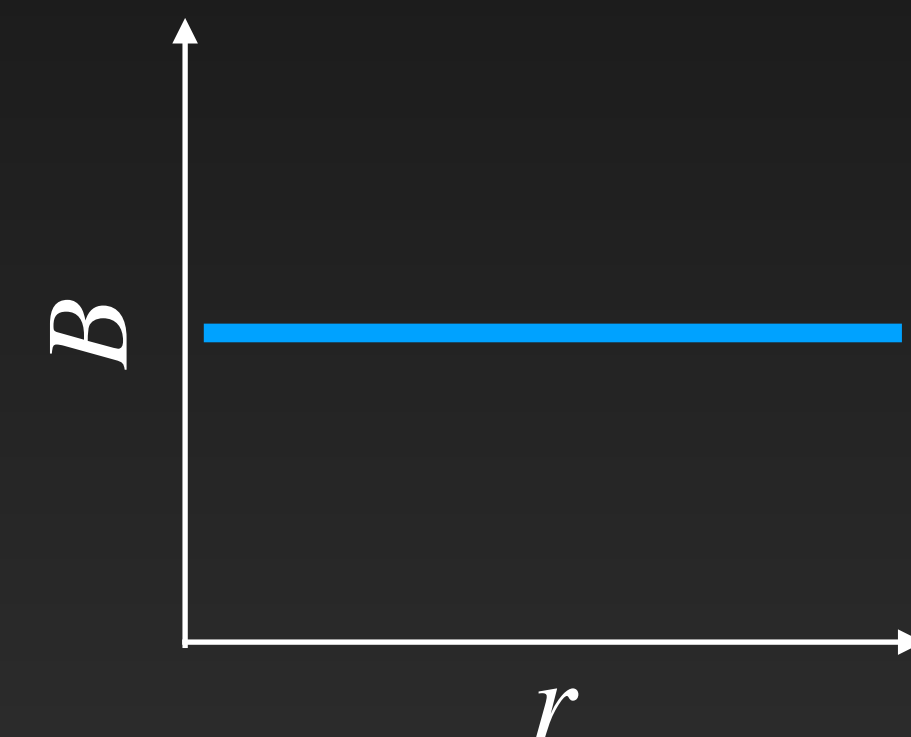


We test all 4 scenarios

Modeling the B field of the host galaxy

Constant B field

[e.g. LHAASO Collaboration
2023, Sci. Adv., 9, 46]

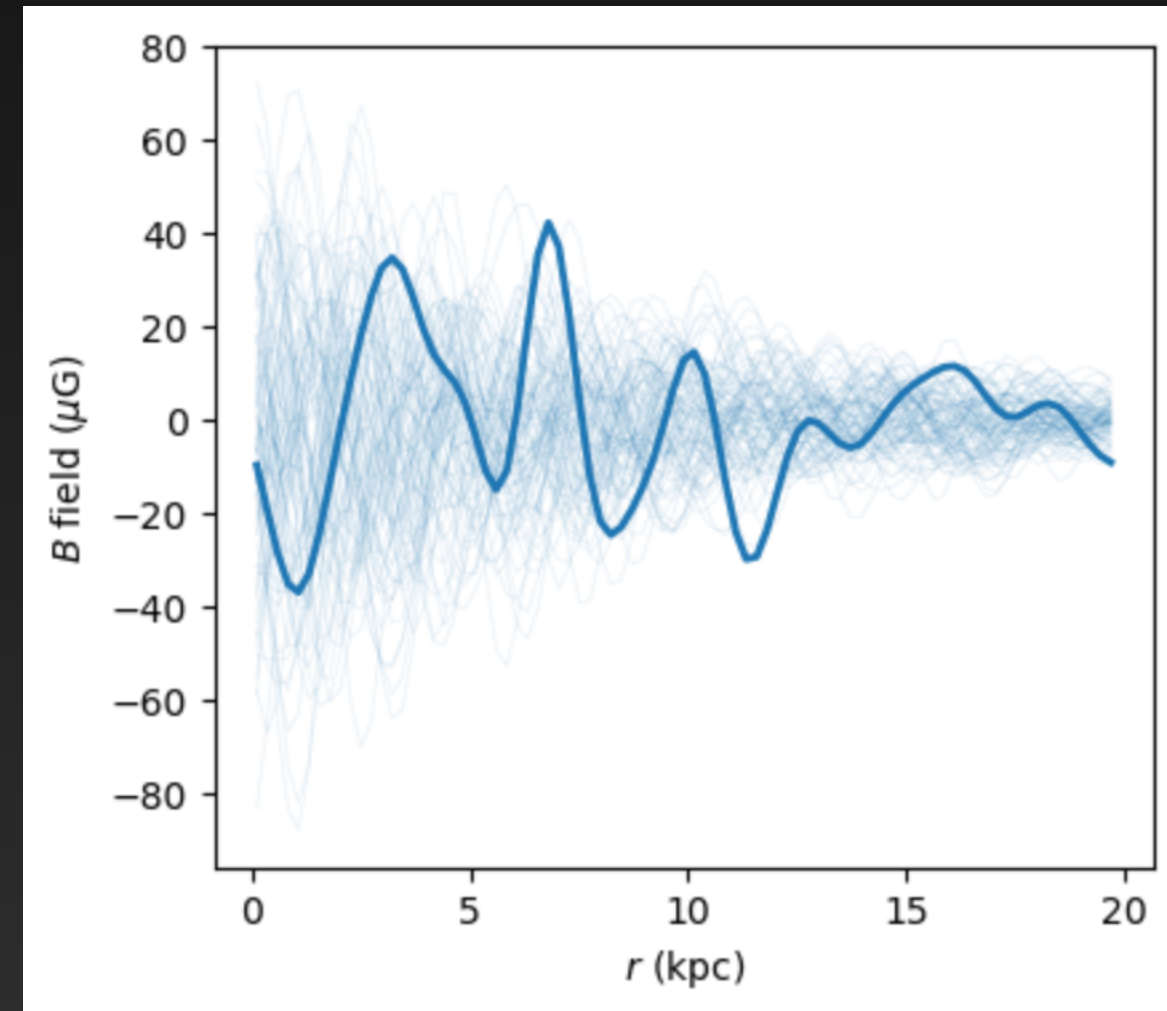


$$B_0 = 5\mu\text{G}$$

$$L_0 = 2R_e$$

Turbulent B fields (spiral and starburst)

[Galanti et al. (2023)]



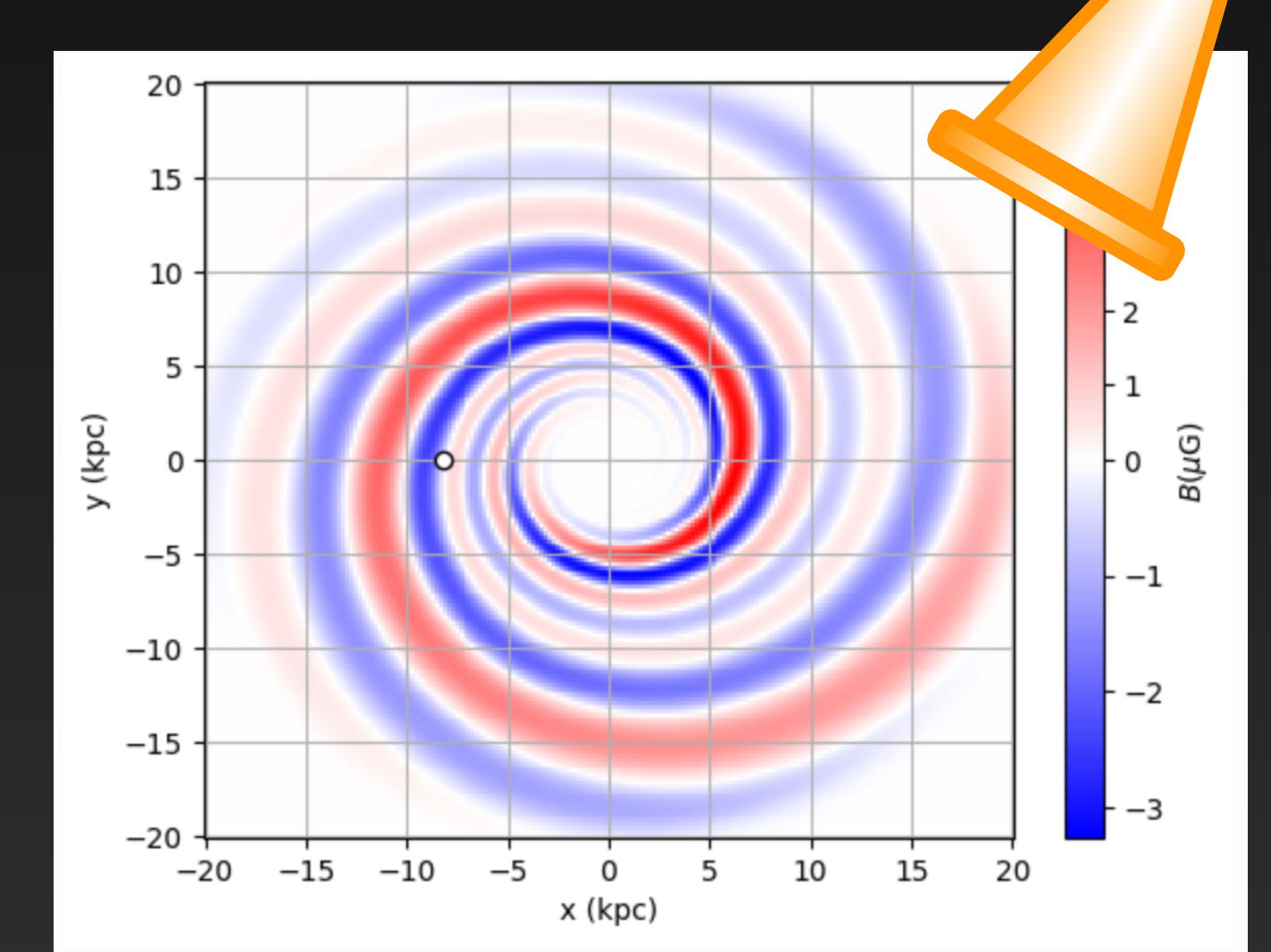
$$B_0 = (20,50)\mu\text{G} \times \exp(-r/r_0)$$

$$r_0 = (15,10) \text{ kpc}$$

Spiral-like galaxy

[e.g. Carenza & Marsh (2022),
Troitsky (2024)]

Work in progress



We test all 4 scenarios

Statistical analysis

Statistical analysis

- LHAASO errorbars asymmetric, flux values given by $y_i^{+\sigma_i^{\text{pos}}}_{-\sigma_i^{\text{neg}}}$

LHAASO data:
EPL or LP reconstruction

Statistical analysis

LHAASO data:
EPL or LP reconstruction

- LHAASO errorbars asymmetric, flux values given by $y_i^{+\sigma_i^{\text{pos}}}_{-\sigma_i^{\text{neg}}}$
- Model:

Statistical analysis

LHAASO data:
EPL or LP reconstruction

- LHAASO errorbars asymmetric, flux values given by $y_i^{+\sigma_i^{\text{pos}}}_{-\sigma_i^{\text{neg}}}$
- Model:

$$F(E) = N \left(\frac{E}{E_0} \right)^{-\alpha - \beta \ln(E/E_0)} P_{\gamma\gamma}(E, m_a, g_{a\gamma}, B)$$

Statistical analysis

- LHAASO errorbars asymmetric, flux values given by $y_i^{+\sigma_i^{\text{pos}}}_{-\sigma_i^{\text{neg}}}$
- Model:

$$F(E) = N \left(\frac{E}{E_0} \right)^{-\alpha - \beta \ln(E/E_0)} P_{\gamma\gamma}(E, m_a, g_{a\gamma}, B)$$

LHAASO data:
EPL or LP reconstruction

Milky B-field model:
Jansson & Farrar (2012) or
Unger & Farrar (2024)
base model

Statistical analysis

- LHAASO errorbars asymmetric, flux values given by $y_i^{+\sigma_i^{\text{pos}}}_{-\sigma_i^{\text{neg}}}$

- Model:

$$F(E) = N \left(\frac{E}{E_0} \right)^{-\alpha - \beta \ln(E/E_0)} P_{\gamma\gamma}(E, m_a, g_{a\gamma}, B)$$

- No ALPs case: $P_{\gamma\gamma} \rightarrow \exp(-\tau_{\gamma\gamma})$ for $g_{a\gamma} \rightarrow 0$

LHAASO data:

EPL or LP reconstruction

Milky B-field model:

Jansson & Farrar (2012) or
Unger & Farrar (2024)
base model

EBL model:

Finke et al. (2022) or
Saldana-Lopez et al.
(2021) or Franceschini et
al. (2017)

Statistical analysis

- LHAASO errorbars asymmetric, flux values given by $y_i^{+\sigma_i^{\text{pos}}}_{-\sigma_i^{\text{neg}}}$

- Model:

$$F(E) = N \left(\frac{E}{E_0} \right)^{-\alpha - \beta \ln(E/E_0)} P_{\gamma\gamma}(E, m_a, g_{a\gamma}, B)$$

- No ALPs case: $P_{\gamma\gamma} \rightarrow \exp(-\tau_{\gamma\gamma})$ for $g_{a\gamma} \rightarrow 0$

LHAASO data:

EPL or LP reconstruction

Milky B -field model:

Jansson & Farrar (2012) or
Unger & Farrar (2024)
base model

EBL model:

Finke et al. (2022) or
Saldana-Lopez et al.
(2021) or Franceschini et
al. (2017)

Host galaxy B field:

Constant

Turbulent (spiral /
starburst)

Spiral model

Statistical analysis

- LHAASO errorbars asymmetric, flux values given by $y_i^{+\sigma_i^{\text{pos}}}_{-\sigma_i^{\text{neg}}}$

- Model:

$$F(E) = N \left(\frac{E}{E_0} \right)^{-\alpha - \beta \ln(E/E_0)} P_{\gamma\gamma}(E, m_a, g_{a\gamma}, B)$$

- No ALPs case: $P_{\gamma\gamma} \rightarrow \exp(-\tau_{\gamma\gamma})$ for $g_{a\gamma} \rightarrow 0$
- We use an asymmetric χ^2 :

LHAASO data:

EPL or LP reconstruction

Milky B -field model:

Jansson & Farrar (2012) or
Unger & Farrar (2024)
base model

EBL model:

Finke et al. (2022) or
Saldana-Lopez et al.
(2021) or Franceschini et
al. (2017)

Host galaxy B field:

Constant

Turbulent (spiral /
starburst)

Spiral model

Statistical analysis

- LHAASO errorbars asymmetric, flux values given by $y_i^{+\sigma_i^{\text{pos}}}_{-\sigma_i^{\text{neg}}}$

- Model:

$$F(E) = N \left(\frac{E}{E_0} \right)^{-\alpha - \beta \ln(E/E_0)} P_{\gamma\gamma}(E, m_a, g_{a\gamma}, B)$$

- No ALPs case: $P_{\gamma\gamma} \rightarrow \exp(-\tau_{\gamma\gamma})$ for $g_{a\gamma} \rightarrow 0$
- We use an asymmetric χ^2 :

$$\chi^2 = \sum_i^N \frac{(y_i - F(E_i))^2}{\sigma_i^2}, \quad \sigma_i = \begin{cases} \sigma_i^{\text{pos}}, & y_i - F(E_i) > 0 \\ \sigma_i^{\text{neg}}, & y_i - F(E_i) \leq 0 \end{cases}$$

LHAASO data:

EPL or LP reconstruction

Milky B-field model:

Jansson & Farrar (2012) or
Unger & Farrar (2024)
base model

EBL model:

Finke et al. (2022) or
Saldana-Lopez et al.
(2021) or Franceschini et
al. (2017)

Host galaxy B field:

Constant

Turbulent (spiral /
starburst)

Spiral model

Statistical analysis

- LHAASO errorbars asymmetric, flux values given by $y_i^{+\sigma_i^{\text{pos}}}_{-\sigma_i^{\text{neg}}}$

- Model:

$$F(E) = N \left(\frac{E}{E_0} \right)^{-\alpha - \beta \ln(E/E_0)} P_{\gamma\gamma}(E, m_a, g_{a\gamma}, B)$$

- No ALPs case: $P_{\gamma\gamma} \rightarrow \exp(-\tau_{\gamma\gamma})$ for $g_{a\gamma} \rightarrow 0$

- We use an asymmetric χ^2 :

$$\chi^2 = \sum_i^N \frac{(y_i - F(E_i))^2}{\sigma_i^2}, \quad \sigma_i = \begin{cases} \sigma_i^{\text{pos}}, & y_i - F(E_i) > 0 \\ \sigma_i^{\text{neg}}, & y_i - F(E_i) \leq 0 \end{cases}$$

- ALPs preferred? $\text{TS} = \chi^2(g_{a\gamma} = 0) - \chi^2(m_a, g_{a\gamma}) > 0$

LHAASO data:

EPL or LP reconstruction

Milky B-field model:

Jansson & Farrar (2012) or
Unger & Farrar (2024)
base model

EBL model:

Finke et al. (2022) or
Saldana-Lopez et al.
(2021) or Franceschini et
al. (2017)

Host galaxy B field:

Constant
Turbulent (spiral /
starburst)
Spiral model

Statistical analysis

- LHAASO errorbars asymmetric, flux values given by $y_i^{+\sigma_i^{\text{pos}}}_{-\sigma_i^{\text{neg}}}$

- Model:

$$F(E) = N \left(\frac{E}{E_0} \right)^{-\alpha - \beta \ln(E/E_0)} P_{\gamma\gamma}(E, m_a, g_{a\gamma}, B)$$

- No ALPs case: $P_{\gamma\gamma} \rightarrow \exp(-\tau_{\gamma\gamma})$ for $g_{a\gamma} \rightarrow 0$
- We use an asymmetric χ^2 :

$$\chi^2 = \sum_i^N \frac{(y_i - F(E_i))^2}{\sigma_i^2}, \quad \sigma_i = \begin{cases} \sigma_i^{\text{pos}}, & y_i - F(E_i) > 0 \\ \sigma_i^{\text{neg}}, & y_i - F(E_i) \leq 0 \end{cases}$$

- ALPs preferred? $\text{TS} = \chi^2(g_{a\gamma} = 0) - \chi^2(m_a, g_{a\gamma}) > 0$
- Best-fit parameters / constraints: $\Delta\chi^2 = \chi^2(m_a, g_{a\gamma}) - \min(\chi^2(m_a, g_{a\gamma}))$

LHAASO data:

EPL or LP reconstruction

Milky B-field model:

Jansson & Farrar (2012) or
Unger & Farrar (2024)
base model

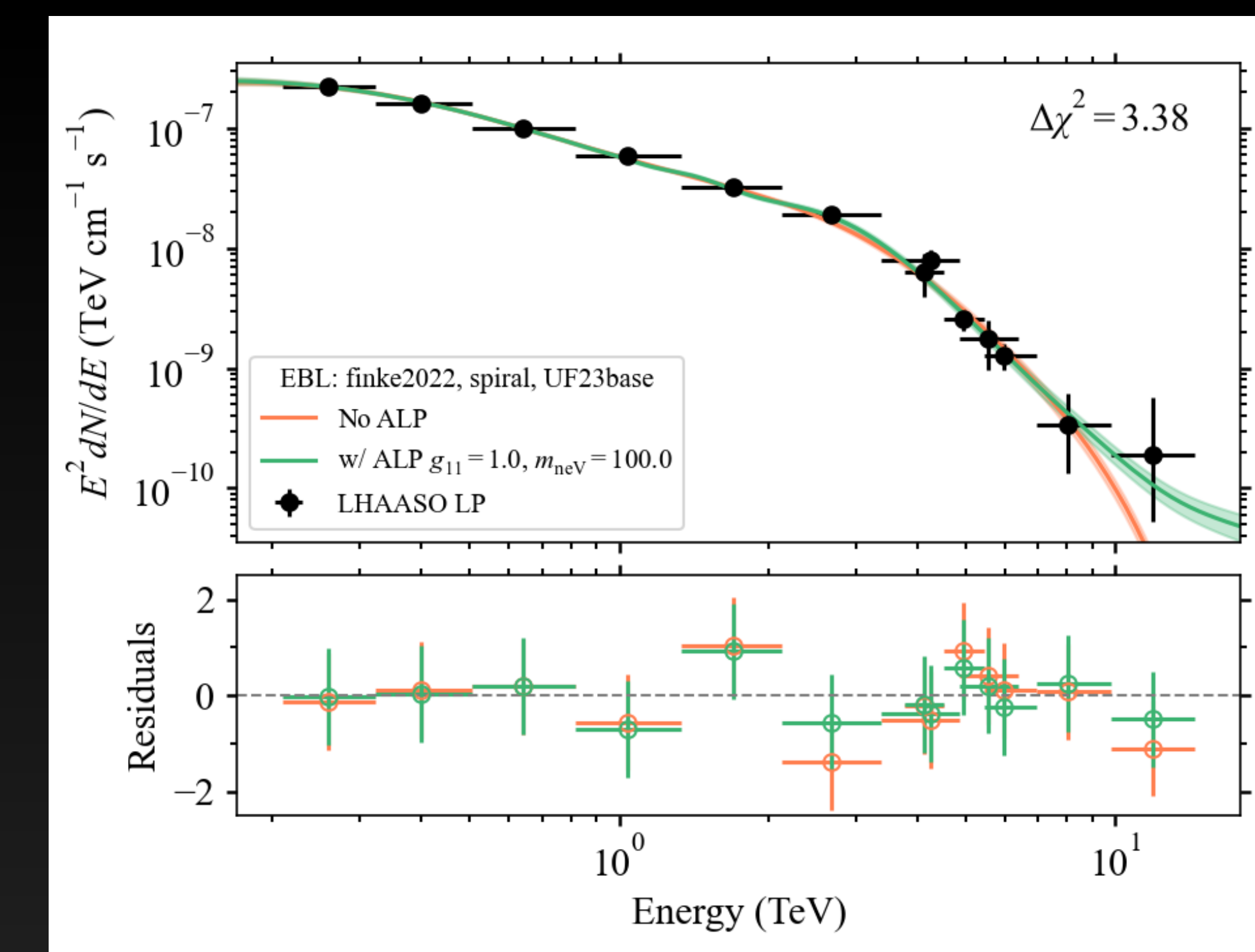
EBL model:

Finke et al. (2022) or
Saldana-Lopez et al.
(2021) or Franceschini et
al. (2017)

Host galaxy B field:

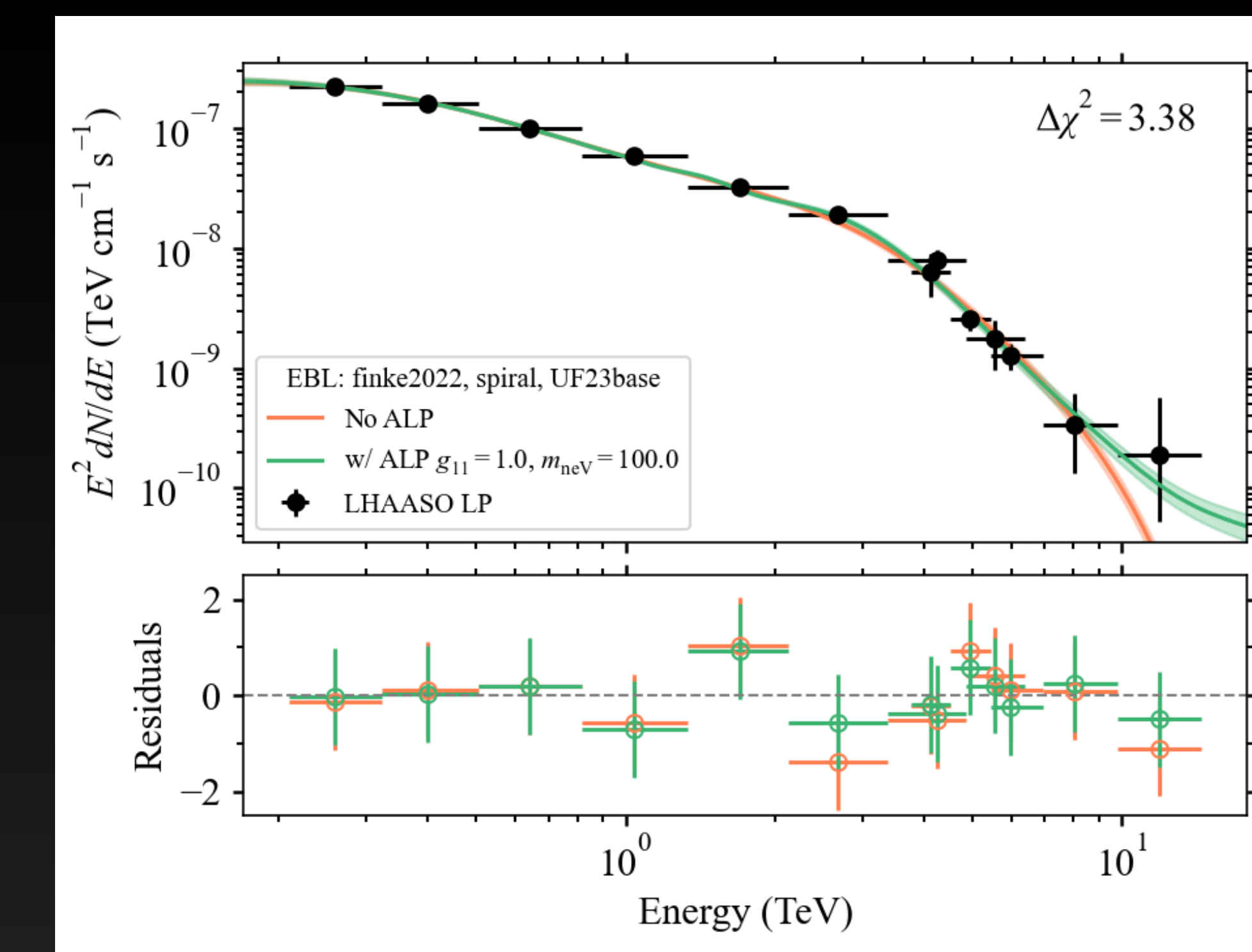
Constant
Turbulent (spiral /
starburst)
Spiral model

Results - General trends



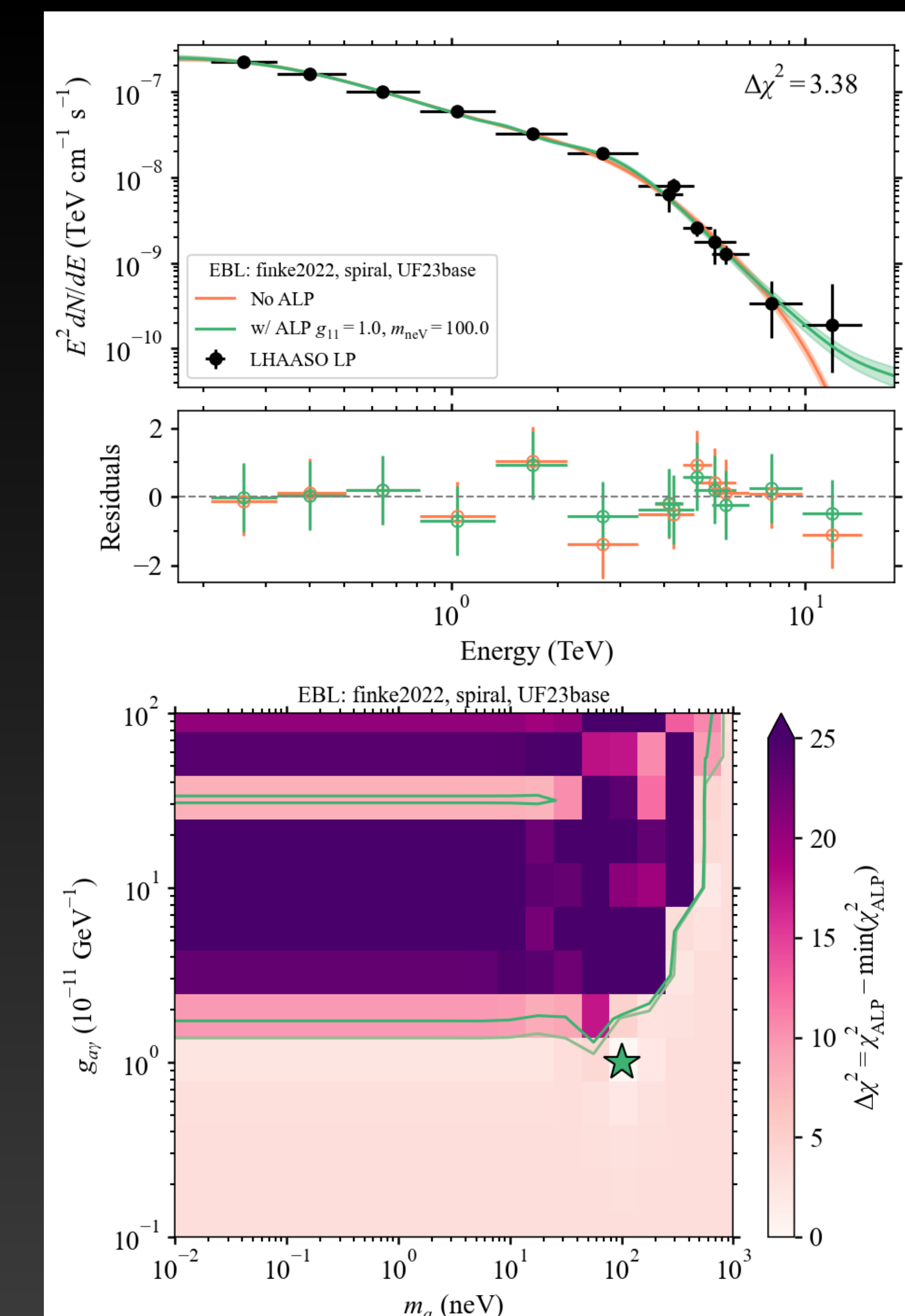
Results - General trends

- Almost all model combinations result in no preference for ALPs, $p_{local} < 2\sigma$ for LP and EPL reconstructed data



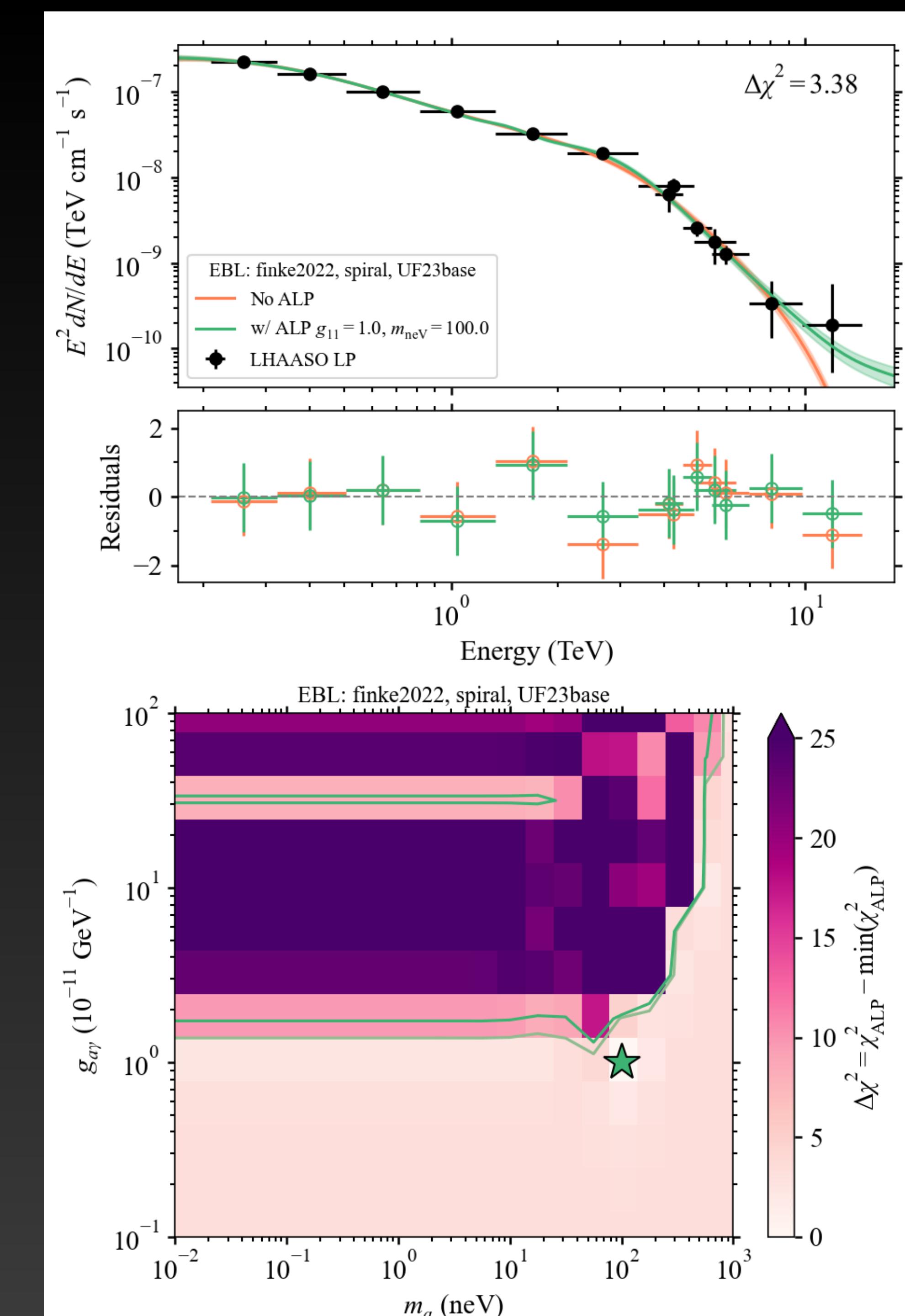
Results - General trends

- Almost all model combinations result in no preference for ALPs, $p_{local} < 2\sigma$ for LP and EPL reconstructed data
- Most models yield very similar constraints



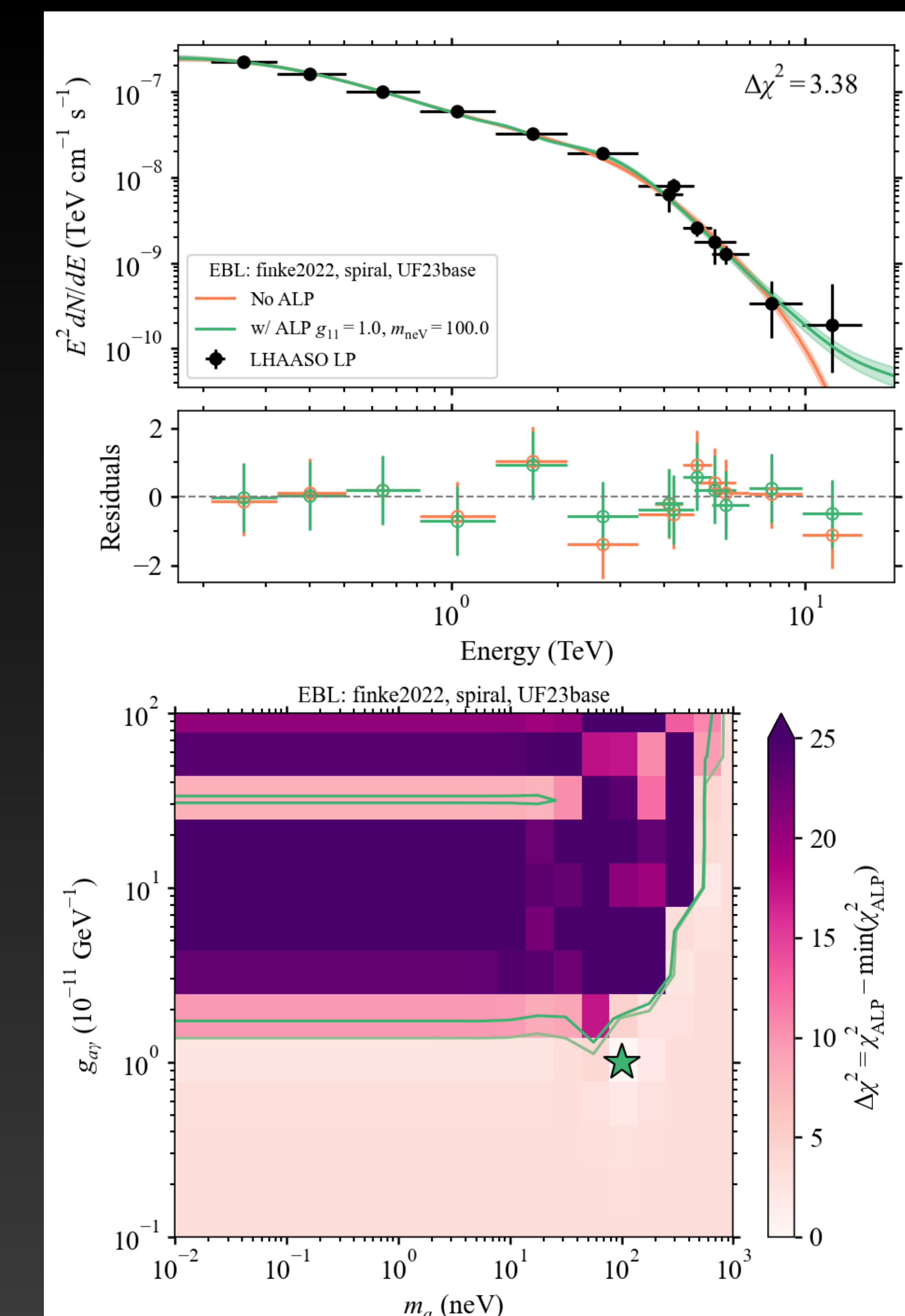
Results - General trends

- Almost all model combinations result in no preference for ALPs, $p_{local} < 2\sigma$ for LP and EPL reconstructed data
- Most models yield very similar constraints
- UF23 model results in slightly higher preferences for ALPs



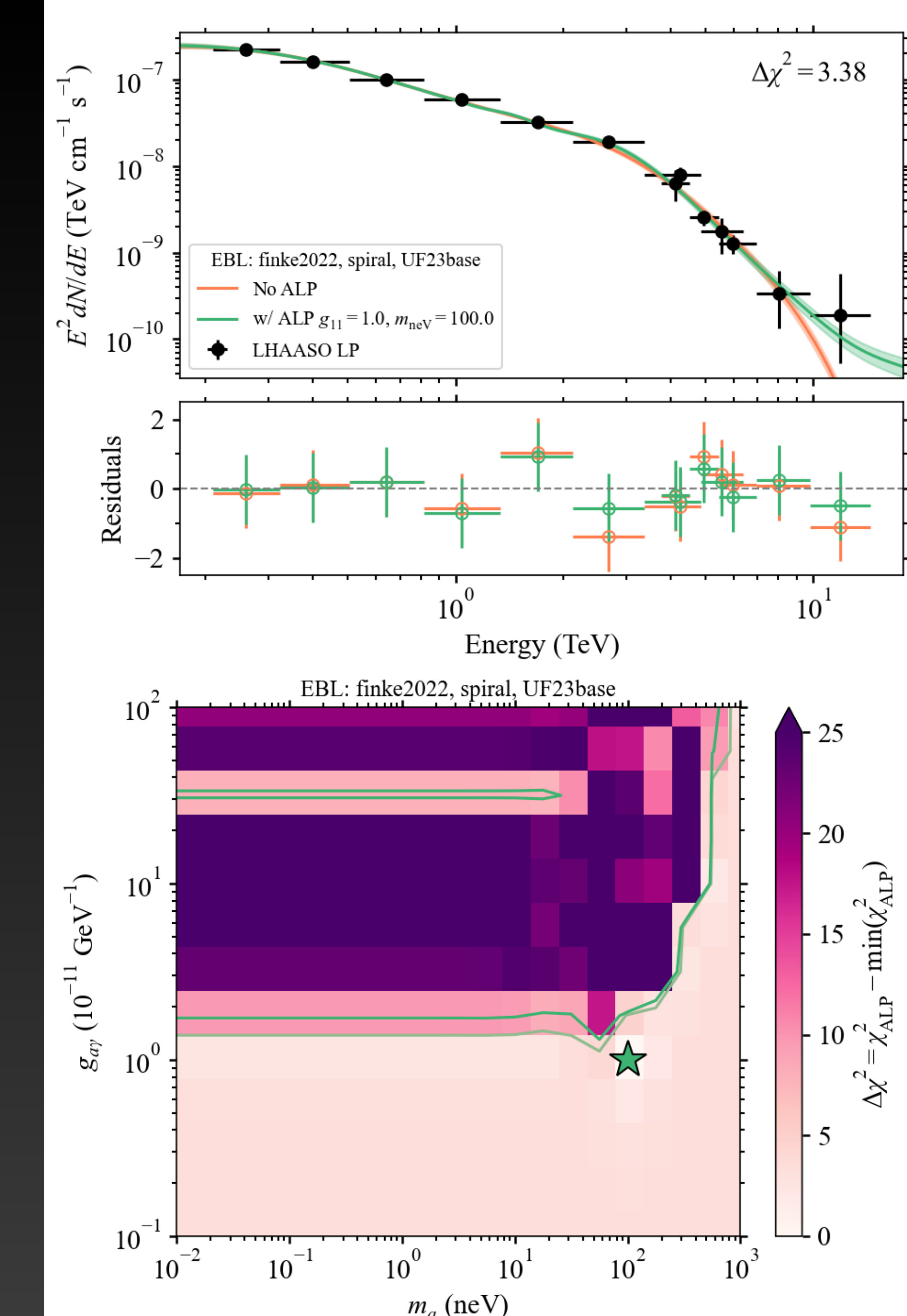
Results - General trends

- Almost all model combinations result in no preference for ALPs, $p_{local} < 2\sigma$ for LP and EPL reconstructed data
- Most models yield very similar constraints
- UF23 model results in slightly higher preferences for ALPs
- EBL with stronger absorption results in slightly higher preferences for ALPs



Results - General trends

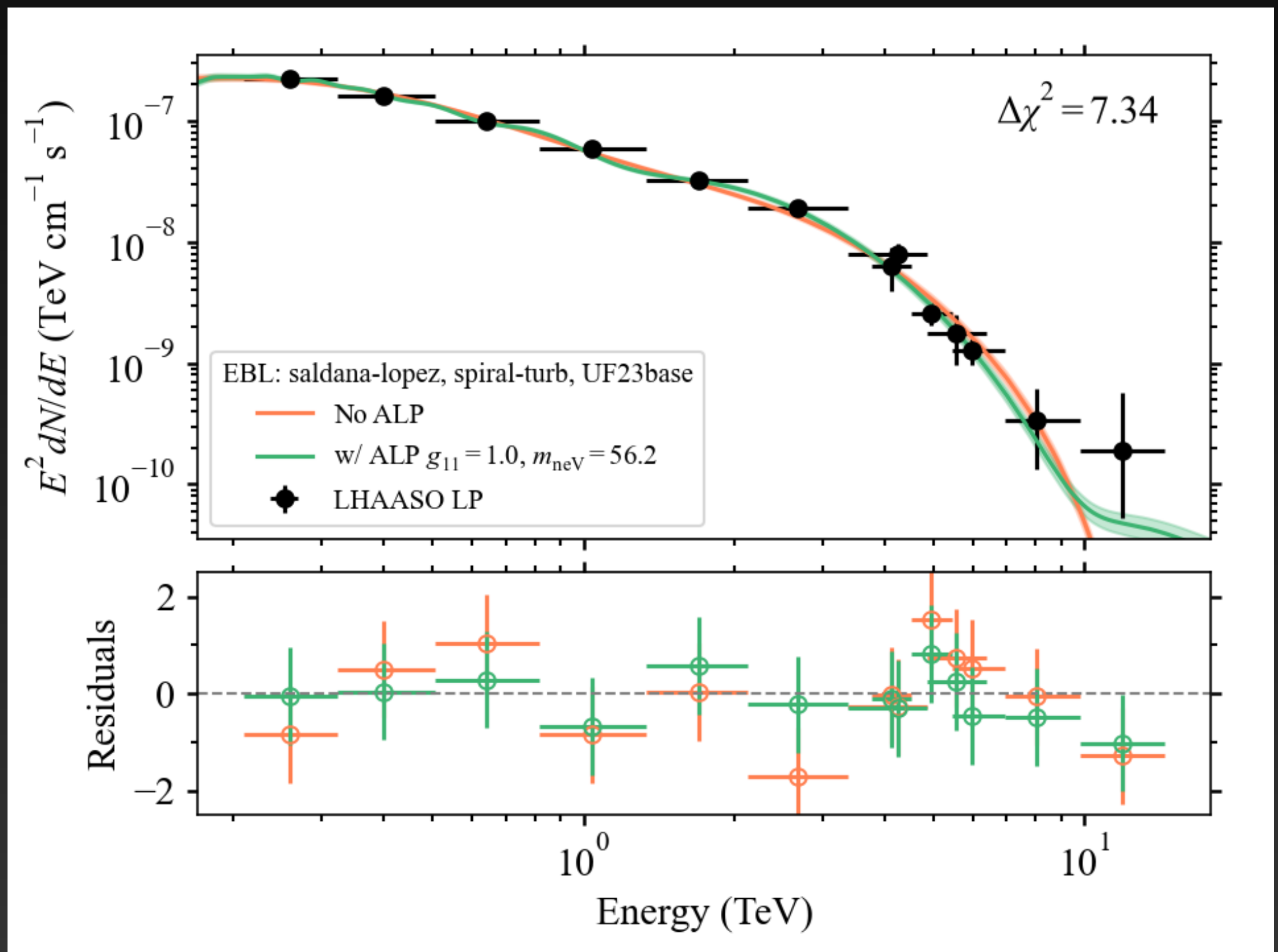
- Almost all model combinations result in no preference for ALPs, $p_{local} < 2\sigma$ for LP and EPL reconstructed data
- Most models yield very similar constraints
- UF23 model results in slightly higher preferences for ALPs
- EBL with stronger absorption results in slightly higher preferences for ALPs
- For EPL (LP) data, significance with $p_{local} \sim 2\sigma$ (3σ) found for turbulent models, Saldana-Lopez (Franceschini) EBL model



EPL data: Model combination with highest preference for ALPs

$$p_{local} = 2.23\sigma$$

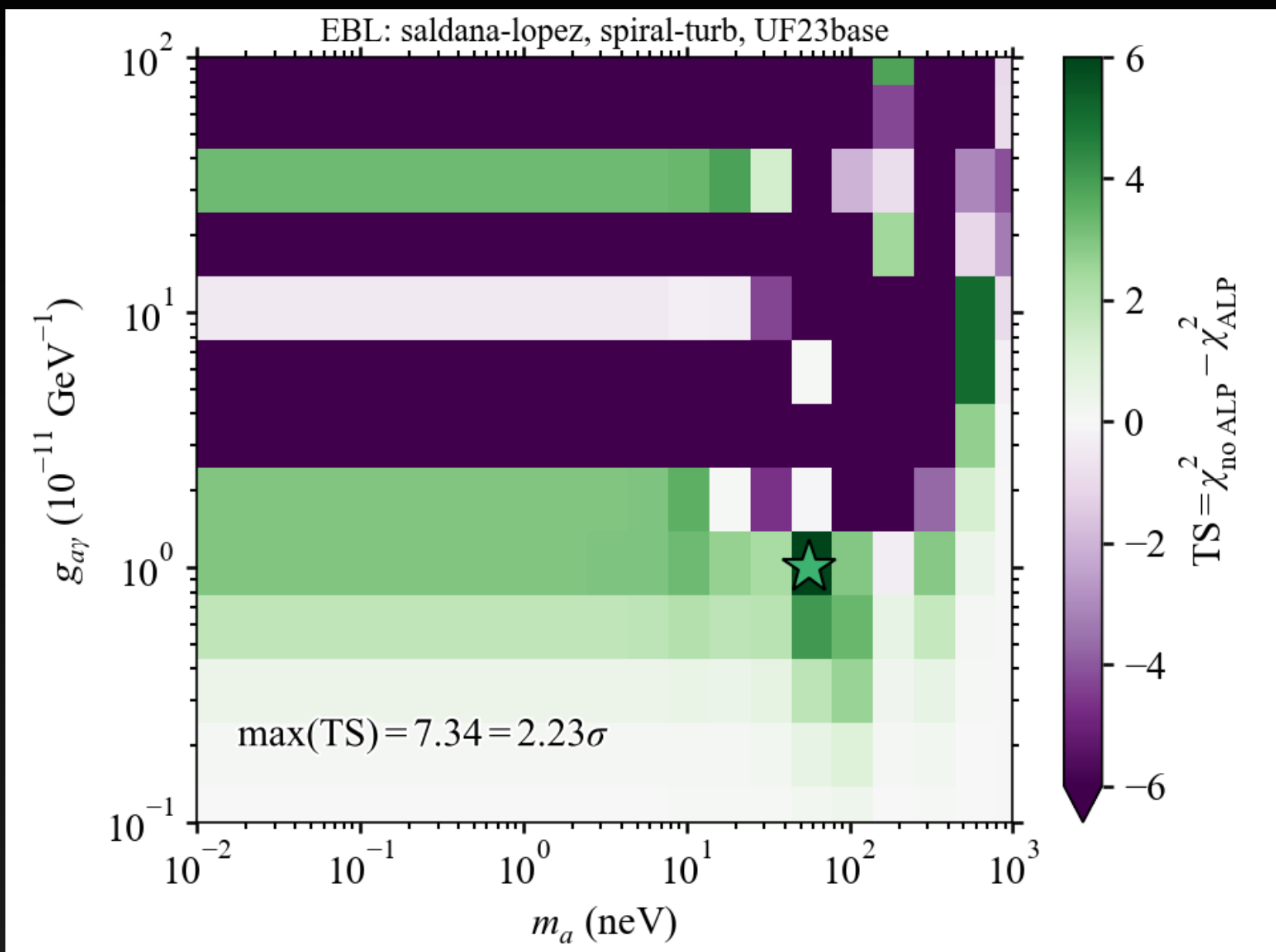
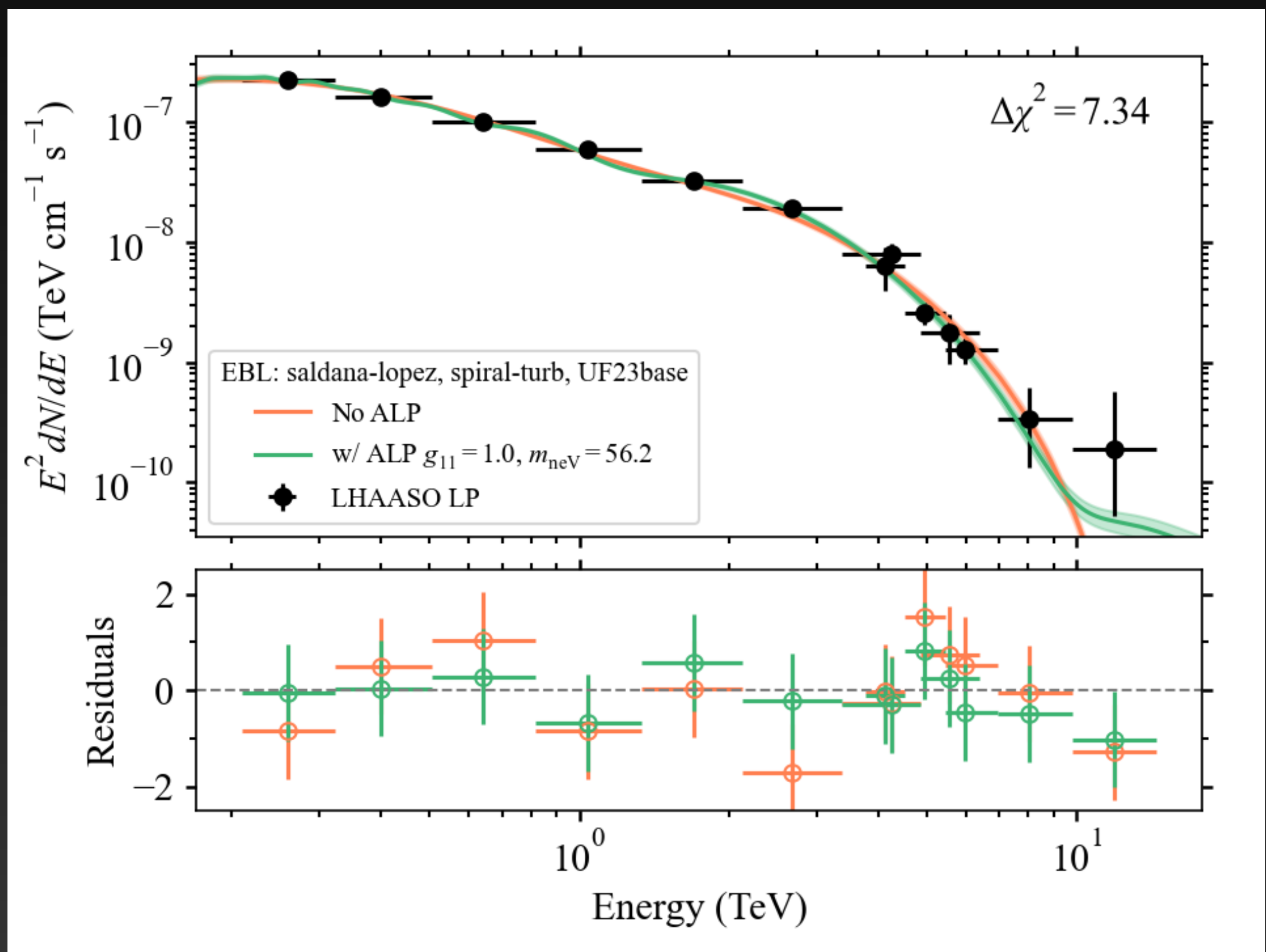
(Not corrected for trials!)



EPL data: Model combination with highest preference for ALPs

$$p_{local} = 2.23\sigma$$

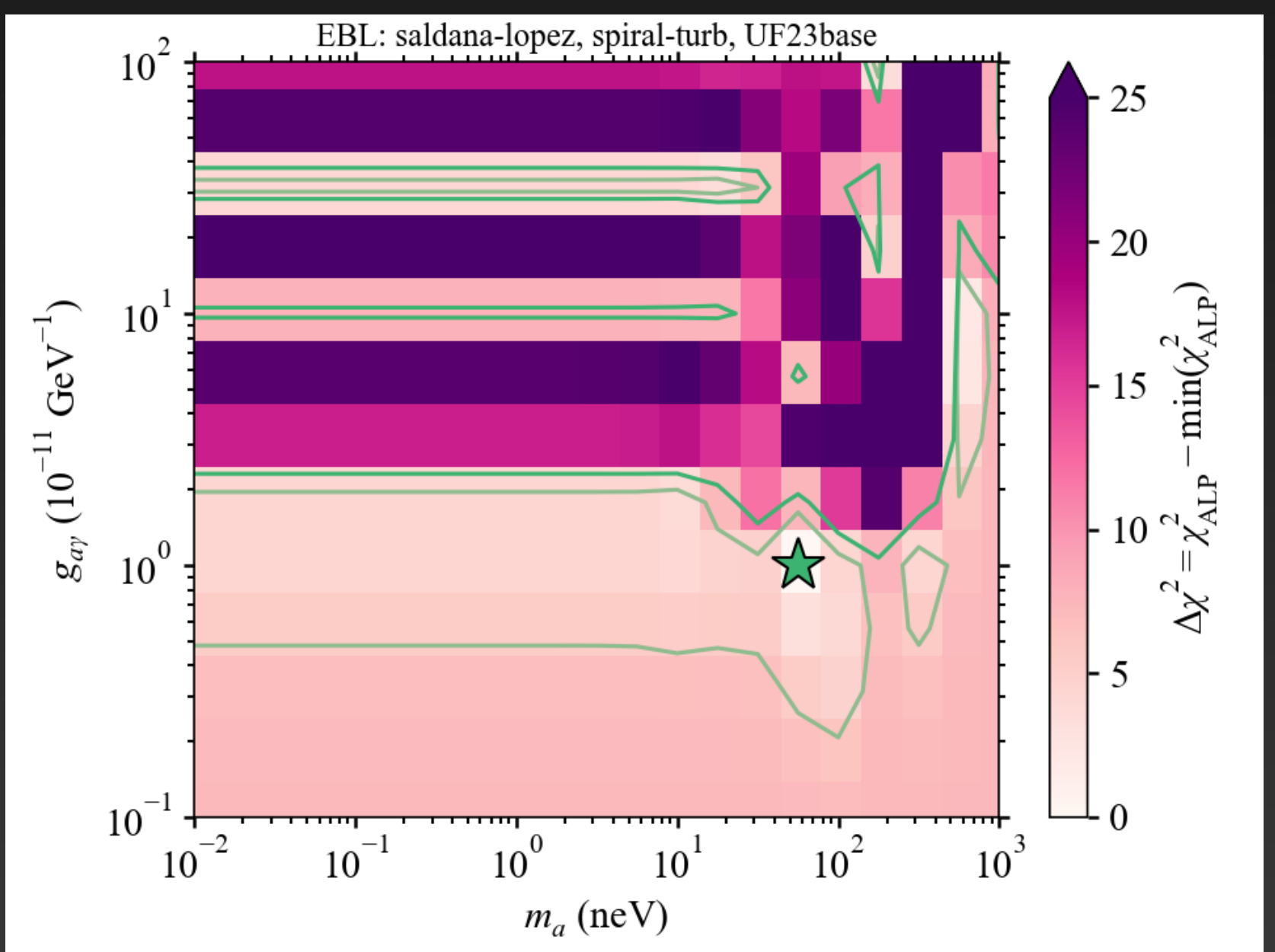
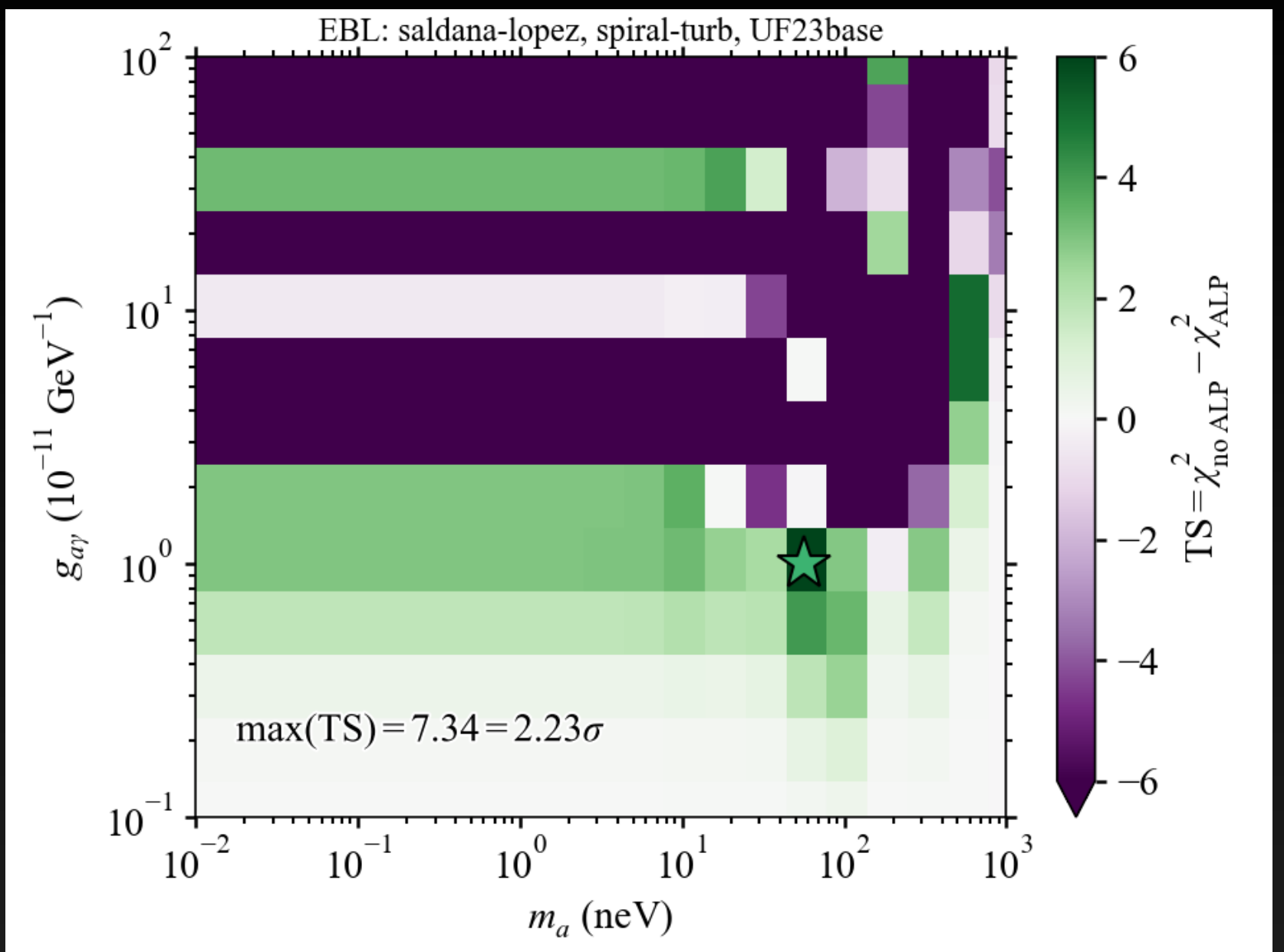
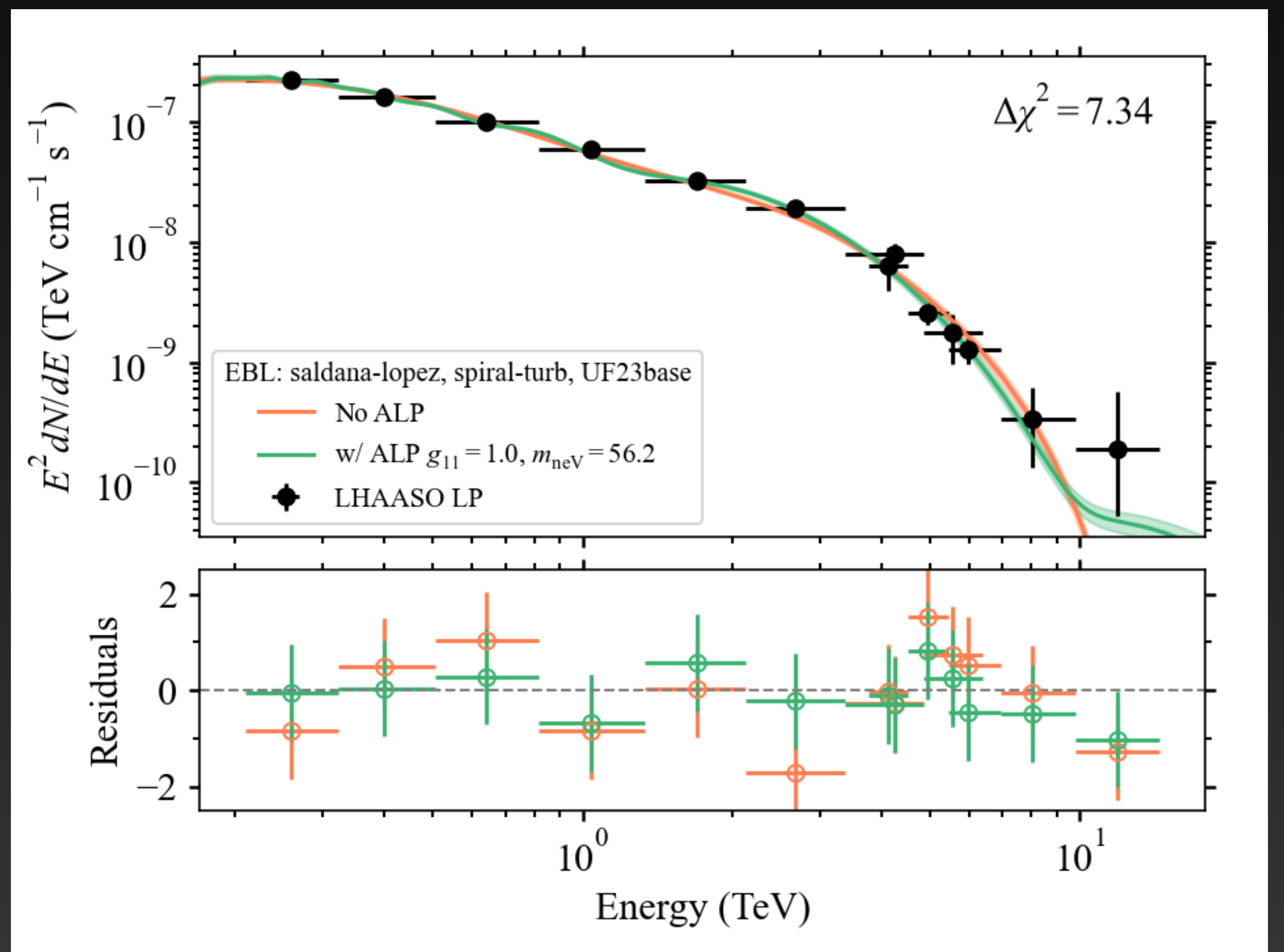
(Not corrected for trials!)



EPL data: Model combination with highest preference for ALPs

$p_{local} = 2.23\sigma$

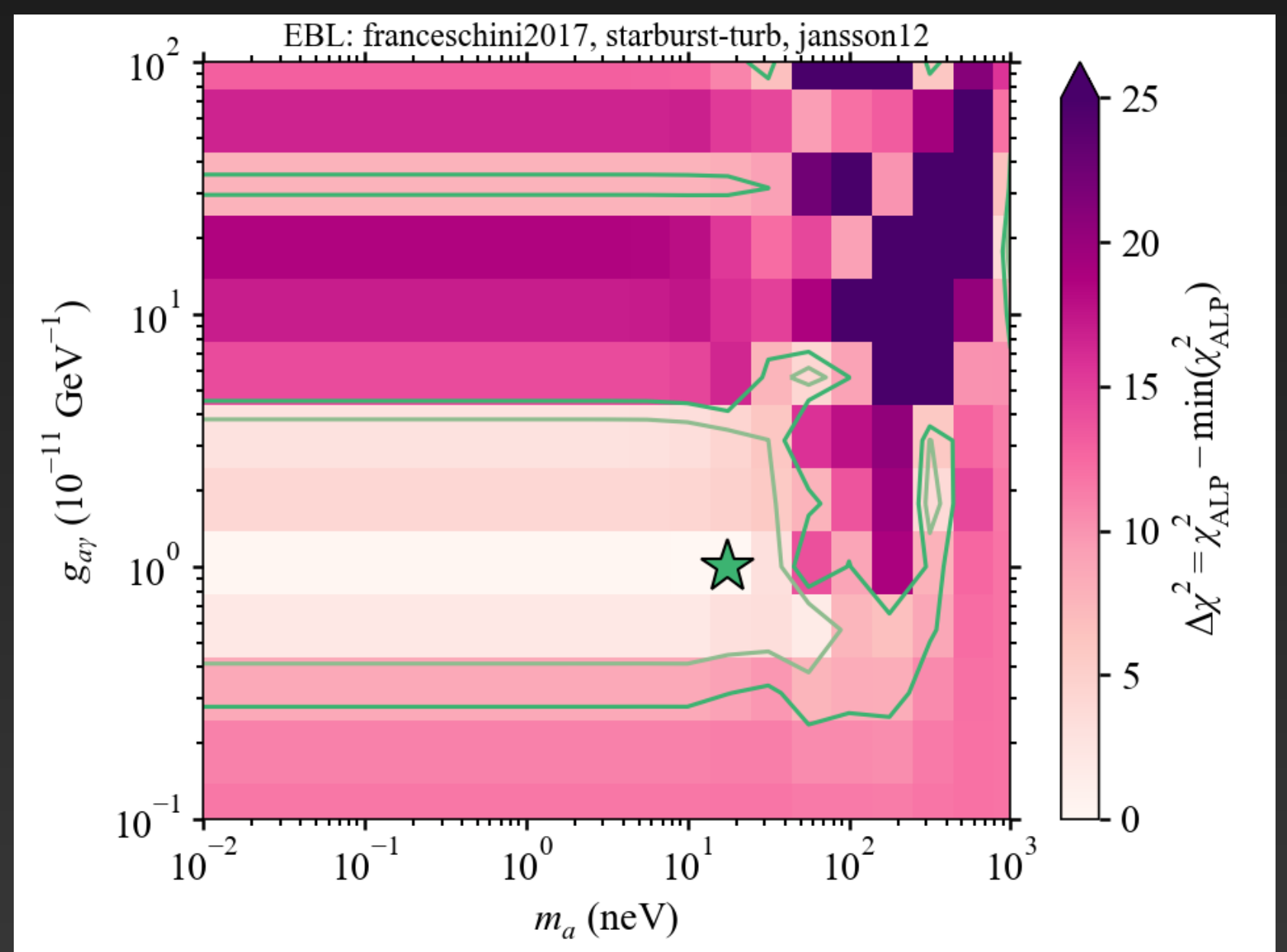
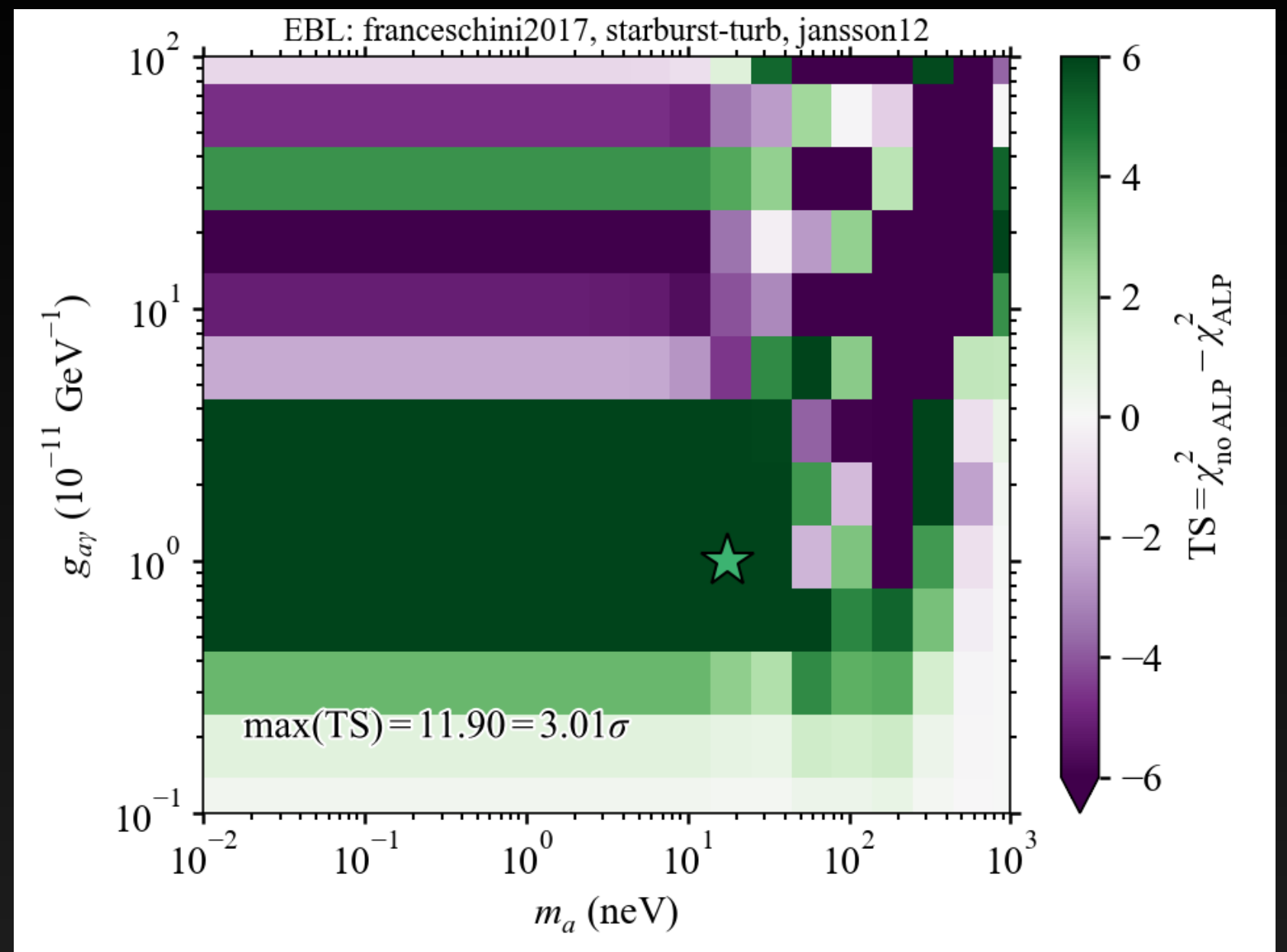
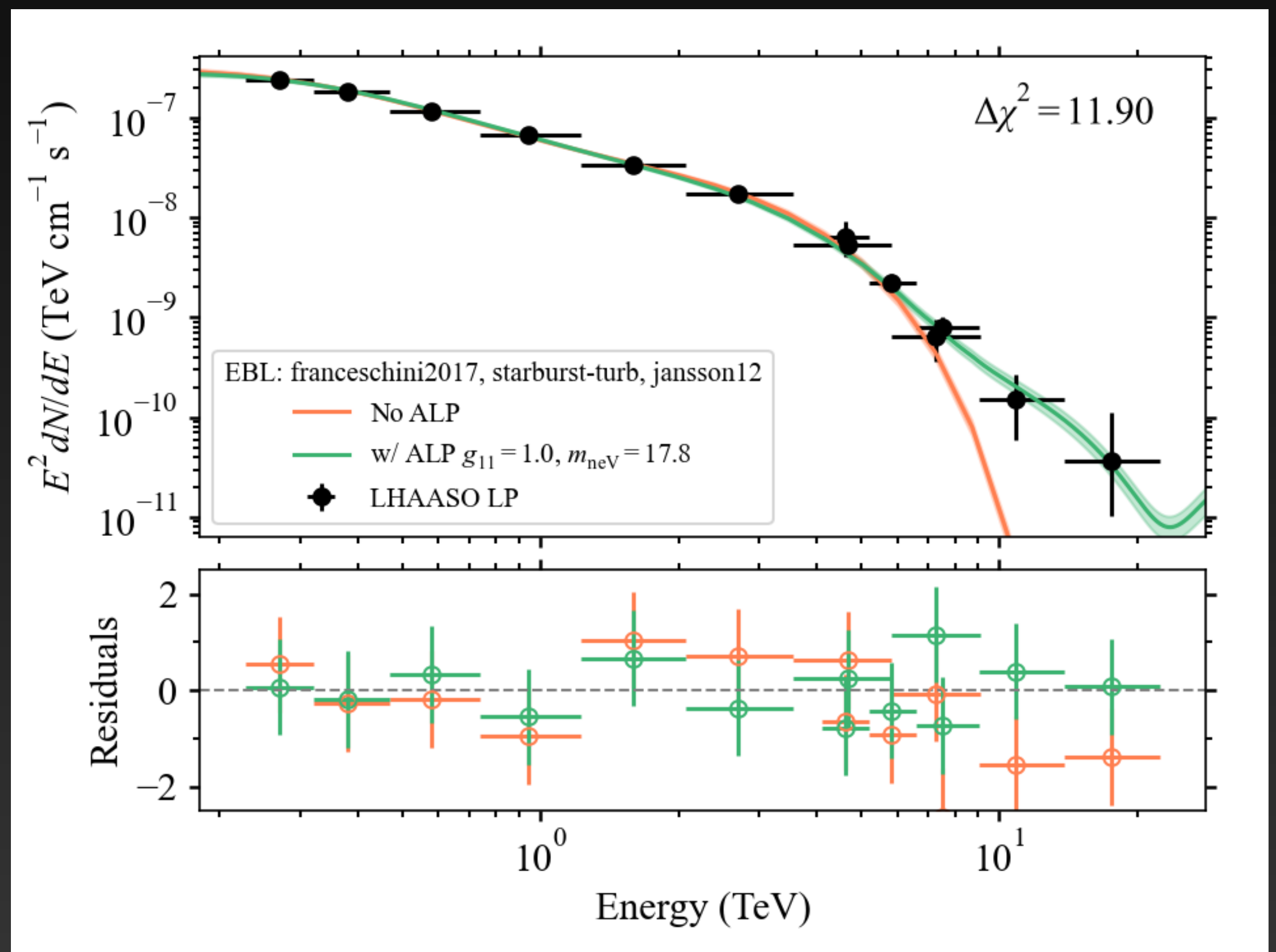
(Not corrected for trials!)



LP data: Model combination with highest preference for ALPs

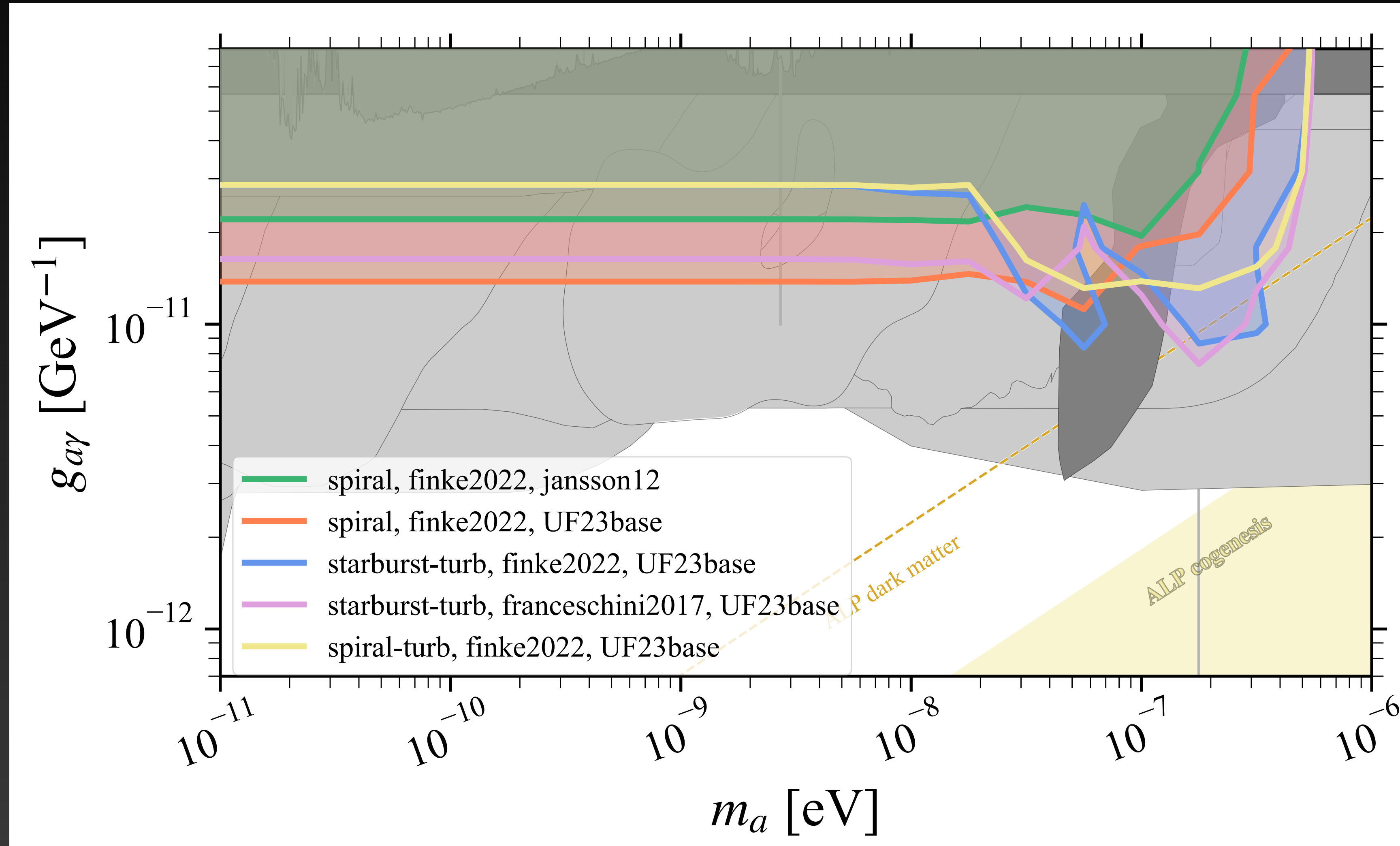
$p_{local} = 3.01\sigma$

(Not corrected for trials!)



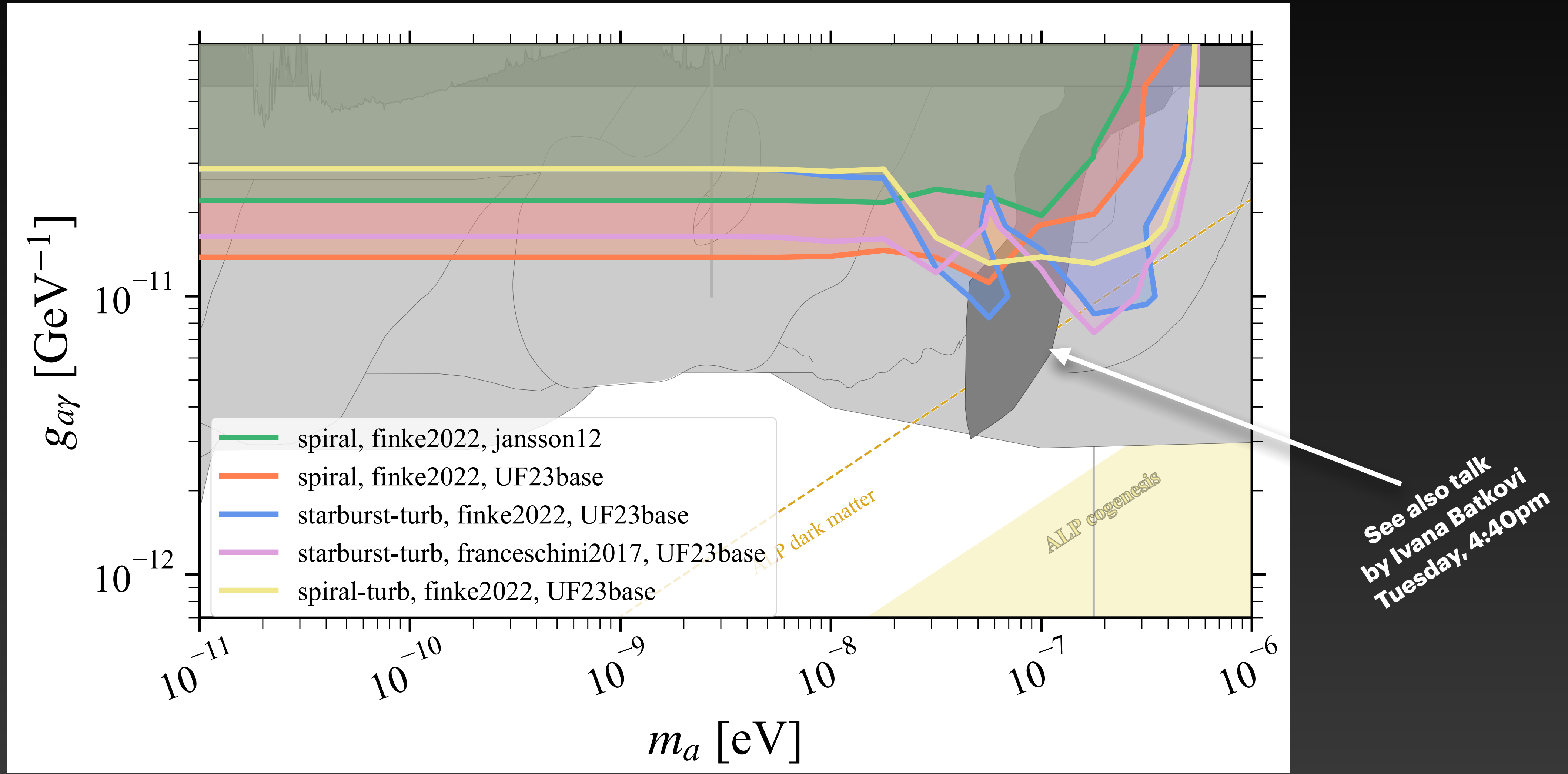
Constraints from GRB221009A in perspective

(Model combinations with $p_{local} < 2\sigma$)



Constraints from GRB221009A in perspective

(Model combinations with $p_{local} < 2\sigma$)



More surprises...?

- Potential detection of photon with 300 TeV in spatial and temporal coincidence with GRB
- Detection with Carpet Air shower array
- If indeed photon from GRB, photon-ALP conversion would not suffice as explanation
- Lorentz invariance violation?

Carpet-3 detection of a photon-like air shower with estimated primary energy above 100 TeV in a spatial and temporal coincidence with GRB 221009A

D. D. Dzhappuev,¹ I. M. Dzaparova,¹ T. A. Dzhatdoev,^{1, 2} E. A. Gorbacheva,¹ I. S. Karpikov,¹ M. M. Khadzhiev,¹ N. F. Klimenko,¹ A. U. Kudzhaev,¹ A. N. Kurenja,¹ A. S. Lidvansky,¹ O. I. Mikhailova,¹ V. B. Petkov,¹ E. I. Podlesnyi,³ N. A. Pozdnukhov,^{1, *} V. S. Romanenko,¹ G. I. Rubtsov,¹ S. V. Troitsky,^{1, 2} I. B. Unatlokov,¹ N. A. Vasiliev,² A. F. Yanin,¹ and K. V. Zhuravleva¹
(Carpet-3 Group)

¹*Institute for Nuclear Research of the Russian Academy of Sciences,
60th October Anniversary Prospect 7a, Moscow 117312, Russia*

²*Lomonosov Moscow State University, 1-2 Leninskie Gory, Moscow 119991, Russia*

³*Norwegian University for Science and Technology (NTNU), Institutt for fysikk, Trondheim, Norway*

The brightest cosmic gamma-ray burst (GRB) ever detected, GRB 221009A, was accompanied by photons of very high energies. These gamma rays may be used to test both the astrophysical models of the burst and our understanding of long-distance propagation of energetic photons, including potential new-physics effects. Here we present the observation of a photon-like air shower with the estimated primary energy of 300^{+43}_{-38} TeV, coincident (with the chance probability of $\sim 9 \cdot 10^{-3}$) with the GRB in its arrival direction and time. Making use of the upgraded Carpet-3 muon detector and new machine learning analysis, we estimate the probability that the primary was hadronic as $\sim 3 \cdot 10^{-4}$. This is the highest-energy event ever associated with any GRB.

arXiv:2502.02425

Conclusions

Conclusions

- GRB221009A was an exceptional event

Conclusions

- GRB221009A was an exceptional event
- Allows to probe photon propagation at high optical depth

Conclusions

- GRB221009A was an exceptional event
- Allows to probe photon propagation at high optical depth
- Observations can be reconciled with EBL models with lower photon density

Conclusions

- GRB221009A was an exceptional event
- Allows to probe photon propagation at high optical depth
- Observations can be reconciled with EBL models with lower photon density
- Photon-ALP oscillations generally not necessary to explain observations

Conclusions

- GRB221009A was an exceptional event
- Allows to probe photon propagation at high optical depth
- Observations can be reconciled with EBL models with lower photon density
- Photon-ALP oscillations generally not necessary to explain observations
- All tested model combinations yield at most a $p_{local} \sim 3\sigma$ preference for ALPs, however, not corrected for trials

Conclusions

- GRB221009A was an exceptional event
- Allows to probe photon propagation at high optical depth
- Observations can be reconciled with EBL models with lower photon density
- Photon-ALP oscillations generally not necessary to explain observations
- All tested model combinations yield at most a $p_{local} \sim 3\sigma$ preference for ALPs, however, not corrected for trials
- Limits on photon-ALP coupling $g_{a\gamma} \gtrsim 2 \times 10^{-11} \text{ GeV}^{-1}$ (95% confidence)
for $m_a \lesssim 2 \times 10^{-7} \text{ eV}$

In case you're fed up with astrophysical uncertainties...

FAXE
Fabry-Pérot Axion Experiment
Jacob Egge & Manuel Meyer

SDU erc

Introduction

- Effective volume of closed resonators $V \propto \lambda^3$
- Remove transverse boundary $\rightarrow V \propto \lambda$
- Microwave Fabry-Pérot resonators can have high $Q > 10^6$
- Simple, large, high-Q resonators at high frequencies

Spherical mirrors

- Need to keep eigenmode away from edge to minimize diffractive losses
- Trade-off between effective volume and quality factor
- Optimized for best signal power using COMSOL
- Formfactor $C \sim 0.3$

Graded-phase mirrors

- Can we increase the effective volume without reducing Q-factor?
- Design super-Gaussian eigenmode
- Fills resonator volume more efficiently
- $C \sim 0.6$
- Requires a more complex mirror profile

Graded-phase design process

- Pick desired mode profile: super-gaussian, flat top....
- Free space propagation of desired mode profile: diffraction changes phase-fronts
- Extract mirror spatial profile: mirror profile needs to follow phase-front phase of diffracted mode profile $-p/2$

Conclusion

- Fabry-Pérot resonators can provide large resonator volumes at high frequencies
- Graded-phase mirrors can increase effective volume by a factor of two

For more info visit arxiv:2506.03091
Sensitivity of a Gigahertz Fabry-Pérot Resonator for Axion Dark Matter Detection

Towards ultra-low backgrounds for high-efficiency cryogenic single photon detection in optical and infrared axion searches

Manuel Meyer¹, Katharina Sophie Isleif², Friederike Januschek³, Axel Lindner³, Gulden Othman², José Alejandro Rubiera Gimeno², Elmeri Rivasto¹, Christina Schwemmbauer³

¹CP3-origins, University of Southern Denmark (SDU), Campusvej 55, 5230 Odense, Denmark
²Deutsches Elektronen-Synchrotron DESY, Notkestr. 85, 22607 Hamburg, Germany
³Helmholtz-Schmidt-Universität, Heisenbergweg 85, 22043 Hamburg, Germany

Motivation: Any Light Particle Search (ALPS) II

- Light shining through a wall experiment
- Located at DESY, Hamburg
- Model independent lab-experiment for:
- Axions
- Axion-like particles (ALPs)

Black-body photon background

- $E \pm \Delta E_{\text{TES}}$ indistinguishable from signal photons \rightarrow Limiting background source for TES and also Superconducting Nanowire Single-Photon Detectors (SNSPDs)
- Rates for our TES setup are $\sim 1\text{ mHz}$ in agreement with simulations [2]

Need to improve energy resolution

- Cold filter with transmission window $E \pm \Delta E$ absorbs majority of black-body photons if $\Delta E_{\text{filter}} \ll \Delta E_{\text{TES}}$
- Improves effective energy resolution of the TES detection SNSPDs
- Main problem: Thermal contraction misaligns filter bench resulting in high optical losses

Determining system detection efficiency

- System detection efficiency (SDE) determined by ratio of power sent to TES and detected photon rate P_{TES} [4]:
$$\eta = \frac{P_{\text{TES}}}{P_{\text{TES}, \text{in}}} = n_{\text{TES}} \frac{\hbar c}{\lambda} P_{\text{TES}, \text{in}}$$
- Power sent in depends on beam splitter ratio r and attenuation L , $P_{\text{TES}, \text{in}} = r P_{\text{in}} 10^{L/10}$
- L determined with photodiode B , P_{in} determined from diode A
- Preliminary results suggest $\eta \gtrsim 80\%$

Transition edge sensor

- Optimized for detecting 1064 nm photons
- Readout using SQUIDS
- Energy resolution (FWHM): $\Delta E_{\text{TES}} \approx 0.15\text{ eV}$ [5]
- Without fiber connected, we achieve record low intrinsic dark current rate: $\text{IDCR} \lesssim 7 \times 10^{-6}\text{ Hz}$ after pulse-shape analysis optimized for 1064nm photons [3, 6]

Cold optical filter bench

- Ultra-narrow band pass filter, specs: $\Delta E_{\text{filter}} \pm \Delta E_{\text{filter}} = (1.16 \pm 0.002)\text{ eV}$ or $(1064 \pm 2)\text{ nm} \Rightarrow$ potentially improving TES energy resolution by factor of 75!
- 90% transmission (0.46 dB attenuation losses) for perfect alignment
- Transmission window shifts as a function of temperature \Rightarrow Compensated by changing angle of incidence
- Cryo-compatible piston stages (JPE) for remote auto-alignment of filter bench \Rightarrow Compensates for misalignment by thermal contraction
- So far: achieved above 80% transmission for single-mode fibers (without filter) at room temperature
- Actively developed in SDU, cold tests in DESY later this year

Fig. 1: schematic layout of the ALPS II detector for a potential TES science run and the Feynman diagram for photon-ALP conversion.

Fig. 2: Current filter bench setup at SDU

Fig. 3: Sketch of the CNN used for signal and background discrimination

Fig. 4: Experimental layout to determine the system detection efficiency

References

- I. Isleif, K. for the ALPS Collaboration (2022), arXiv:2205.07306
- Rubiera Gimeno, J. A. et al. (2025), Phys. Rev. D 112, 032001
- Shah, R. et al. (2022), J. Low Temp. Phys. 2022, 209, 355
- Gerrits, T. et al. (2020), Metrologia 57, 015002
- Rubiera Gimeno, J. A. et al. (2024), PoS EPS-HEP2023, 567
- Meyer, M. et al. (2024), Annalen Phys. 536, 1, 2200545

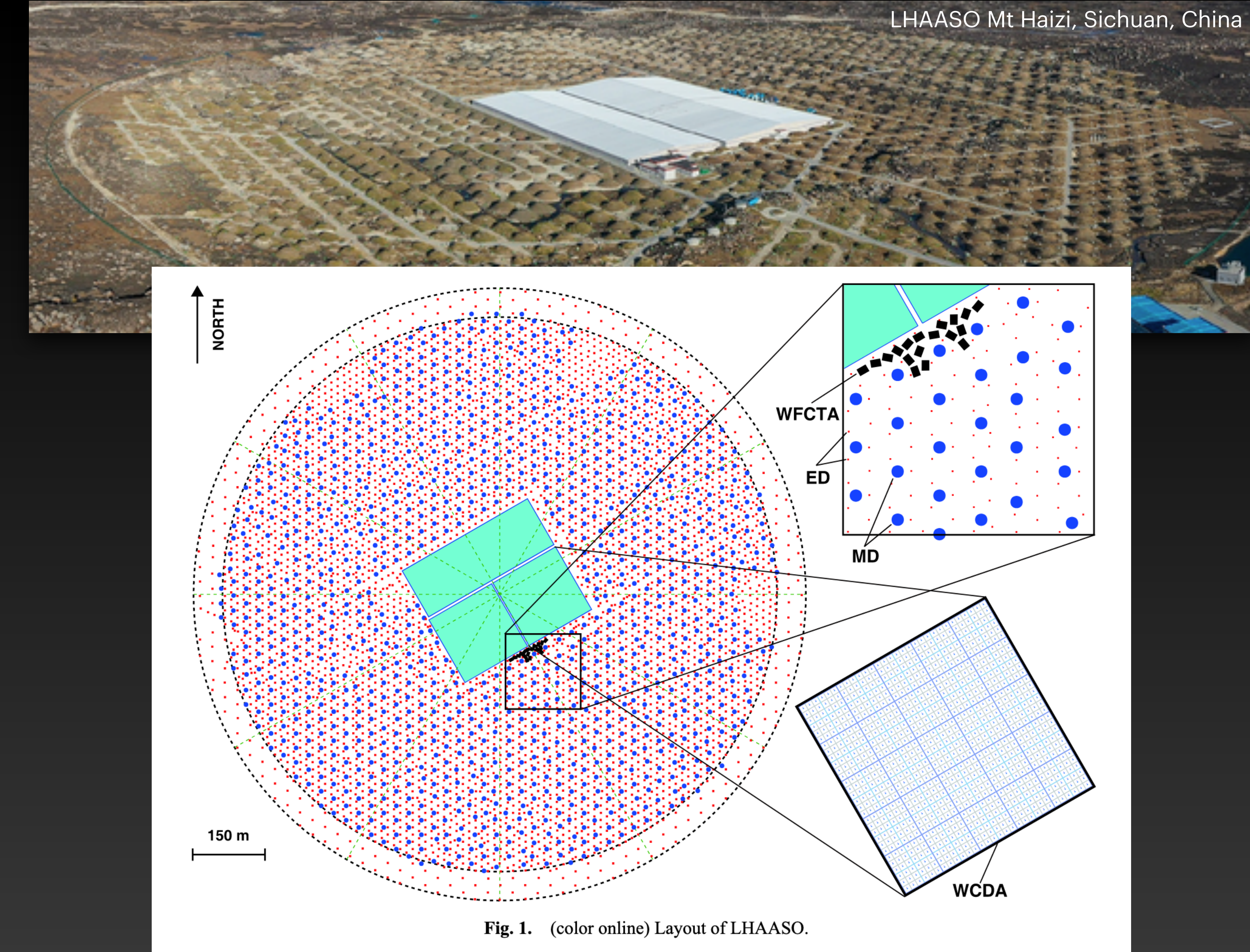
Back up

VHE photons seen with LHAASO



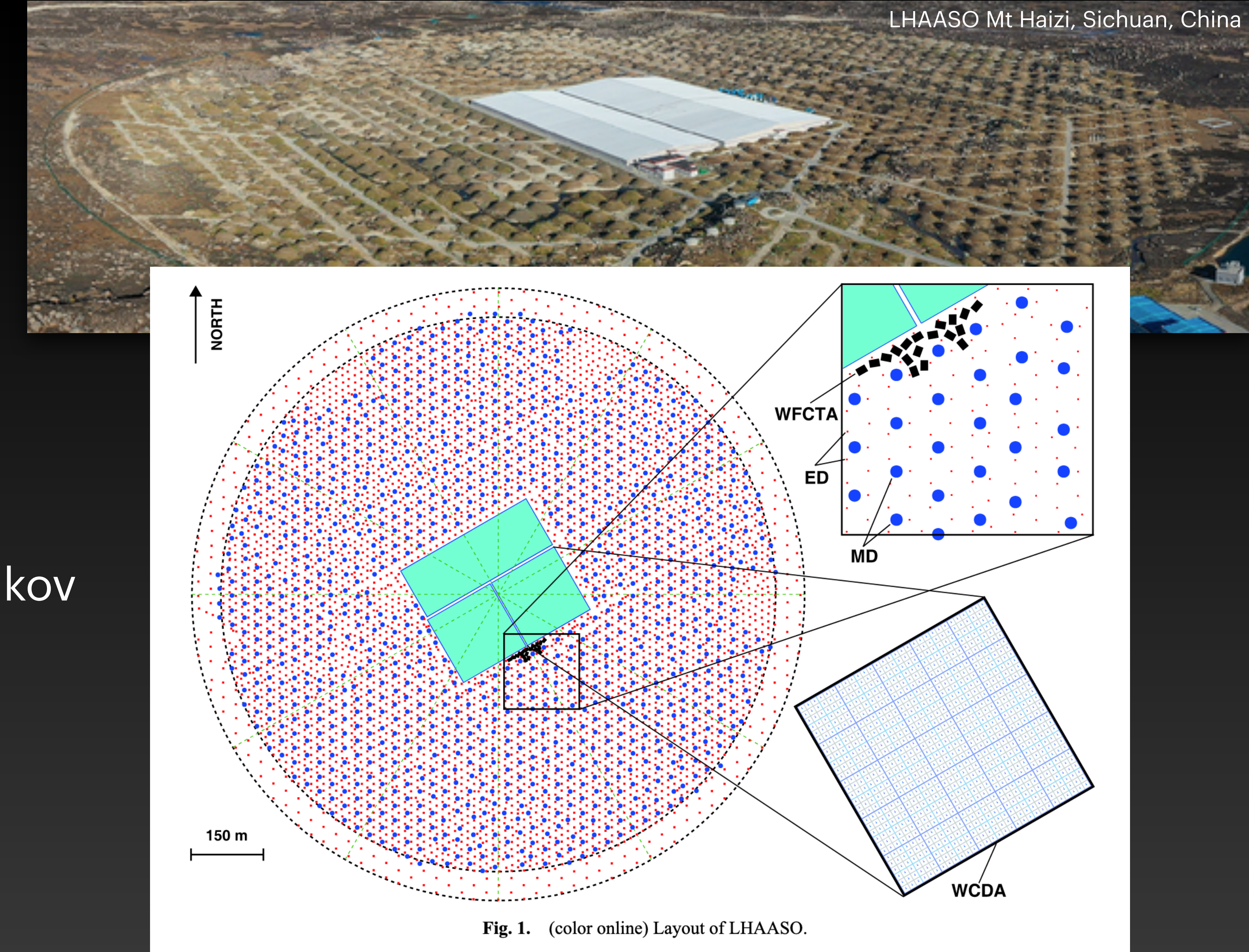
LHAASO Mt Haizi, Sichuan, China

VHE photons seen with LHAASO



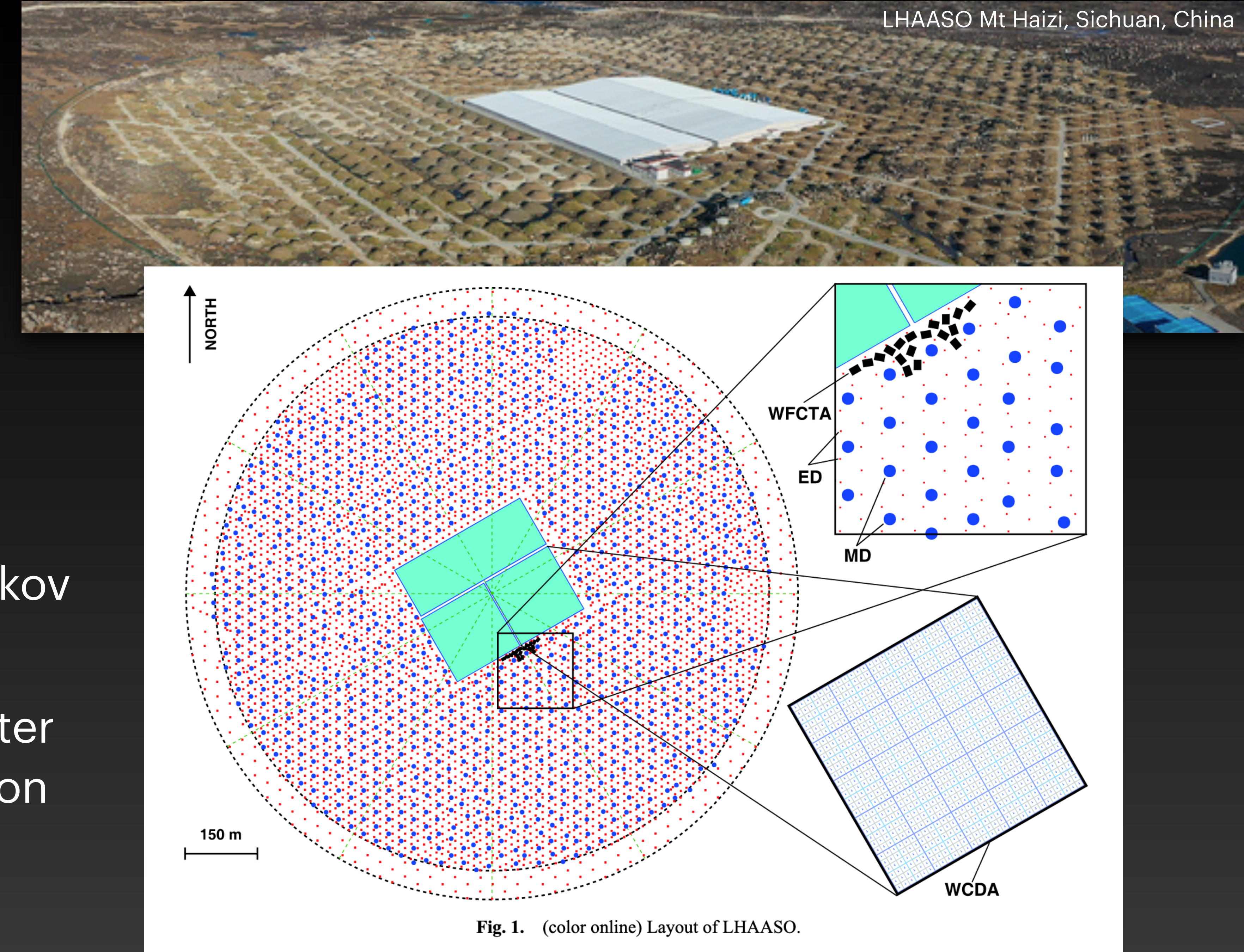
VHE photons seen with LHAASO

- **WCDA:** Water Cherenkov
Detector $78,000\text{ m}^2$

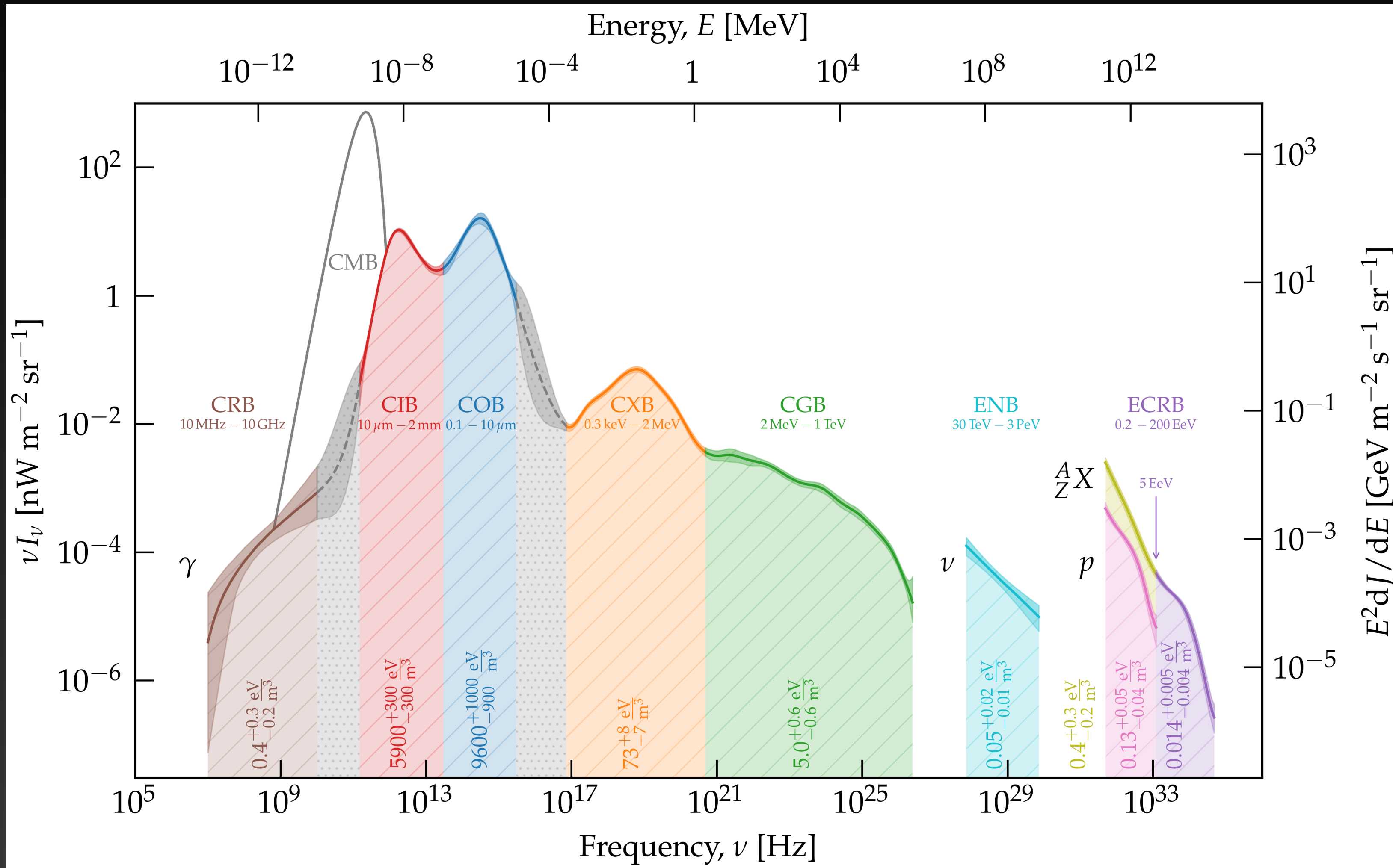


VHE photons seen with LHAASO

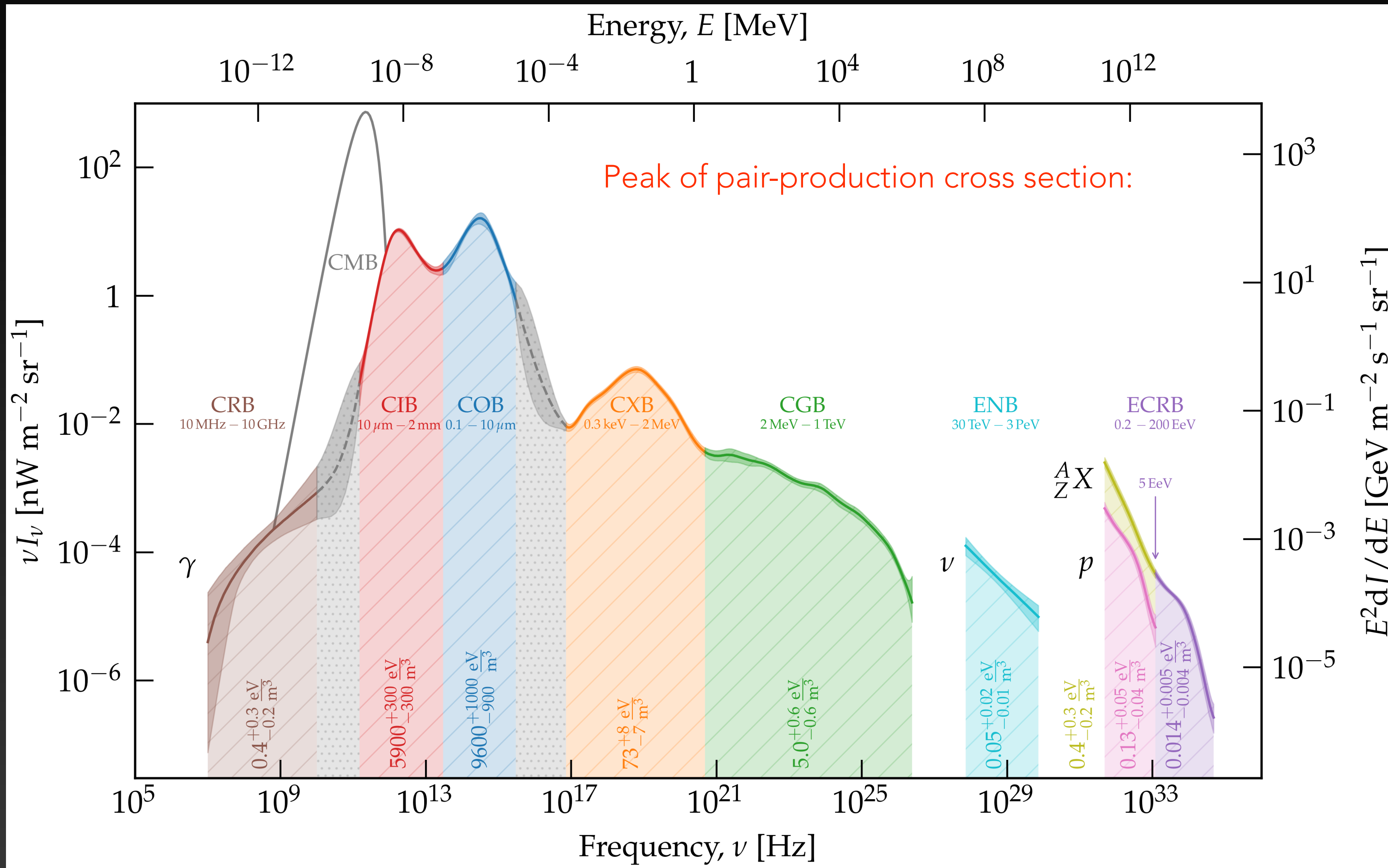
- **WCDA:** Water Cherenkov Detector $78,000\text{ m}^2$
- **KM2A:** square kilometer array with EM and muon detectors



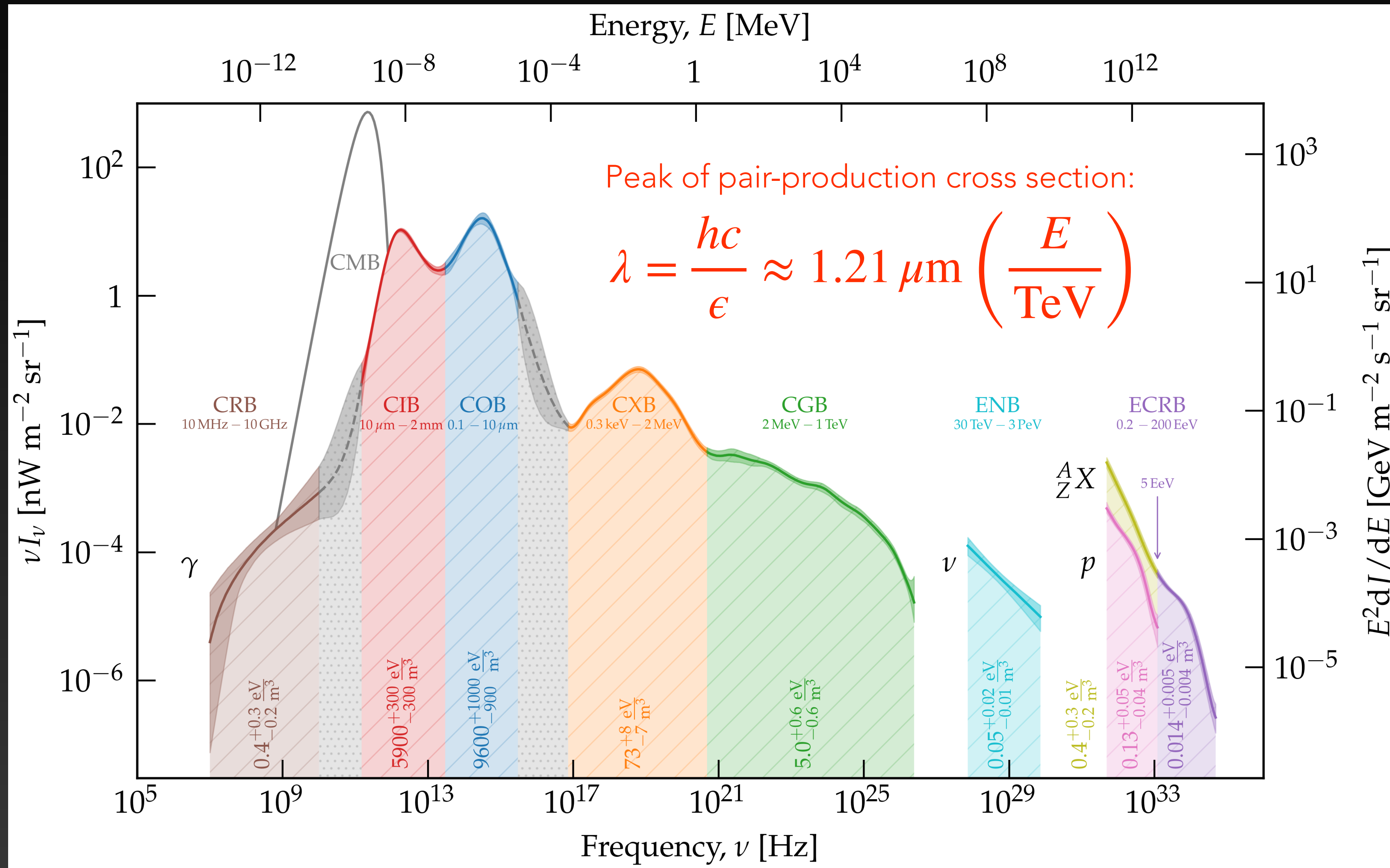
Background radiation fields



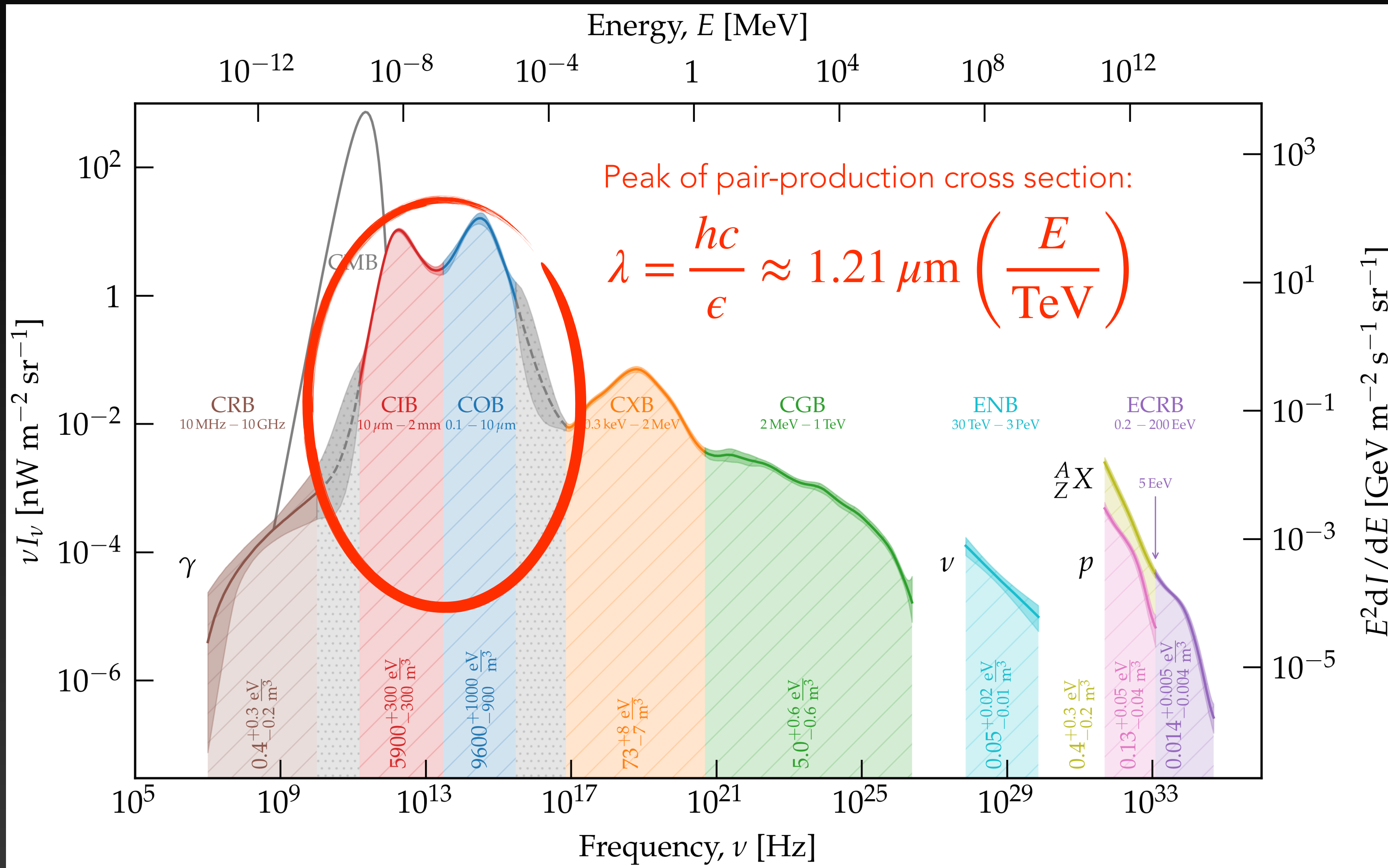
Background radiation fields



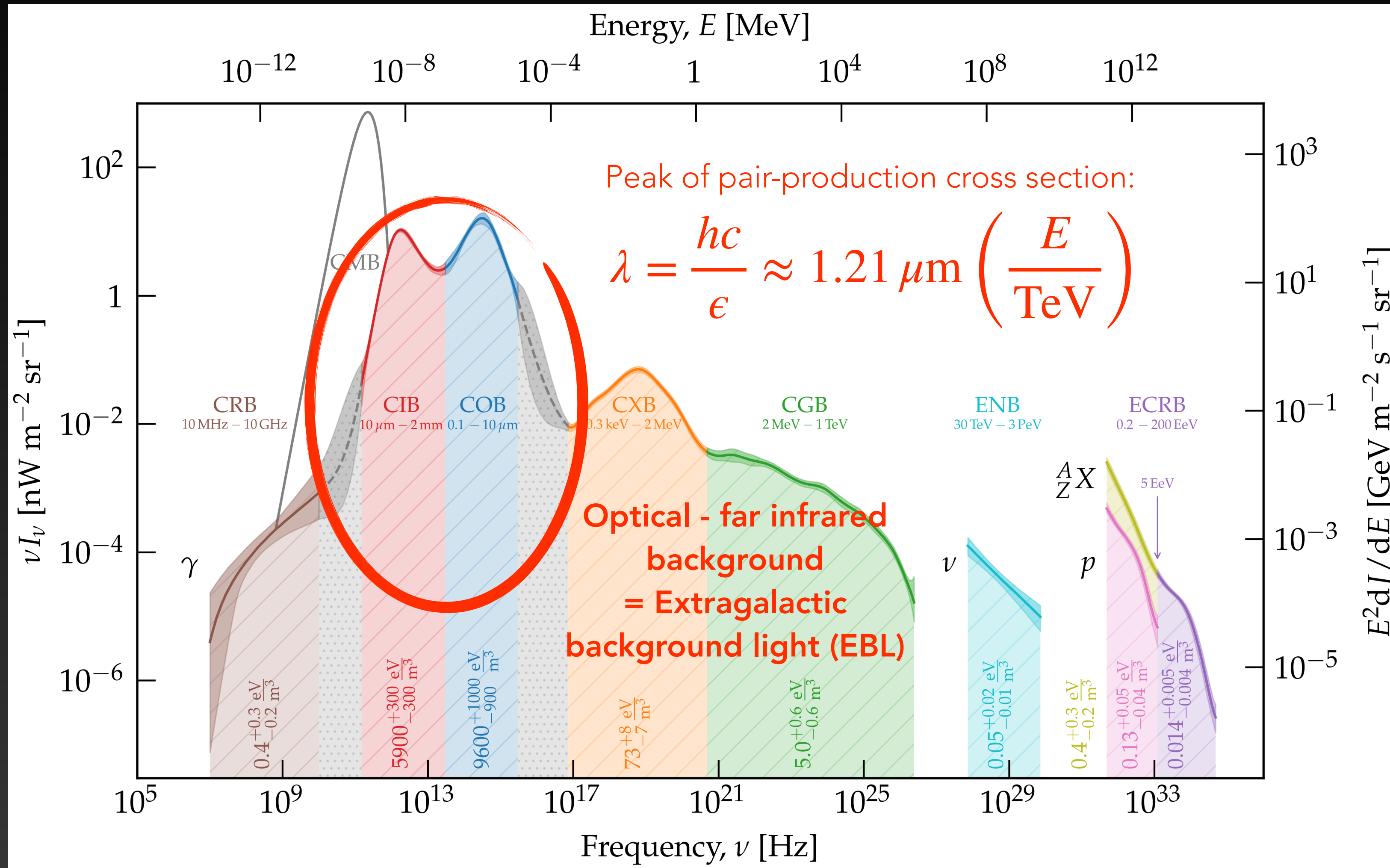
Background radiation fields



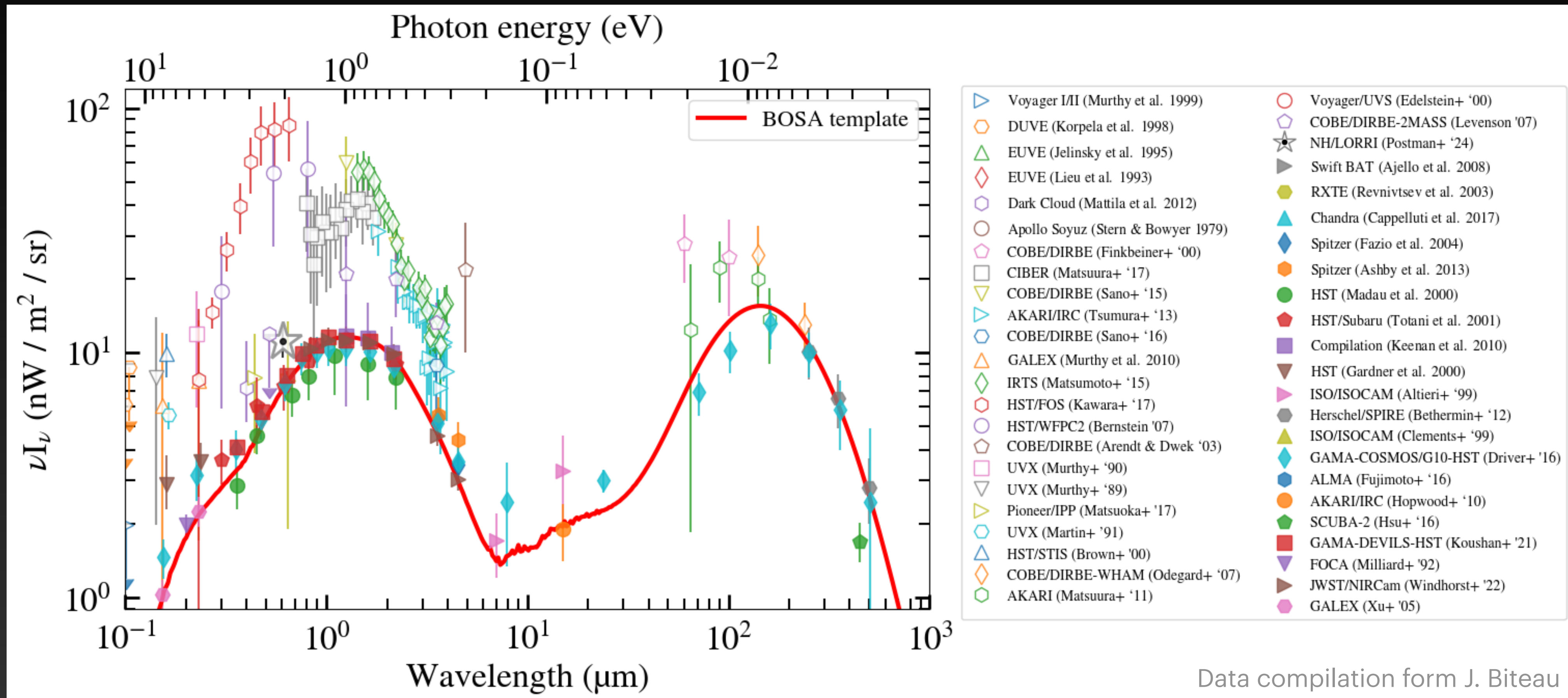
Background radiation fields



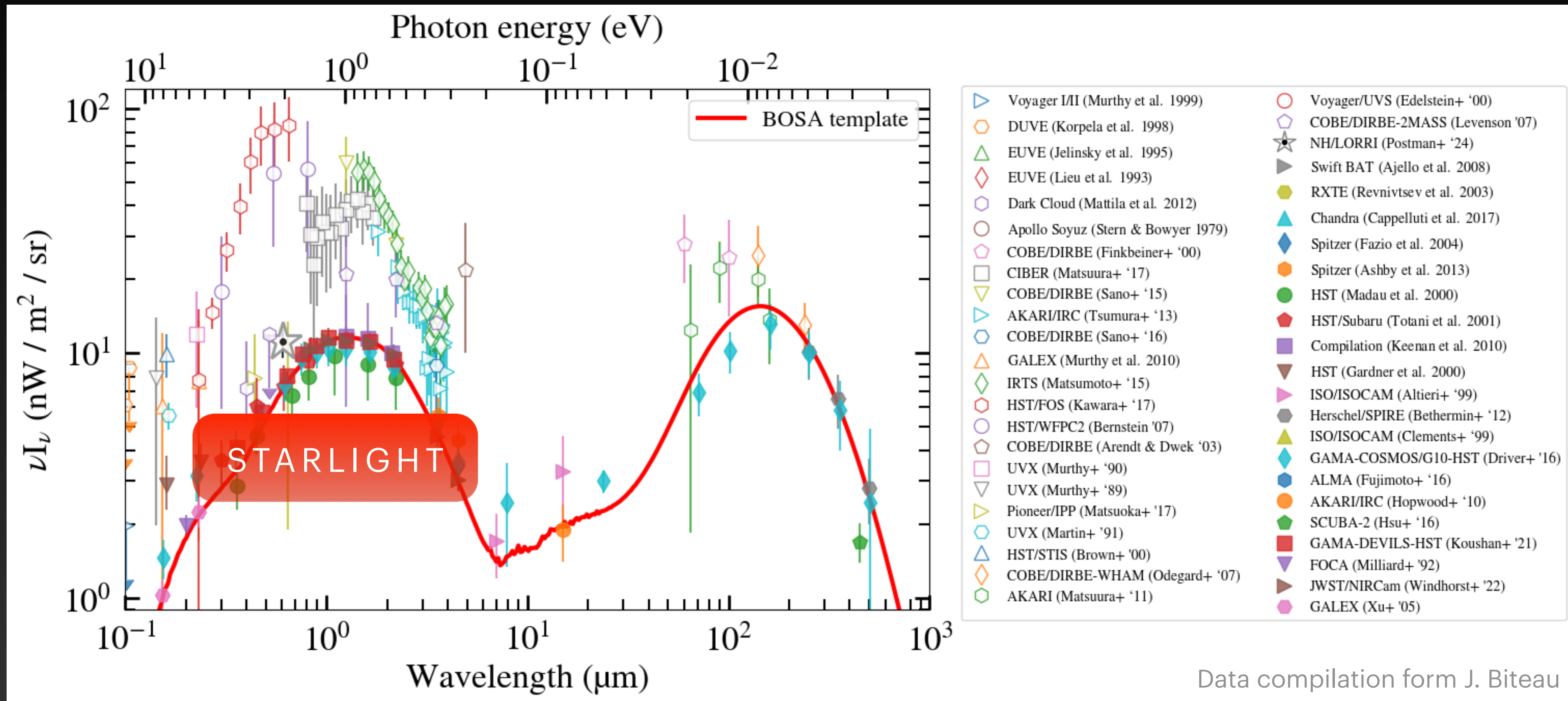
Background radiation fields



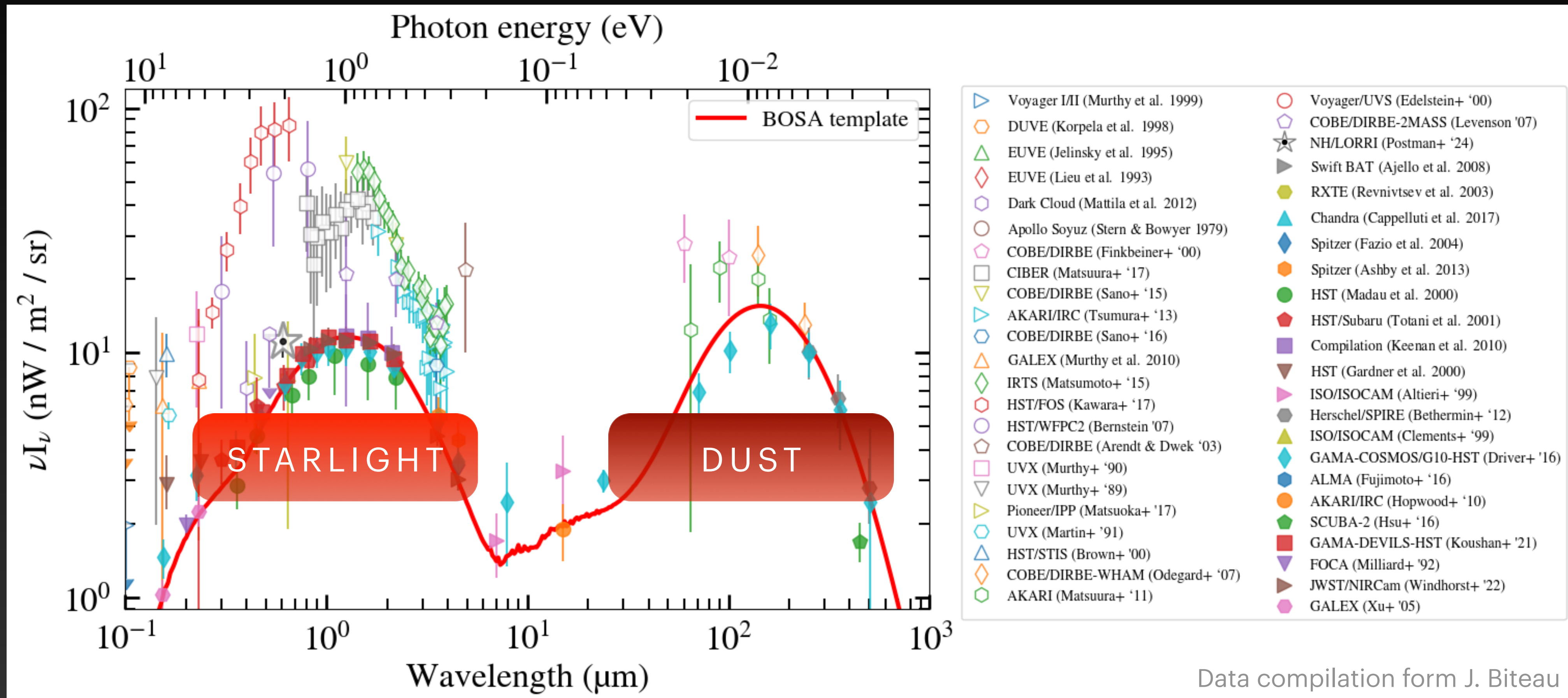
EBL Measurements



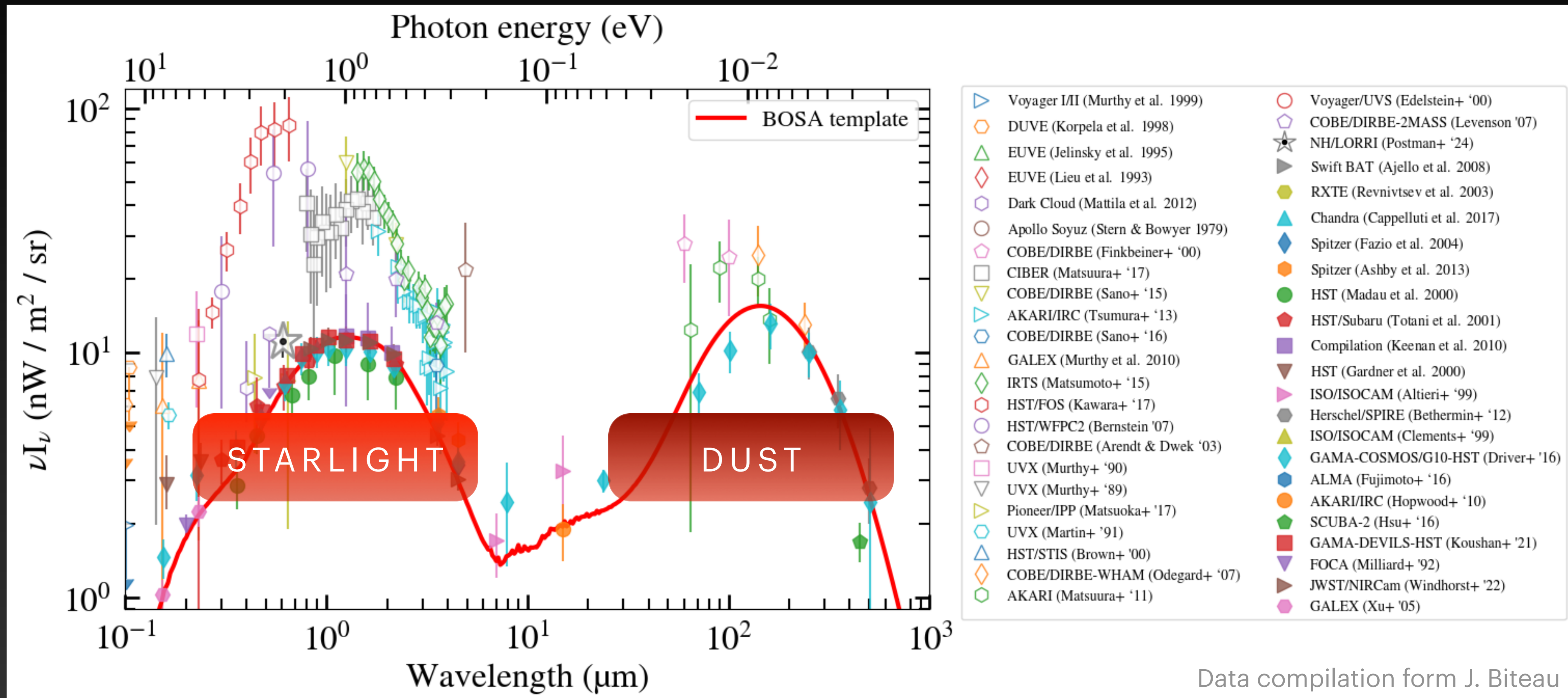
EBL Measurements



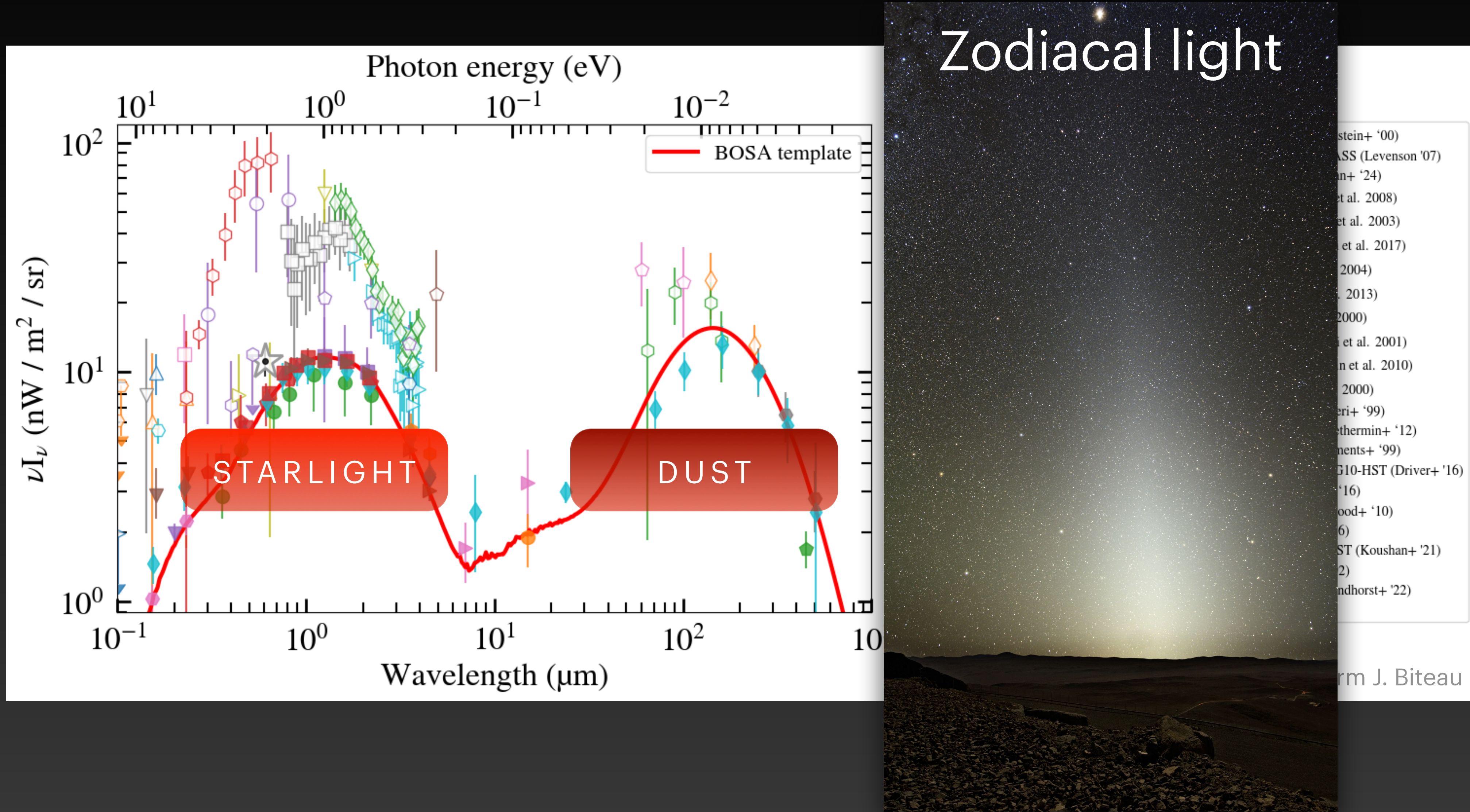
EBL Measurements



EBL Measurements



EBL Measurements



Optical Depth

$$\tau_{\gamma\gamma}(E, z_0) = \int_0^{z_0} dz \left| \frac{dL}{dz} \right| \int_0^{\infty} d\epsilon \frac{dn}{d\epsilon}(\epsilon, z) \int_{-1}^1 d\mu \frac{1 - \mu}{2} \sigma_{\gamma\gamma}(\beta)$$

Optical Depth

$$\tau_{\gamma\gamma}(E, z_0) = \int_0^{z_0} dz \left| \frac{dL}{dz} \right| \int_0^{\infty} d\epsilon \frac{dn}{d\epsilon}(\epsilon, z) \int_{-1}^1 d\mu \frac{1 - \mu}{2} \sigma_{\gamma\gamma}(\beta)$$

Line of sight integral
to source

Optical Depth

$$\tau_{\gamma\gamma}(E, z_0) = \int_0^{z_0} dz \left| \frac{dL}{dz} \right| \int_0^{\infty} d\epsilon \frac{dn}{d\epsilon}(\epsilon, z) \int_{-1}^1 d\mu \frac{1 - \mu}{2} \sigma_{\gamma\gamma}(\beta)$$

Line of sight integral
to source

Integral over energy over
photon density of
background radiation field

Optical Depth

$$\tau_{\gamma\gamma}(E, z_0) = \int_0^{z_0} dz \left| \frac{dL}{dz} \right| \int_0^{\infty} d\epsilon \frac{dn}{d\epsilon}(\epsilon, z) \int_{-1}^1 d\mu \frac{1 - \mu}{2} \sigma_{\gamma\gamma}(\beta)$$

Line of sight integral to source

Integral over energy over photon density of background radiation field

Integral over angle $\mu = \cos \theta$ between photon momenta over pair-production cross section

Data	GMF	EBL	Host	p_{local}
EPL	Jansson12	Saldana-Lopez	Constant	1.26σ
EPL	UF23, base	Saldana-Lopez	Constant	1.79σ
EPL	Jansson12	Finke	Constant	0.97σ
EPL	UF23, base	Finke	Constant	1.33σ
EPL	Jansson12	Franceschini	Constant	1.17σ
EPL	UF23, base	Franceschini	Constant	1.68σ

Data	GMF	EBL	Host	p_{local}
EPL	Jansson12	Saldana-Lopez	Turbulent, spiral	2.01σ
EPL	UF23, base	Saldana-Lopez	Turbulent, spiral	2.23σ
EPL	Jansson12	Finke	Turbulent, spiral	1.36σ
EPL	UF23, base	Finke	Turbulent, spiral	0.83σ
EPL	Jansson12	Franceschini	Turbulent, spiral	1.19σ
EPL	UF23, base	Franceschini	Turbulent, spiral	1.22σ

Data	GMF	EBL	Host	p_{local}
EPL	Jansson12	Saldana-Lopez	Turbulent, starburst	1.84σ
EPL	UF23, base	Saldana-Lopez	Turbulent, starburst	2.02σ
EPL	Jansson12	Finke	Turbulent, starburst	0.86σ
EPL	UF23, base	Finke	Turbulent, starburst	0.86σ
EPL	Jansson12	Franceschini	Turbulent, starburst	1.20σ
EPL	UF23, base	Franceschini	Turbulent, starburst	1.15σ

Data	GMF	EBL	Host	p_{local}
LP	Jansson12	Saldana-Lopez	Constant	1.46σ
LP	UF23, base	Saldana-Lopez	Constant	1.74σ
LP	Jansson12	Finke	Constant	1.71σ
LP	UF23, base	Finke	Constant	1.90σ
LP	Jansson12	Franceschini	Constant	2.75σ
LP	UF23, base	Franceschini	Constant	2.85σ

Data	GMF	EBL	Host	p_{local}
LP	Jansson12	Saldana-Lopez	Turbulent, spiral	1.54σ
LP	UF23, base	Saldana-Lopez	Turbulent, spiral	1.62σ
LP	Jansson12	Finke	Turbulent, spiral	1.68σ
LP	UF23, base	Finke	Turbulent, spiral	1.70σ
LP	Jansson12	Franceschini	Turbulent, spiral	2.88σ
LP	UF23, base	Franceschini	Turbulent, spiral	2.92σ

Data	GMF	EBL	Host	p_{local}
LP	Jansson12	Saldana-Lopez	Turbulent, starburst	1.59σ
LP	UF23, base	Saldana-Lopez	Turbulent, starburst	1.74σ
LP	Jansson12	Finke	Turbulent, starburst	1.82σ
LP	UF23, base	Finke	Turbulent, starburst	1.89σ
LP	Jansson12	Franceschini	Turbulent, starburst	3.01σ
LP	UF23, base	Franceschini	Turbulent, starburst	2.89σ